

Biochemical Interrogation of Polyketide Ketoreductase and Dehydratase Domain
Stereoselectivity, Stereospecificity and Mechanism via Synthetic, Truncated Substrates

A DISSERTATION
SUBMITTED TO THE FACULTY OF THE GRADUATE SCHOOL
OF THE UNIVERSITY OF MINNESOTA
BY

William D. Fiers

IN PARTIAL FULFILLMENT OF THE REQUIREMENTS
FOR THE DEGREE OF
DOCTOR OF PHILOSOPHY

Dr. Robert A. Fecik, Dr. Courtney C. Aldrich

April, 2016

Acknowledgements

Firstly, I would like to convey my gratitude to my primary advisor Prof. Robert A. Fecik for his initial direction and advice on my thesis work. The freedom he gave me during these past years has allowed me to develop my own skills as a researcher: to generate my own hypotheses, as well as drive several projects to completion. Secondly, I would like to express my appreciation towards my co-Advisor, Prof. Courtney C. Aldrich. His guidance in the last couple of years of my dissertation work allowed me to hone my scientific writing skills and develop my interest in exploring new areas of biology outside of my initial training. My thanks go out to Prof. Thomas R. Hoye and Prof. Rodney L. Johnson for advice and suggestions while acting as my committee members. I would also like to acknowledge the essential advice and structural expertise of Prof. Janet L. Smith (University of Michigan) and her students (Dr. Steffen M. Bernard, Greg J. Dodge and Meredith Skiba). Crystallography experiments in their lab will undoubtedly have a lasting impact on the field. From the Fecik lab, I would like to thank my wife, Dr. Yang Li for her guidance and support in all efforts inside and outside of the lab. I would also like to acknowledge the past Fecik group members: Professors Erick K. Leggans (Grinnell College) and Amber J. Onorato (Northern Kentucky University) for laying the foundations for much of the polyketide work as well as my graduate training in organic chemistry. Additionally, Bryan C. Murray (Pfizer) deserves recognition for inspiring research conversations. I would like to acknowledge my appreciation for the invaluable biochemical and analytical expertise and guidance of Dr. Benjamin P. Duckworth (Beckman Coulter) and Prof. Bruce A. Witthuhn (University of Minnesota-Center for Mass Spectrometry). Additionally, expression of proteins and their purification would not have been possible without assistance from Daniel Wilson (Center for Drug Design) From the Aldrich lab I would like to thank Dr. Ce Shi (Promega), Dr. Surendra Dawadi, Carter G. Eiden, Matthew R. Bockman, Joseph A. Buonomo and Evan M. Alexander for useful discussions while participating in their group meetings. Finally, I would like to acknowledge the Department of Medicinal Chemistry for their generous funding and support during the last two years of my Ph.D. training.

Dedication

I dedicate this thesis and dissertation to my mother and father (Julie A. and Douglas F. Fiers), my sister (Elise M. Fiers) and my wife (Yang Li). My parents have supported my education both financially and emotionally, seeing me through both trying times and times of success. Without their encouragement and understanding I fear I would never have been able to complete this work and come so far in my training. Furthermore, their inspiration as successful and caring healthcare providers has perhaps impacted me in more ways than I will ever know.

My sister has been a constant source of inspiration as a model of creativity and resourcefulness. Though our life paths have diverged to some extent, she remains my most reliable friend and staunchest ally. As always, I look forward to finding out to what endeavors lie ahead for both of us, confident that the journey will prove the most fulfilling reward.

Finally, I would like to dedicate this work to my wife, Yang Li. Through a chance of fate we met at the beginning of our graduate careers and she has been a pillar of comic wisdom, emotional support, and motivation throughout this process. I have had the opportunity to traverse the globe, learn a new language, explore a new culture and love a beautiful and intelligent woman. I cannot imagine desiring anything more and look forward to where this crazy life will take us together!

Abstract

Polyketide natural products are secondary metabolites produced in fungi, plants and bacteria. Since their discovery, these versatile small molecules have served as pharmaceuticals in many fields of medicine. From use as antibiotics to anti-cancer agents to immunosuppressants, polyketides remain staple components in the pharmacopeia. Nature biosynthesizes members of this natural product class through use of a complex network of enzymes known as polyketide synthases.

There is an interest in studying enzymatic pathways that install chemical functional groups and unique three-dimensional form in hopes of rationally modifying them to create new drug molecules. This is an attractive prospect as enzyme catalysis can be predicted by genetic examination of the pathway. In theory, swapping, deleting or inserting a catalytic domain in the pathway would offer a means of controlled alteration of the natural product. While initial efforts have led to limited success, recently the focus has been shifted to understanding the mechanistic and structural details of these pathways with the aim of improving rational pathway diversification.

Three aspects of polyketide synthesis: cryptic domains, distal stereochemistry and non-canonical domain architecture; remain relatively unexplored in the polyketide literature. Cryptic domains involve the configuration of polyketide intermediates obscured by later domain action. Stereochemistry distal to the site of manipulation on the polyketide may be a factor in pathway alteration, as the new catalytic site may not accept subtle changes made by prior enzymes. Modern genetics has revealed many pathways don't follow the rules pertaining to the presence and order of catalytic domains. Bizarre exceptions to canonical domain architecture are difficult to reproduce and predict in modified pathways. Additionally, discovering how the product is ultimately produced may offer insight and new strategies for the coupling of polyketide synthase modules to create new products. We hypothesized that all three aspects of polyketide synthases (cryptic domains, distal stereochemistry and non-canonical domain architecture) could be studied

through interrogation of individual catalytic domains with synthetic, diffusible substrates.

In our studies we revealed several key elements of polyketide synthases that were previously unknown in the literature. We biochemically verified that cryptic stereochemistry and geometry can be accurately predicted based on genetic patterns in a polyketide synthase. A novel, mass spectrometry-based method of quantifying enzyme turnover in polyketide synthases was developed. This new technique allowed for the direct comparison of substrates with changes in distal stereochemistry in a dehydratase domain. Single inversions in configuration in substrates were found to result in a 14- to 45-fold loss in enzyme activity. Additionally, we were able to elucidate a unique mechanism for vinylogous dehydration in the curacin A pathway. This discovery explains why the polyketide synthase is missing domains and provides a clear exception to the notion of enzyme-product co-linearity. The combined work suggests that many potential pitfalls in the rational design of polyketide synthases can be anticipated and avoided through increased knowledge of pathway mechanisms and limitations.

Table of Contents

Acknowledgements	i
Dedication	ii
Abstract	iii
Table of Contents	v
List of Tables	vii
List of Figures	vii
List of Schemes	xi
List of Abbreviations	x
Chapter 1: Introduction to Polyketide Synthase Function	
1.1 Polyketide natural products: Occurrence and value	1
1.2 Polyketide synthases: Natural product assembly lines.....	4
Chapter 2: Tylosin Module 3 Cryptic Ketoreductase and Dehydratase Domains	
2.1 Cryptic β -processing in polyketide synthase domains.....	12
2.2 Chemical strategy and rationale.....	13
2.3 Synthesis of native substrate and product compounds.....	17
2.3.1 Chemical synthesis of two-carbon homologue thioethers.....	17
2.3.2 Synthesis of thioester substrates.....	19
2.3.3 Unsuccessful synthesis of one-carbon homologs of the TylKR3 substrate.....	20
2.4 Expression of tylosin module 3 β -processing domains.....	22
2.5 Enzymatic analysis of TylDH3-KR3.....	23
2.5.1 Analysis of ketoreductase activity.....	23
2.5.2 Analysis of dehydratase activity.....	23
2.6 Synthesis and activity of epimeric DH substrates.....	27
2.7 Tylosin module 3 summary.....	29
2.8 Chemistry experimental section.....	31
2.9 Biology experimental section.....	66

Chapter 3: Curacin Module K Cryptic Dehydratase

3.1 Background on the natural product curacin.....	72
3.2 Chemical strategy and rationale.....	73
3.3 Synthesis of truncated CurK DH substrates.....	75
3.4 CurK DH-catalyzed production and characterization of triene intermediate.....	76
3.5 Quantitative analysis of CurK DH-catalyzed dehydration.....	79
3.6 Chemistry experimental section.....	80
3.7 Biology experimental section.....	85

Chapter 4: Curacin Module I and J Vinylogous Dehydration

4.1 Unusual architectural features of the curacin PKS.....	89
4.2 Chemical strategy and rationale.....	91
4.3 Synthesis of truncated CurJ DH substrates and product.....	92
4.4 Comparative analysis of curacin DHs and predicted CurJ substrates.....	93
4.5 Vinylogous dehydration theory for anomalous elimination.....	94
4.6 Chemical strategy and rationale for vinylogous substrates.....	95
4.7 Synthesis of CurJ DH vinylogous elimination substrates.....	96
4.8 Comparative analysis of vinylogous elimination in the curacin pathway.....	98
4.9 Chemistry experimental section.....	100
4.10 Biology experimental section.....	116

Chapter 5: Curacin Module G dehydratase substrates

5.1 Formation of the cis-alkene within curacin biosynthetic pathway.....	117
5.2 Chemical strategy and rationale.....	118
5.3 Synthesis activity of the putative CurG substrate.....	119
5.4 A holistic hypothesis for curacin biosynthesis.....	124
5.5 Vinylogous dehydration- Unknowns and future directions.....	126
5.6 Chemistry experimental section.....	130

References.....	136
------------------------	------------

Appendix.....	140
----------------------	------------

List of Tables

Table 2.1 Steady-state kinetic analysis of TyIDH3 substrates.....	26
Table 2.2 LC-MS/MS analysis of analytes 2.6 , 2.7 , 2.10 , 2.8 , 2.9 , and 2.11	69
Table 3.1 CurK DH substrate, product and internal standard LC-MS/MS properties....	86
Table 3.2 CurK DH standard curve data.....	86
Table 3.3 LC-MS/MS data for CurK DH substrate 3.5	88
Table 4.1 LC-MS/MS data for 4.2–4.6 , 4.13 and 4.14	116
Table 5.1 Temperature-dependent diastereomeric ratio of ketone reduction.....	123

List of Figures

Figure 1.1 Simple and complex polyketides.....	2
Figure 1.2 Natural and semi-synthetic macrolide antibiotics.....	2
Figure 1.3 Lovastatin, compactin and derived antihypolipodemic agents.....	2
Figure 1.4 A representative collection of polyketide and polyketide-derived pharmaceutical agents.....	3
Figure 1.5 The total synthesis of the polyketide oricinol.....	4
Figure 1.6 Birch's isotopic labeling of 2-hydroxy-6-methylbenzoic acid.....	4
Figure 1.7 Type I, II and III polyketide synthases.....	5
Figure 1.8 Polyketide chain extension via enzyme-catalyzed Claisen reactions.....	6
Figure 1.9 Proposed mechanisms of polyketide C-methyltransferase domains.....	7
Figure 1.10 The fundamental mechanism for the KR-catalyzed ketone reduction.....	8
Figure 1.11 Ketoreductase classification by stereoselectivity.....	8
Figure 1.12 Elimination catalyzed by polyketide dehydratase domain.....	9
Figure 1.13 The proposed ene-mechanism of reduction by enoyl reductase domains....	10
Figure 1.14 Polyketide chain termination by a thioesterase domain.....	10
Figure 1.15 Polyketide tailoring by post-PKS enzymes.....	11
Figure 1.16 PKS and post-PKS biosynthesis of the antibiotic erythromycin.....	12
Figure 2.1 Cryptic stereochemistry in a polyketide synthase.....	13

Figure 2.2 The modular PKS of tylactone (2.1).....	14
Figure 2.3 Native and synthetic TyIKR3 substrates with their possible β -processing products.....	16
Figure 2.4 LC-MS/MS traces of <i>in vitro</i> ketoreduction and dehydration reactions.....	25
Figure 2.5 Linear regression analysis of TyIDH3KR3 kinetic data with substrates 2.7 , 2.9 , 2.41 , and 2.42	27
Figure 2.6 SDS-PAGE image of TyIDH3-KR3 purification.....	68
Figure 2.7 Mass spectrometry analysis of TyIDH3-KR3.....	68
Figure 2.8 LC-MS/MS trace of dienethiolate 2.53	71
Figure 3.1 The curacin A biosynthetic pathway.....	73
Figure 3.2 A comparison of natural curacin geometric isomers.....	74
Figure 3.3 Curacin module K DH substrate and product design.....	75
Figure 3.4 Graphical display of the stereoselective action of the CurK DH.....	77
Figure 3.5 LC-MS/MS analysis of the incubation of 3.5 and 3.6 with the CurK DH....	78
Figure 3.6 The diagnostic α , β -protons used to assign geometry in the CurK DH product.....	79
Figure 3.7 Michaelis-Menten analysis of substrate 3.5	80
Figure 3.8 Standard curve of product 3.7	87
Figure 4.1 The curacin A biosynthetic pathway with proposed polyketide module intermediates.....	90
Figure 4.2 A depiction of stuttered dehydration.....	90
Figure 4.3 The predicted full length CurJ DH substrate (4.1) and designed small molecule substrates.....	91
Figure 4.4 LC-MS/MS analysis of predicted CurJ DH substrate activity.....	94
Figure 4.5 Vinylogous elimination catalyzed by the CurJ module.....	95
Figure 4.6 Designed vinylogous elimination substrates for CurJ DH.....	96
Figure 4.7 Incubation of substrates 4.13 and 4.14 with the curacin dehydratases.....	99
Figure 5.1 The actions of the CurF-CurG di-module from the curacin pathway.....	118
Figure 5.2 Design of synthetic CurG dehydratase product and substrate.....	119
Figure 5.3 Proposed vinylogous elimination between modules CurG and CurH.....	125

Figure 5.4 Proposed pathway incorporating vinylogous eliminations for curacin A biosynthesis.....	126
Figure 5.5 Depiction of allylic strain in vinylogous dehydration substrates.....	128
Figure 5.6 The proposed mechanistic basis for <i>cis</i> alkene formation through vinylogous elimination.....	129

List of Schemes

Scheme 2.1 Synthesis of thioether 2.9	17
Scheme 2.2 Synthesis of enantiomeric thioether 2.8	18
Scheme 2.3 Synthetic route to ketoreductase substrate 2.5	19
Scheme 2.4 Synthesis of thioester TylKR3 product 2.7	19
Scheme 2.5 Synthesis of thioester TylKR3 substrate 2.4	20
Scheme 2.6 Synthesis of thioester substrate 2.6	20
Scheme 2.7 Unsuccessful synthesis of one-carbon thioether substrate.....	22
Scheme 2.8 Synthetic route towards dehydratase substrate 2.41	28
Scheme 2.9 Synthesis of substrate 2.42	29
Scheme 2.10 Synthetic route towards authentic product standard 2.53	29
Scheme 2.11 Chemoenzymatic synthesis of diene products.....	64
Scheme 3.1 Synthetic route towards CurK DH substrate 3.5	76
Scheme 4.1 Synthesis of CurJ DH substates 4.2 and 4.3	92
Scheme 4.2 Synthetic route towards CurJ DH product 4.6	93
Scheme 4.3 Intramolecular cyclization of δ -hydroxyl-thioesters.....	96
Scheme 4.4 The short synthesis of vinylogous dehydration substrate 4.13	97
Scheme 4.5 The synthesis of di-dehydration substrate 4.15	98
Scheme 5.1 Retrosynthetic analysis of CurG DH substrates 5.2/5.3	120
Scheme 5.2 Failed synthesis of key aldehyde 5.5	121
Scheme 5.3 Failed decarboxylative Claisen reaction.....	122
Scheme 5.4 Successful Claisen condensation to form 5.16	122
Scheme 5.5 Completion of CurG DH substrates 5.2/5.3	123

List of Abbreviations

Å	angstrom
A	adenylation domain
A ^{1,2}	1,2-allylic strain
A ^{1,3}	1,3-allylic strain
ACP	acyl-carrier protein
Asp	aspartic acid
AT	acyltransferase domain
Bn	benzyl
Bu	butyl
¹³ C	carbon 13
Calcd	calculated
CDI	1,1'-carbonyldiimidazole
CMT	carbon methyltransferase domain
CoA	coenzyme A
cps	counts per second
Cur	curacin
Cy	cyclization domain
Da	dalton
DCC	<i>N,N'</i> -dicyclohexylcarbodiimide
DDQ	2,3-dichloro-5,6-dicyano-1,4-benzoquinone
DEBS	6-deoxyerythronolide B synthase
DH	dehydratase domain
DIBAL-H	diisobutylaluminum hydride
DIPEA	diisopropylethylamine
DMAP	4-dimethylaminopyridine
DMF	dimethylformamide
DMP	Dess-Martin periodinane
DMSO	dimethyl sulfoxide

DNA	deoxyribonucleic acid
DPPA	diphenyl phosphoryl azide
<i>E. coli</i>	<i>Escherichia coli</i>
ECH	enoyl-coenzyme A hydratase domain
EDCI	1-ethyl-3-(3-dimethylaminopropyl)carbodiimide
equiv	equivalents
ER	enoyl reductase domain
ESI	electrospray ionization
Et	ethyl
Et ₂ O	diethyl ether
EtOAc	ethyl acetate
FabA	<i>Escherichia coli</i> fatty acid dehydratase-isomerase enzyme
G	gravity
GCN5	yeast histone <i>N</i> -acetyltransferase enzyme
GNAT	GCN5-related <i>N</i> -acetyltransferase
GroEL	bacterial heat shock protein 60
GroES	bacterial heat shock protein 10
GST	glutathione <i>S</i> -transferase
h	hour(s)
¹ H	hydrogen 1
His	histidine
HPLC	high-performance liquid chromatography
HRMS	high-resolution mass spectrometry
HWE	Horner-Wadsworth-Emmons
Hz	hertz
IBX	2-iodoxybenzoic acid
Imid.	imidazole
<i>i</i> PrOH	isopropanol
IPTG	isopropyl β-D-1-thiogalactopyranoside

k_{cat}	turnover number
kDa	kilodalton
K_M	Michaelis constant
KR	ketoreductase domain
KS	ketosynthase domain
LC-MS/MS	liquid chromatography tandem mass spectrometry
LDA	lithium diisopropylamide
LIC	ligation independent cloning
LOD	limit of detection
LRMS	low-resolution mass spectrometry
M	molar
m/z	mass-to-charge ratio
Me	methyl
MeCN	acetonitrile
min	minute(s)
MeOH	methanol
MHz	megahertz
mM	millimolar
mmol	millimoles
mOCR	monomeric overcome classical restriction protein
MRM	multiple reaction monitoring
MT	methyltransferase domain
NAC	<i>N</i> -acetylcysteamine
NADPH	nicotinamide adenine dinucleotide phosphate
NaHMDS	sodium bis(trimethylsilyl)amide
nM	nanomolar
NMO	<i>N</i> -methylmorpholine <i>N</i> -oxide
NMR	nuclear magnetic resonance
OD ₆₀₀	optical density at a wavelength of 600 nanometers
PCP	peptide carrier protein

PEG	polyethylene glycol
pg	prep grade
PKS	polyketide synthase
pLysS	T7 lysozyme coding sequence
PPG	polypropylene glycol
ppm	parts per million
pyr	pyridine
QTOF	quadrupole time-of-flight
quant.	quantitative yield
R^2	coefficient of determination
R_f	retention factor
RPM	revolutions per minute
SAH	<i>S</i> -adenosylhomocysteine
SAM	<i>S</i> -adenosylmethionine
SDS-PAGE	sodium dodecyl sulfate-polyacrylamide gel electrophoresis
[<i>S</i>]	substrate concentration
Ser	serine
SUMO	small ubiquitin-like modifier
TE	thioesterase domain
TEA	triethylamine
<i>tert</i> -BuOAc	<i>tert</i> -butyl acetate
TES	triethylsilyl
TESOTf	trifluoromethanesulfonate trifluoromethanesulfonate
Tf ₂ O	trifluoromethanesulfonic anhydride
TFA	trifluoroacetic acid
THF	tetrahydrofuran
TIPS	triisopropylsilyl
TIPSOTf	triisopropylsilyl trifluoromethanesulfonate
TLC	thin-layer chromatography
TMSCl	trimethylsilyl chloride

TOF	time-of-flight
TPAP	tetrapropylammonium perruthenate
Tris	tris(hydroxymethyl)aminomethane
tRNA	transfer ribonucleic acid
Tyl	tylosin
Tyr	tyrosine
v_0	initial velocity
μM	micromolar
UV	ultraviolet

Chapter 1: Introduction to the Polyketides

1.1 Polyketide natural products: Occurrence and value

Polyketide natural products represent a chemically broad, multifaceted family of secondary metabolites. Members of this class are commonly isolated from fungal, bacterial and botanical organisms, ranging from simple (5-methyl-1-naphthoic acid, **1.1**) to complex (rifamycin B, **1.2**) molecules (**Figure 1.1**). A consequence of the wide structural diversity of polyketides is their extensive use in many therapeutic areas. Erythromycin (**1.3**) was isolated and marketed by Eli Lilly as a broad-spectrum antibiotic in 1955, paving the way for a host of other natural and semi-synthetic macrolides.¹ The natural product analogs of erythromycin range from subtle transformations (*O*-methylation, clarithromycin, **1.4**) to a series of intricate functional group manipulations (telithromycin, **1.5**) each bestowing favorable pharmacokinetic, drug-stabilizing, efficacy and reduced drug resistance properties to the original scaffold (**Figure 1.2**). The field of cholesterol regulation was greatly advanced by polyketide antihypolipodemic agents. The discovery of lovastatin (**1.6**), compactin (**1.7**) and related pharmaceuticals (simvastatin (**1.8**), and pravastatin (**1.9**)) provided clinicians safe and reliable therapeutic medications (**Figure 1.3**). Highlights of polyketide usage in other therapeutic areas include: immunosuppressants tacrolimus (**1.10**) and rapamycin (**1.11**), antineoplastic agents ixabepilone (**1.12**, an epothilone B analog) and the antibody-drug conjugate Kadcyla (**1.13**, derived from maytansine and the monoclonal antibody trastuzumab), as well as the antifungal drug amphotericin B (**1.14**) (**Figure 1.4**)

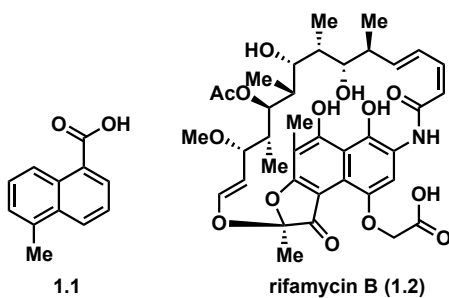


Figure 1.1. Simple and complex polyketide natural products.

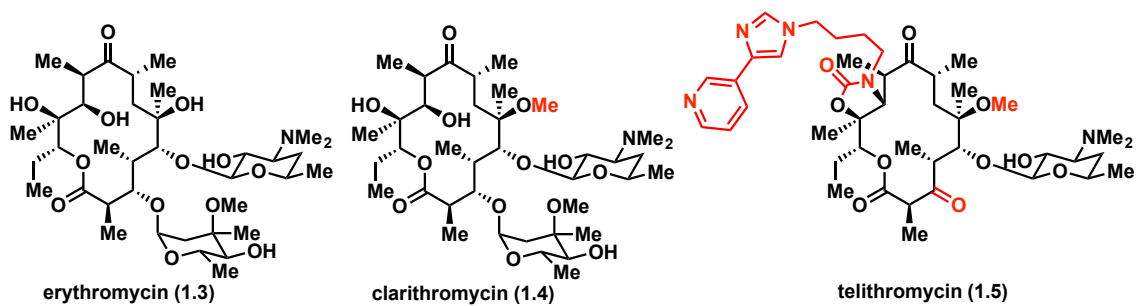


Figure 1.2. Natural and semi-synthetic macrolide antibiotics. Erythromycin analogs clarithromycin and telithromycin are shown with modifications highlighted in red.

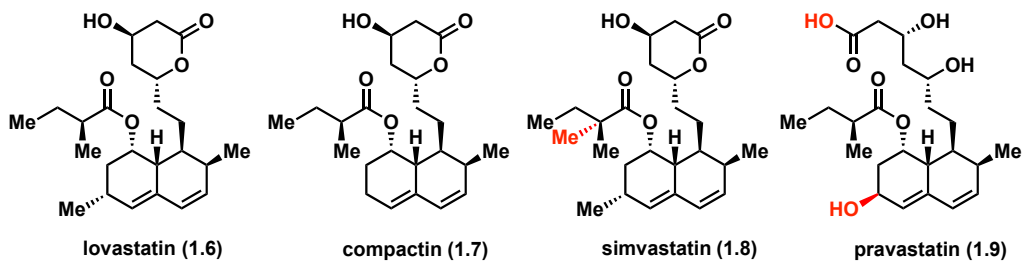


Figure 1.3. Lovastatin, compactin and derived antihypolipodemic agents. The semi-synthetic manipulations are shown in red for simvastatin and pravastatin.

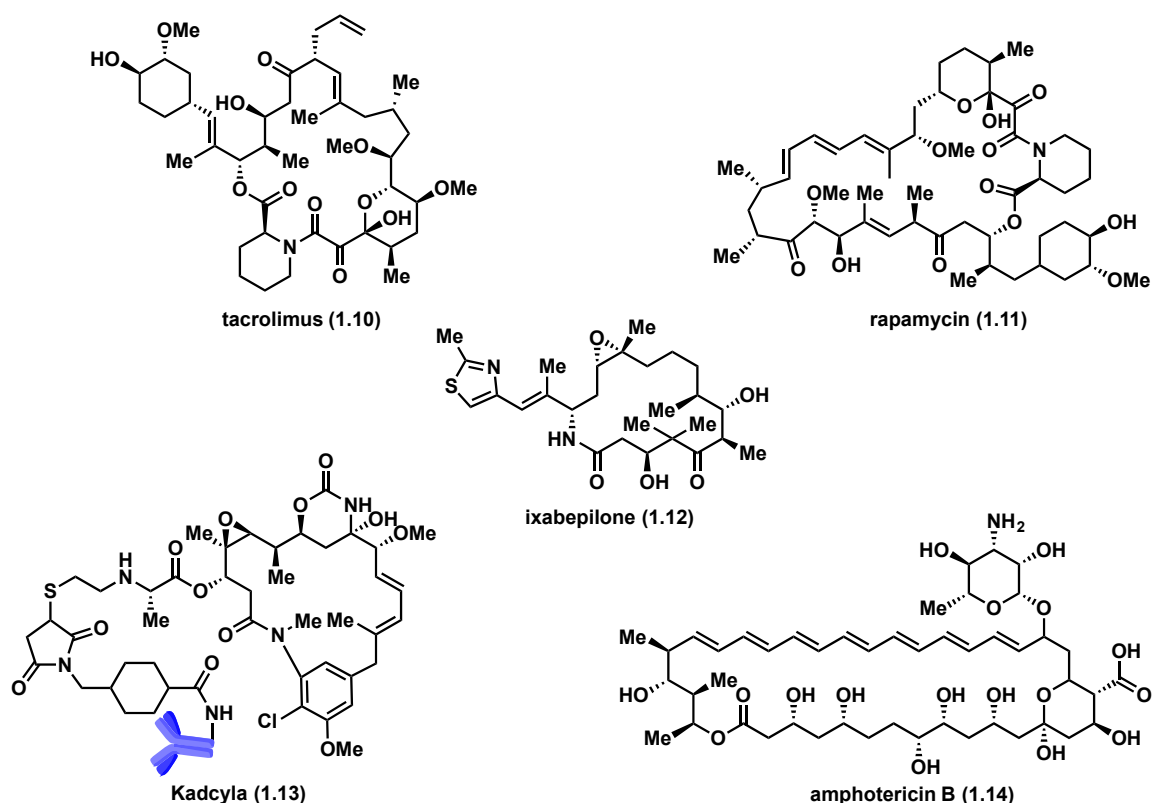


Figure 1.4. A representative collection of polyketide and polyketide-derived pharmaceutical agents.

Prior to the first use of the term, polyketides were defined as “multiple keten” by John Norman Collie as early as 1907.² This descriptor was used to define the hypothetical biosynthetic intermediates responsible for many early natural products. As evidence towards his proposal, Collie highlighted the total synthesis of the natural product orcinol (**1.15**) from diacetylacetone (**1.16**) after heating under strong alkaline conditions (**Figure 1.5**).³ The biosynthetic theory lay unproven until 1955 when A. J. Birch and coworkers developed a clever isotope labeling experiment that would lay the groundwork for more than a half-century of fruitful research.⁴ Birch had hypothesized that acetate could serve as the fundamental building block based on common substitution patterns in polyphenolic natural metabolites. In his key experiment, ¹⁴C-labeled sodium acetate (**1.17**) was fed to *Penicillium griseofulvum*, a common mold known for producing 2-hydroxy-6-methylbenzoic acid (**1.18**) (**Figure 1.6**). Analysis revealed an isotope incorporation rate

and pattern consistent with a polyketone intermediate (**1.19**), strikingly similar to diacetylacetone (**1.16**). Isotope feeding experiments, based on Birch's insightful work, would later stitch together the polyketide class of natural products based on their biosynthetic building blocks.

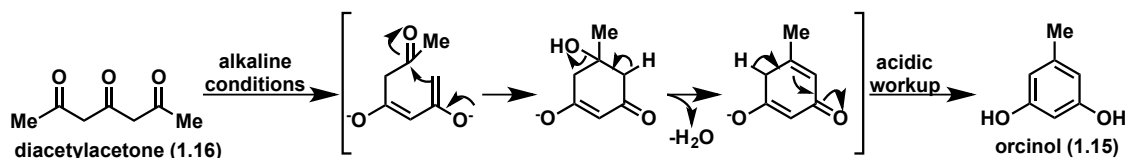


Figure 1.5. The total synthesis of the polyketide orcinol. Diacetylacetone (**1.16**) served as the inspiration for Collie's biosynthetic building blocks.

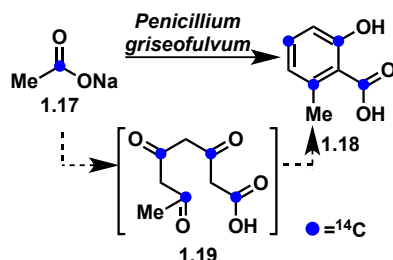


Figure 1.6. Birch's isotopic labeling of 2-hydroxy-6-methylbenzoic acid. The incorporated ^{14}C -labeled carbons are shown in blue.

The next major hurdle in the study of polyketide biosynthesis was proving how producing organisms catalyzed Claisen reactions and controlled cyclization or reduction reactions *in vitro*.

1.2 Polyketide synthases: Natural product assembly lines

The advent of molecular genetics and parallel discoveries in the field of fatty acid biosynthesis led to the isolation and characterization of polyketide-producing enzymes, or polyketide synthases (PKSs). Polyketide synthases are a broad enzyme family ranging from huge megaenzymes to small monofunctional proteins. The synthase enzymes are now subdivided into three distinct types based on their size, function and substrate

preference. Type I polyketide synthases are large multifunctional proteins that are chiefly characterized by their distinct catalytic domains (**Figure 1.7**). Each catalytic domain is responsible for one transformation in the polyketide synthase, instilling a co-linear architecture in the PKS. In contrast, a cluster of individual proteins, each catalyzing a defined step towards polyketide biosynthesis, typifies type II polyketide synthases. Iterative and non-iterative sub-families of type I exist, differing in single use or multiple uses of megaenzyme catalytic domains. Both type I and type II PKSs act upon substrates bound to an acyl-carrier protein (ACP). These are typically derived from acyl-coenzyme A intermediates. Type III polyketide synthases differ by their single active site capable of catalyzing several reactions and their preference for acyl-CoA substrates instead of ACP-bound substrates. For simplicity, the remaining sections will depict all steps as they occur in in type I, bacterial (non-iterative) PKS.

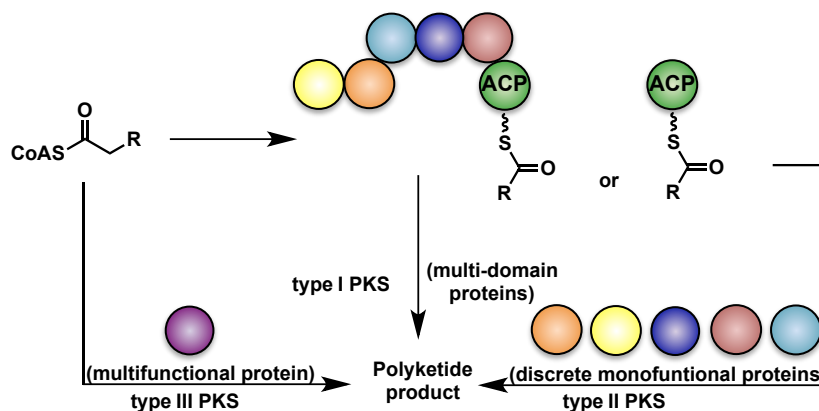


Figure 1.7. Type I, II and III polyketide synthases.

Chain elongation occurs via a ketosynthase catalyzed Claisen reaction that is chemically identical across all three types of polyketide synthases. Enzymatically, the process varies in the substrate identity (ACP-bound in type I and II, CoA-thioester in type III) and intermolecular or intramolecular substrate-protein interaction (type I vs. type II and III). The process begins via intermediate transfer from an ACP domain from a previous module (or loading module ACP if $n = 1$) to the current module's ketosynthase domain (KS) (**Figure 1.8**). The acyltransferase domain (AT) catalyzes a transesterification of the

coenzyme A-thioester extender unit (usually malonyl- or methylmalonyl-CoA) onto itself, forming a new, transient ester. The AT-bound ester is attacked intramolecularly by the current module's ACP domain, transferring the carboxyester building block and priming the module for the key Claisen reaction. The KS domain catalyzes the decarboxylation of the ACP-bound malonate (or methylmalonate) extender unit and guides the resulting enolate in its attack on the KS-bound polyketide intermediate. The formed β -ketone intermediate may be directly passed to the KS domain of the next module (n+1) or it may undergo processing by additional domains in the same module (n).

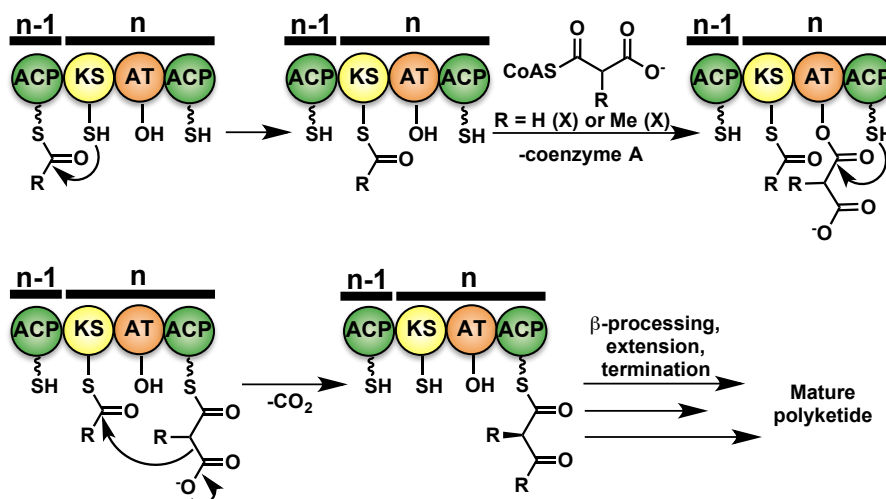


Figure 1.8. Polyketide chain extension via enzyme-catalyzed Claisen reactions. The generic module number is represented as n or $n-1$.

The optional processing of β -ketothioesters by additional domains in the module instills functional group and stereogenic diversity in the final polyketide product. Traditionally known as β -processing, this process can actually modify both the α - and β -carbon centers proximal to the thioester on an extended, ACP-bound thioester intermediate.

The first possible modification is α -methylation catalyzed by a carbon-methyltransferase (CMT) domain. This domain takes advantage of the acidic nature of the α -proton in the

β -carbonyl-intermediate, deprotonating it to form a resonance-stabilized enolate. The enolate's attack on *S*-adenosylmethionine (SAM) fixes a methyl group in the α -position and leaves *S*-adenosylhomocysteine (SAH) as the sole byproduct (**Figure 1.9**). The limited studies on this rare PKS module thus far have focused on the origin of dimethyl units in polyketides. Preliminary work has revealed two possible routes: 1) The action of CMT on a malonyl-CoA prior to condensation by the KS domain ($R = OH$), 2) The dimethylation of an unmethylated intermediate of a polyketide by a CMT ($R =$ growing polyketide).⁵ There is currently a lack of information on the catalytic mechanism, stereoselectivity and structure in CMT domains leaving these unknown aspects attractive subjects of future research.

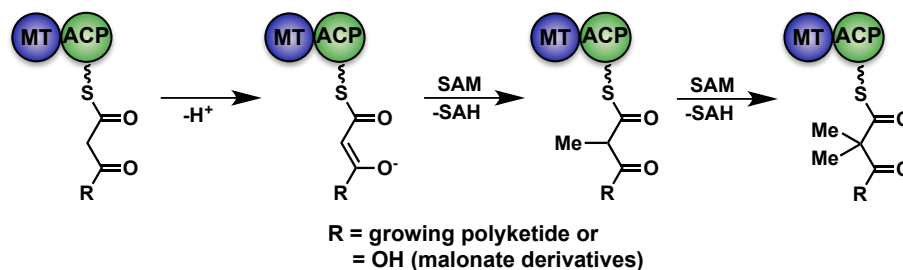


Figure 1.9. Proposed mechanisms of polyketide *C*-methyltransferase domains. Two hypotheses are in effect, one acting on the malonate building blocks prior to ($R = OH$) and following ($R =$ growing chain) KS-catalyzed Claisen reaction.

A ketoreductase (KR) domain catalyzes the reduction of the β -ketone moiety in polyketide chain intermediates. This process utilizes nicotinamide adenine dinucleotide phosphate (NADPH) and stereoselectively forms a β -hydroxythioester intermediate (**Figure 1.10**). In addition to setting the hydroxyl-bearing stereogenic center, the domain also serves to fix the α -stereocenter in appropriately substituted substrates. The native *2S*-configuration resulting from the KS-catalyzed condensation may be epimerized by ketoreductase employing the same catalytic residues used for catalyzing stereoselective reduction.^{6,7} KR domains have been classified as types A and B for production of L- and D-alcohols, respectively (**Figure 1.11**).⁸ Type C ketoreductases fail to catalyze reduction.

Further sub-types 1 and 2 denote the ketoreductases' ability or inability to catalyze epimerization of the α -stereocenter to 2*R*-configuration.

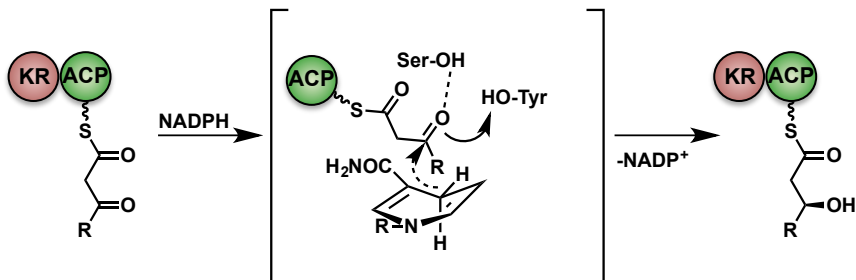


Figure 1.10. The fundamental mechanism for the KR-catalyzed ketone reduction. The essential serine and tyrosine residues of the KR domain are shown with their hypothesized roles in catalysis. The delivery of the pro-*S* hydride from NADPH is invariant. Polyketide substrate orientation determines stereoselectivity.

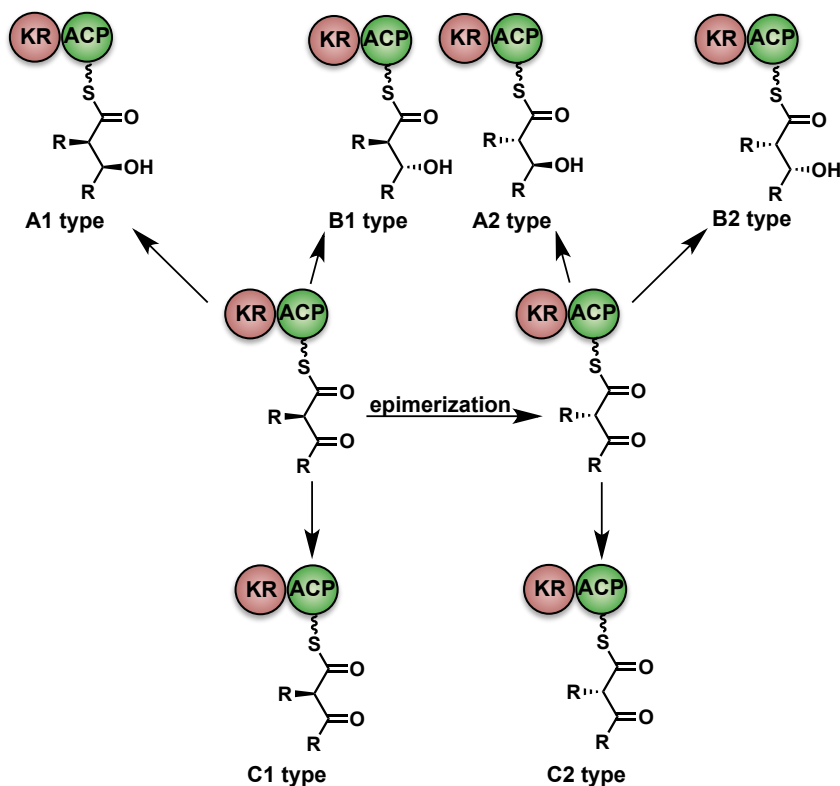


Figure 1.11. Ketoreductase classification by stereoselectivity.

Once the β -hydroxythioester intermediate is formed, water can be eliminated by a dehydratase (DH) domain to form an olefin product. Although their study has lagged behind that of the ketoreductase domain, there has been resurgence in interest in DH domains. The polyketide dehydration is stereospecific in respect to both α - and β -stereogenic centers.⁹ The net reaction is a *syn*-dehydration, similar to elimination in fatty acid biosynthesis and utilizes a catalytic histidine-aspartic acid dyad (**Figure 1.12**). Both *cis*- and *trans*-alkenes are present in polyketides, though little is known about *cis*-alkene formation as it has yet to be observed *in vitro*.

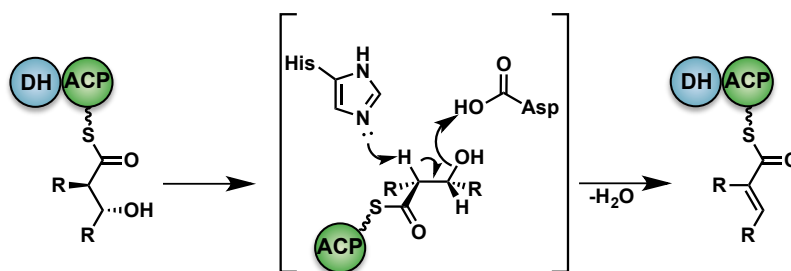


Figure 1.12. Elimination catalyzed by polyketide dehydratase domain. The proposed mechanism for *syn*-elimination with DH catalytic residues is displayed in brackets. In the example a *trans*-olefin product is formed after elimination of water.

The final reductive processing event is the enoyl reductase (ER) domain. As its name suggests, the ER domain catalyzes the reduction of thioenoates, formed by dehydratase domains, yielding saturated alkanes in the process. This reduction utilizes NADPH in a similar to ketoreduction catalyzed by KR domains. The α -stereoselectivity appears to rely heavily on the presence or absence of a tyrosine residue, conferring *2S*- or *2R*-selectivity, respectively.^{10,11} This residue is not essential for catalysis and was determined to be necessary but not sufficient in dictating stereoselectivity. Recently, it has been revealed that the mechanism invokes an ene reaction with a transient, observable adduct (**Figure 1.13**).¹²⁻¹⁴

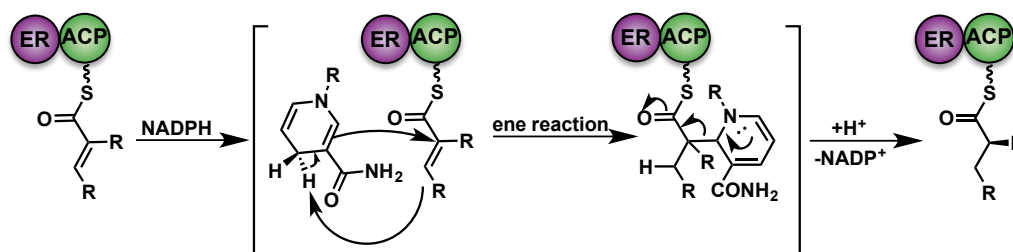


Figure 1.13. The proposed ene-mechanism of reduction by enoyl reductase domains. The stereo-identity of the transient ene-adduct has yet to be deciphered.

The final module of the polyketide synthase usually contains a thioesterase (TE) domain responsible for cleaving the mature chain elongation intermediate. The reaction typically results in macrocyclization or hydrolysis, affording a macrolactone or carboxylic acid product, respectively (**Figure 1.14**). The enzymatic mechanism involves a serine-histidine-aspartic acid triad that loads the module's ACP-bound thioester onto the serine residue via a transesterification. In addition to terminating thioesterases there have also been reports of editing TE (also known as type II or TE II) domains responsible for releasing stalled intermediates in the biosynthetic pathway.^{15,16}

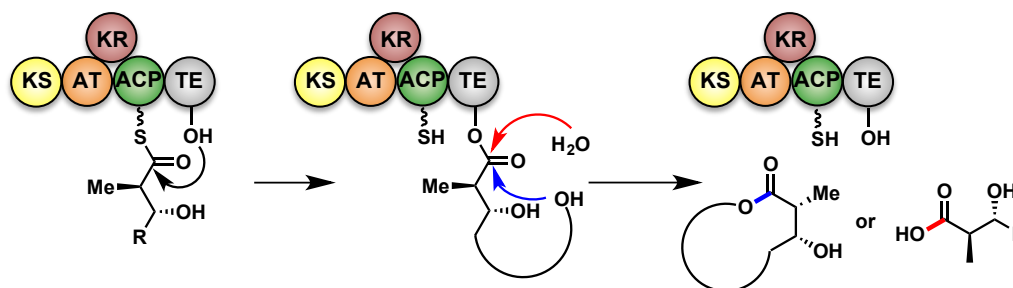


Figure 1.14. Polyketide chain termination by a thioesterase domain. The thioesterase can catalyze macrolactonization (blue arrow) or hydrolysis (red arrow) to release the ester intermediate from the polyketide synthase.

A number of tailoring enzymes can alter the polyketide once it has been released from the PKS (**Figure 1.15**). These enzymes vary widely in their identity and catalytic role in biosynthesis. P450 enzymes are often recruited for C-H oxidation of the polyketide

backbone. Glycosylation is another a common means of modification. Other enzymes catalyze alkene isomerization, epoxidation, cyclopropanation and halogenation. Examining the natural product for deviation from the normal, alternating substitution pattern seen in polyketides can give insight into the post-PKS alterations occurring. Additionally, one can use the genetic sequence of the pathway to tease out functionality that may be the result of a tailoring event, unaccounted for by the central PKS (i.e. reduction, oxidation, elimination or methylation chemistry in the absence of KR, ER, DH or MT domains). The complete biosynthetic pathway to erythromycin (**1.3**) is the archetypal example of polyketide formation in nature (**Figure 1.16**).

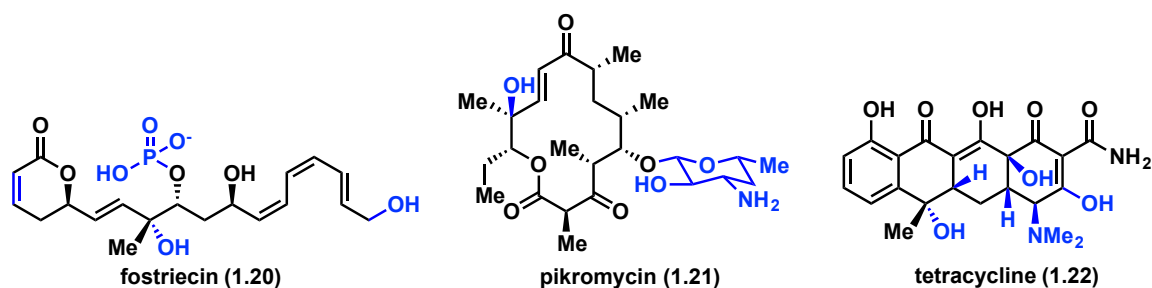


Figure 1.15. Polyketide tailoring by post-PKS enzymes. The modifications made after the polyketide synthase are shown in blue.

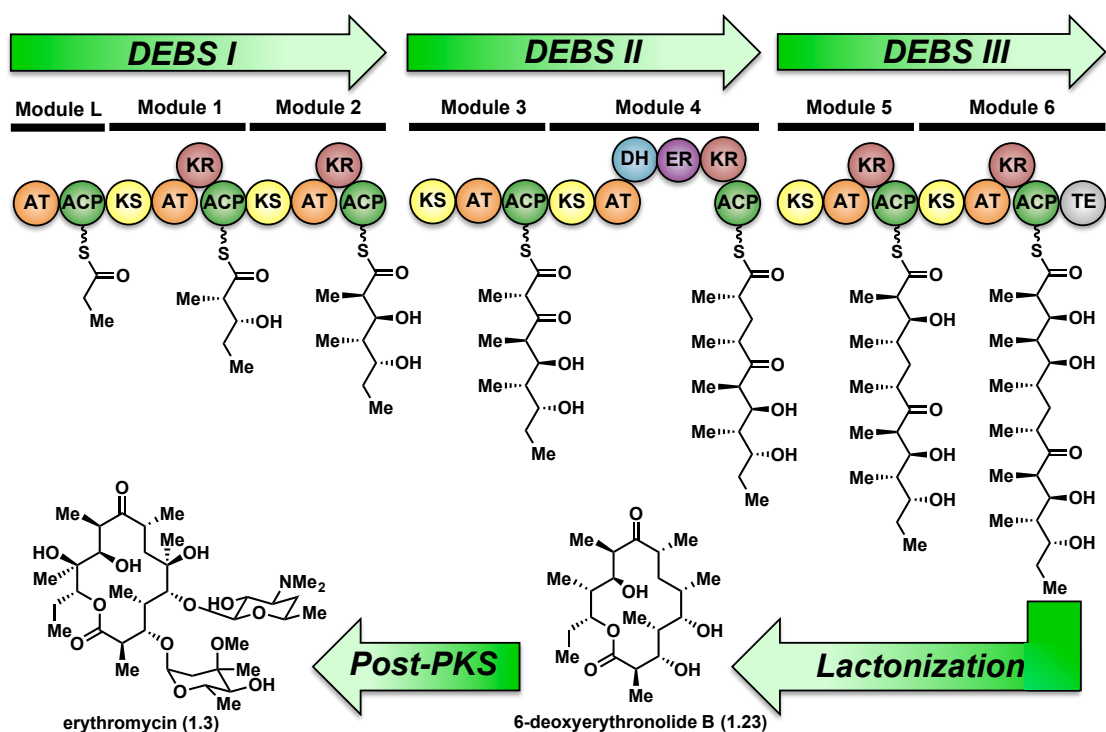


Figure 1.16. PKS and post-PKS biosynthesis of the antibiotic erythromycin. One loading module and 6 extension modules, each incorporating a unit of methylmalonyl-CoA, yield the aglycone, 6-deoxyerythronolide B (**1.23**). P450 enzyme oxidation and glycosylation furnish the final natural product.

Chapter 2: Tylosin Module 3 Cryptic Ketoreductase and Dehydratase Domains

This chapter is based on previously published work appearing in: Fiers, W.D., Dodge, G. J., Li, Y., Smith, J. L., Fecik, R. A., Aldrich, C. C. *Chem. Sci.* **2015**, 6, 5027-5033.

2.1 Cryptic β -processing in polyketide synthase domains

The stereochemical outcome of β -processing domains is often concealed or obscured through subsequent, downstream catalytic events. These instances of hidden domain action can fall into two broad categories: cryptic ketoreductase stereochemistry and cryptic dehydratase geometry (**Figure 2.1**). Cryptic KR reductions arise from presence of

a subsequent DH domain, catalytically eliminating water and, in so doing, removing both α - and β -stereogenic centers. *Trans*-olefin configuration arises from the elimination of D-alcohols while *cis*-olefins emanate from enzyme-mediated isomerization events.^{17,18} Despite recent, compelling evidence suggesting that, in phoslactomycin biosynthesis, PKS DH domain-catalyzed generation of *Z*-olefins occurs from L-alcohols, *in vitro* validation has yet to be obtained.^{19,20} Olefin geometry may be rendered cryptic through successive reduction by an ER domain, potentially yielding a new α -stereogenic center in the process. Cryptic reductions have received a significant amount of attention over the last decade resulting in several novel approaches to their study.^{21,22} Bioinformatic analysis has shown promise in predicting stereogenic centers based on amino acid sequence of the KR domain in question.^{17,23,8}

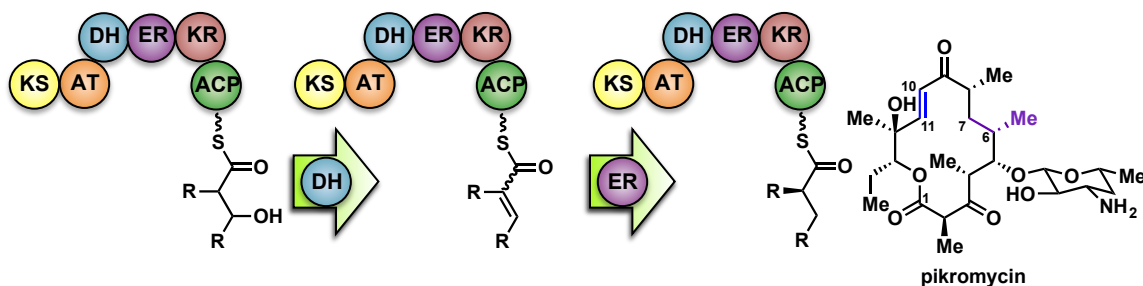


Figure 2.1. Cryptic stereochemistry in a polyketide synthase. Depicted is the obscured stereochemistry placed by the KR domain and the hidden geometry of the dehydratase domain. Pikromycin is shown as an example with cryptic KR activity in blue ($\Delta^{10,11}$) and doubly cryptic KR and DH activity shown in purple (C-6,7).

2.2 Chemical strategy and rationale

Tylosin (**2.1**), a 16-membered macrolactone product of *Streptomyces fradiae*, was chosen as a model system for our initial cryptic domain studies. The tylosin polyketide synthase includes one loading module and seven extension modules terminating in a thioesterase (TE) domain affording the aglycone tylactone (**2.2**) (**Figure 2.2**).²⁴ By virtue of their DH domains, modules 2, 3, and 5 have cryptic KR stereochemistry. Additionally, module 5,

housing an ER domain constitutes a complete reductive sequence further obscuring the geometry of the precursor olefin. Prior methods to study cryptic KRs and DHs using synthetic substrates have generally been limited to diketides. Truncated substrates, while synthetically more accessible, are often poorly tolerated resulting in low conversion and exhibit loose stereochemical discrimination.^{25,26} As a result, the inferred substrate specificity obtained using truncated substrates remains dubious given their significant deviation from the native chain intermediates. Cane and coworkers overcame this limitation through the *in situ* chemoenzymatic synthesis of a triketide from a diketide substrate using a KS-AT didomain and excised ACP domain from 6-deoxyerythronolide B synthase (DEBS).²⁷ However, we anticipated this strategy would be difficult to implement for tetraketides as this would require the use of two complete modules in tandem.

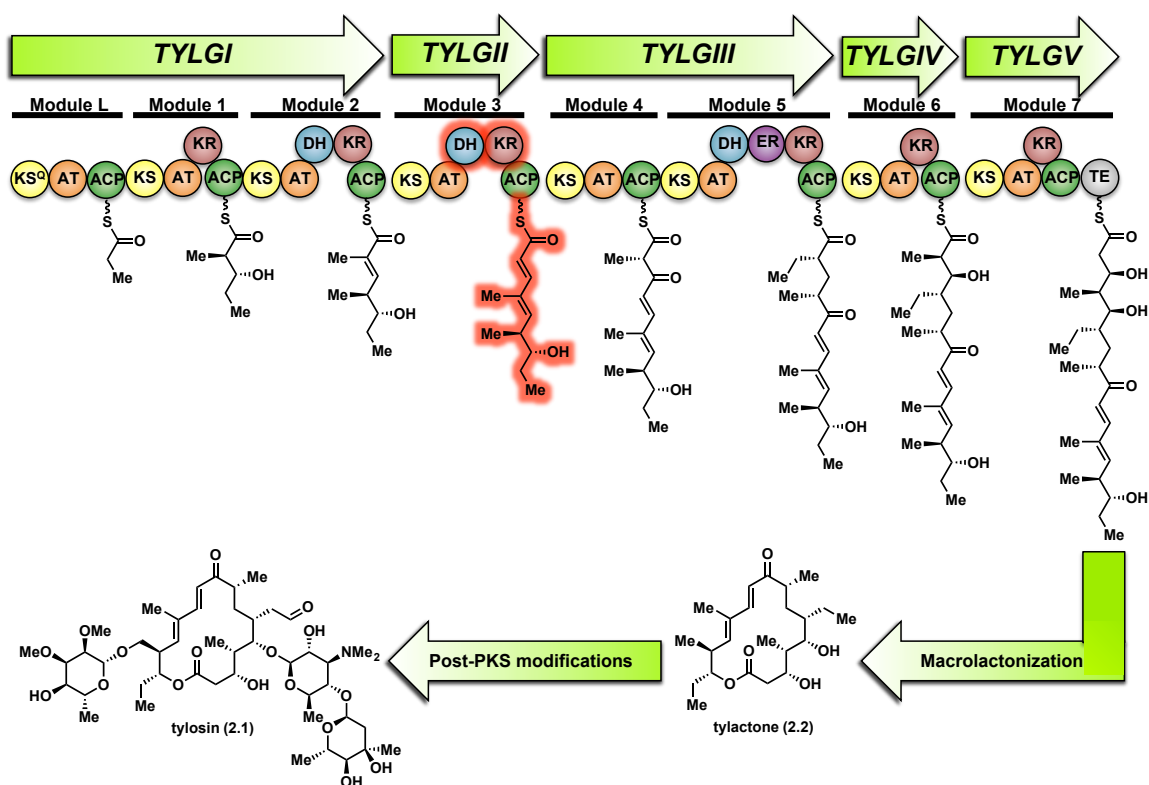


Figure 2.2. The modular PKS of tylosone (2.1). The module 3 β -processing domains and their postulated product are highlighted in red.

As part of ongoing studies in our laboratories, we are interested in the development and use of small molecule tools for exploring innate reactivity within polyketide synthase modules. In the present study we sought to probe the enzyme catalyzed turnover of full-length tetraketide substrates **2.4**, **2.6** and **2.7** by TylKR3 and TylDH3 via LC-MS/MS detection (**Figure 2.3**). One virtue of our chosen tetraketides is that they uniformly lack a δ -hydroxyl moiety which has been shown to spontaneously lactonize with the thioester^{25,27,28}. Our previous strategy utilized stable full-length polyketide intermediate mimics that are resistant to spontaneous intramolecular lactonization through replacement of the labile thioester linkage with a stable thioether moiety.^{22,29} In light of these results, we sought to validate the use of thioether analogs **2.5**, **2.8** and **2.9** for direct comparison with the aforementioned thioester substrates. This would constitute the first steady-state analysis of a polyketide dehydratase domain using native substrates, uncover the cryptic stereochemistry of TylKR3, and would offer a unique, more native context to discover innate substrate biases. The use of a natural full-length tetraketide chain intermediates and epimers at each stereogenic center would also allow us to evaluate the impact of vicinal and distal stereochemistry on KR and DH substrate processing.

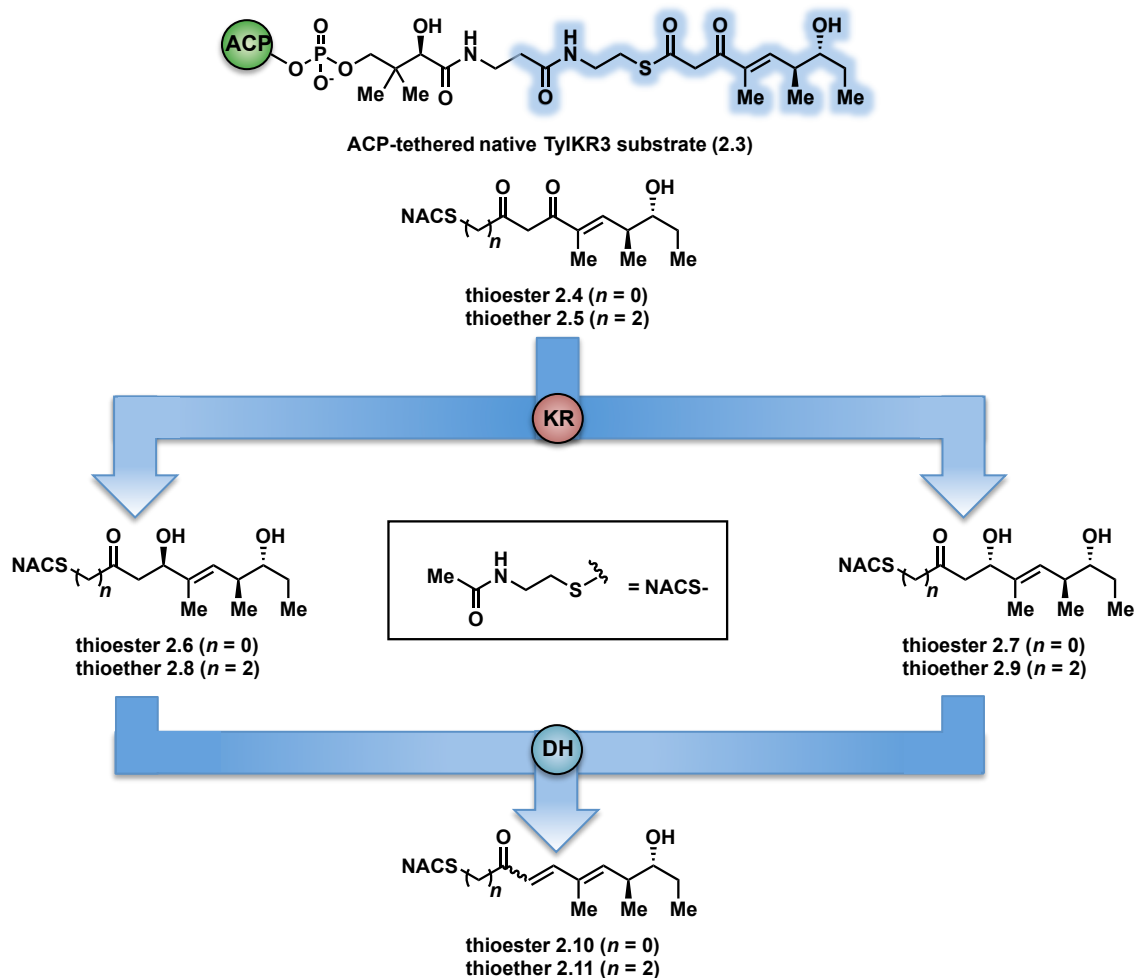


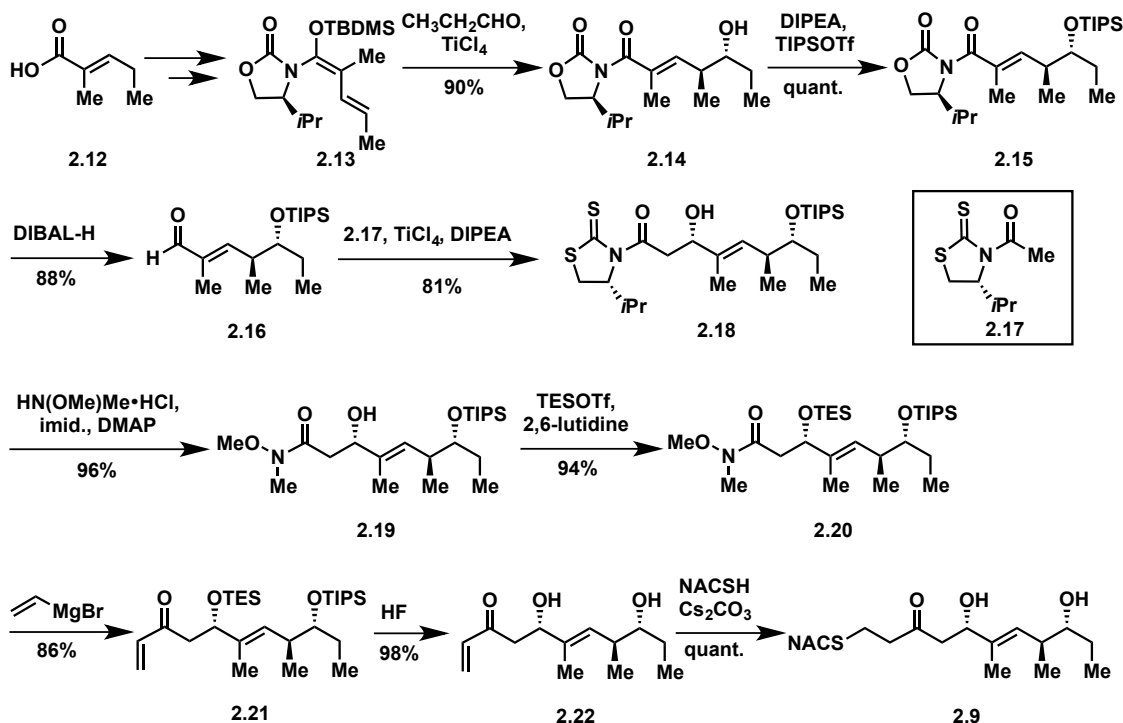
Figure 2.3. Native and synthetic TyIKR3 substrates with their possible β -processing products. The truncated region of the native substrate (2.3) serving as the basis of substrates 2.4 and 2.5 is highlighted in blue.

2.3 Synthesis of substrate and product compounds

2.3.1 Chemical synthesis of two carbon homologue thioethers

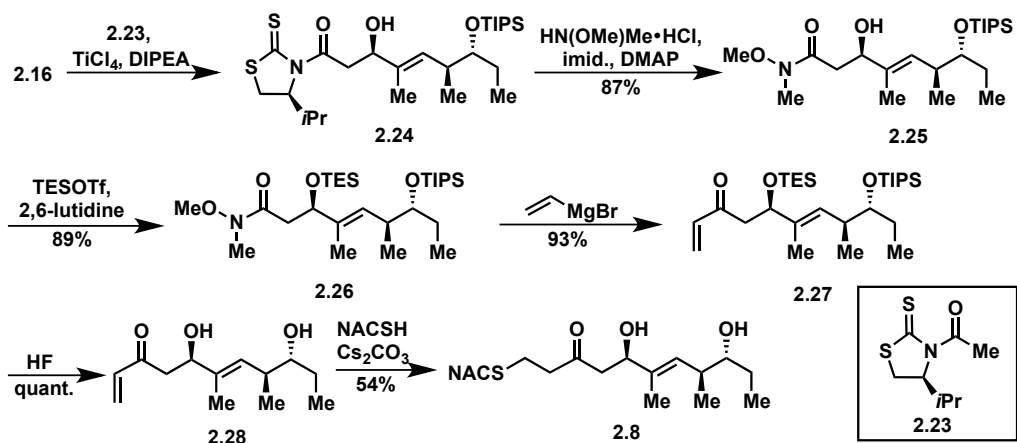
The synthesis of tetraketide substrate mimic **2.9** for TyIDH3 began with known vinylketene silyl *N,O*-acetal **2.13**, obtained in two steps from commercially available *trans*-2-methyl-2-pentenoic acid **2.12** (Scheme 2.1).³⁰ The vinylogous Mukaiyama aldol reaction of **2.13** with propionaldehyde set the two distal stereogenic centers with excellent yield and diastereoselectivity (92%, >98:2 dr), illustrating the power of Kobayashi's methodology for synthesis of this triketide building block.³⁰ The relative and absolute stereochemistry was confirmed by comparison of its NMR spectral data and optical rotation value to the reported enantiomer.³¹ The vinylogous aldol adduct **2.14** was subsequently protected as the TIPS ether **2.15** in quantitative yield and reductive removal of the oxazolidinone auxiliary with DIBAL-H provided aldehyde **2.16**.

Scheme 2.1. Synthesis of thioether **2.9**.



With the enal **2.16** in hand, we were poised to set the unknown stereochemistry of the TylKR3 reduction product. Utilization of Nagao's *N*-acetylthiazolidinethione **2.17** under titanium-catalyzed conditions developed by Vilarrasa, Urpí and coworkers furnished the D-alcohol as the only detectable diastereomer in 81% yield.^{32,33} The thiazolidinethione chiral auxiliary of **2.18** was displaced with HN(OMe)Me to afford the corresponding Weinreb amide **2.19**.³⁴ The newly formed β -hydroxyl group was protected as TES ether **2.20**. Due to susceptibility to α,β -elimination, the strength of base was crucial, as tertiary amines (TEA, DIPEA) yielded exclusively the conjugated dienamide, whereas 2,6-lutidine afforded the desired TES ether. The precise order of this two-step sequence (**2.18** \rightarrow **2.20**) was critical as reversal led to a sterically encumbered, hydroxyl-protected thiazolidine resistant to displacement. Grignard addition of vinylmagnesium bromide to Weinreb amide **2.20** provided **2.21** that was globally deprotected with HF to afford **2.22**. Regioselective Michael addition of *N*-acetylcysteamine (NAC) to the terminal enone of **2.23** produced TYLDH3 substrate mimic **2.9** containing a two-carbon spacer. The L-alcohol diastereomer **2.8** was prepared in an analogous fashion from **2.16** employing the antipode of **2.17** (**2.23**) (Scheme 2.2).

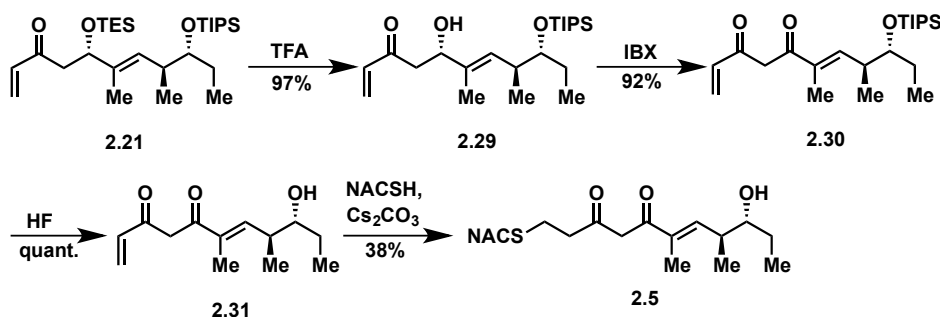
Scheme 2.2. Synthesis of enantiomeric thioether **2.8**.



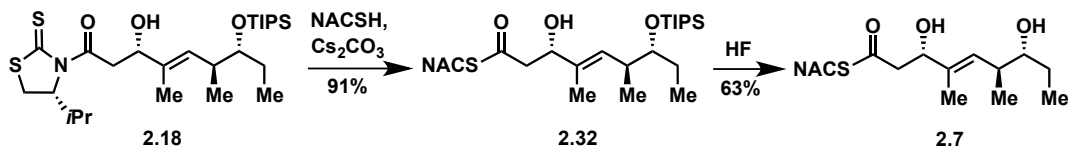
At the onset of the project we had planned to prepare the TylKR3 substrate mimic **2.5** from the corresponding TylDH3 substrate **2.9** through regioselective oxidation of the

allylic alcohol in preference to the distal secondary alcohol. Unfortunately **2.9** and its precursor **2.22** proved recalcitrant to a variety of oxidants (MnO_2 , BaMnO_4 , $\text{Pd}(\text{OAc})_2/\text{O}_2$, etc.), returning starting material or dehydration products under more forcing conditions.³⁵⁻³⁷ In light of these results, we decided to chemoselectively remove the TES protecting group in **2.21** to provide mono-protected **2.29** (Scheme 2.3). A variety of common oxidants were then screened to affect the transformation of alcohol **2.29** to the desired β -diketone **2.30** including the Dess-Martin periodinane, TPAP/NMO, and $\text{SO}_3 \cdot \text{pyr}$. Surprisingly, most common reagents led to quick decomposition of the starting material or unwanted hetero-Michael additions. A recently described β -hydroxyketone oxidation employing iodoxybenzoic acid (IBX) as the oxidant was employed as a mild, neutral method.³⁸ This procedure afforded β -diketone **2.30** in near quantitative yields after simple filtration of the sparingly soluble oxidant from the products. Facile TIPS deprotection with aqueous HF provided **2.31**, which was reacted with NAC to afford TylKR3 substrate **2.5**.

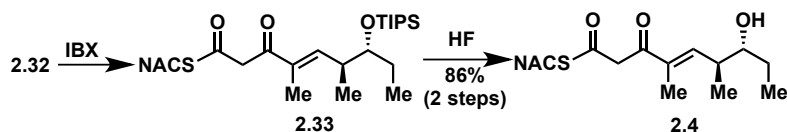
Scheme 2.3. Synthetic route to ketoreductase substrate **2.5**.



Scheme 2.4. Synthesis of thioester TylKR3 product **2.7**.



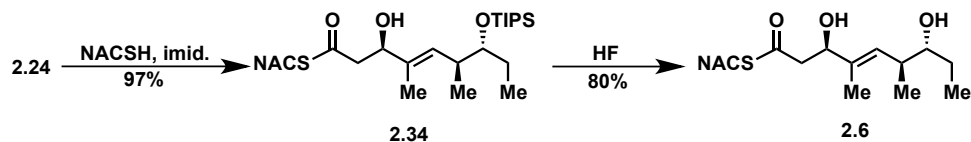
Scheme 2.5. Synthesis of thioester TylKR3 substrate **2.4**.



2.3.2 Synthesis of thioester substrates

The NAC thioester TylKR3 and TylDH3 substrates **2.4** and **2.7** were synthesized in a straightforward approach from intermediates **2.32** and **2.18**, respectively, prepared in Scheme 1. The thiazolidinethione in **2.18** was directly displaced with *N*-acetylcysteamine (NAC) yielding the β -hydroxythioester **2.32** (Scheme 2.4). TIPS deprotection with aqueous HF furnished the TylDH3 NAC thioester substrate mimic **2.7**. As anticipated, this compound displayed reasonable stability at room temperature and was stable for up to three months at 4 °C (determined by repeated ^1H -NMR). Oxidation of β -hydroxythioester **2.32** would provide the required β -ketothioester. Several reaction conditions were studied to affect this transformation and it was found, once again, that IBX afforded near quantitative yield of **2.33** (Scheme 2.5). TIPS deprotection promoted by aqueous HF yielded TylKR3 NAC thioester substrate mimic **2.4**. β -Hydroxy thioester **2.6**, the C-2 epimer of compound **2.7**, could be synthesized in a similar manner to **2.7** (Scheme 2.6).

Scheme 2.6. Synthesis of thioester substrate **2.6**.

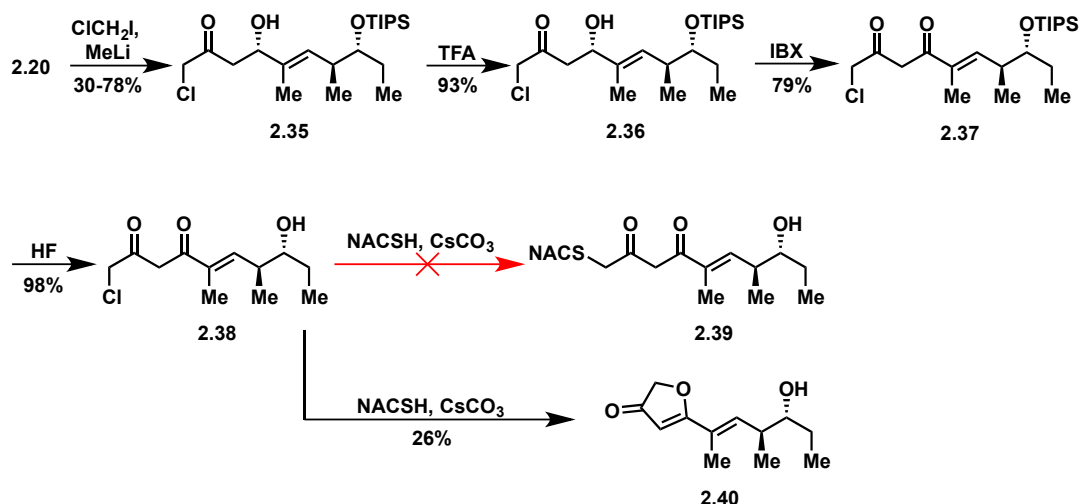


2.3.3 Unsuccessful synthesis of one-carbon homologs of the TylKR3 substrate.

We had initially planned to make one-carbon extended thioether substrate analogs for the tylosin module 3 ketoreductase. This would allow us to assess the intermediary change

between the two-carbon analog (**2.5**) and the thioester (**2.4**) to determine if an optimal length could be obtained. The synthetic route, utilizing common Weinreb (**2.2**) amide, closely parallels that of **2.5** (**Scheme 2.7**). Careful addition of MeLi to a cooled solution of the Weinreb amide and ClCH₂I furnished chloromethyl ketone **2.35** in variable yields (30-78%). Selective TES deprotection and oxidation were carried out in a similar fashion as previous syntheses. Reaction of the fully deprotected product **2.38** with HSNAC yielded one product in moderate conversion by TLC. Surprisingly, upon isolation of the product it was discovered that the product was devoid of the characteristic *N*-acetylcysteamine peaks predicted for thioether **2.39**. Careful ¹H-NMR analysis of the product revealed formation of a new alkene-singlet peak. We rationalized that a cyclization of the keto-enol tautomer occurred during the course of the reaction forming enone **2.40**. In retrospect, this result is not unexpected, as several instances of this transformation have been reported to date in the literature.^{39,40} Attempts to slow the cyclization by reducing the temperature (-20, 0 °C) or the equivalents of base (0.5, 0.1 equiv) either only slowed the formation of the undesired product or led to an increase in recovered starting material. Although the thiol (pKa 7) is expected to act as a better acid than the diketone (pKa 9) the undesired product is the result of an intramolecular reaction, outpacing the desired intermolecular reaction. Attempts to preform the thiol anion (*n*BuLi or Na₂CO₃) also resulted in the sole formation of the undesired furanone product. In light of these results, we decided to forgo the synthesis of TylKR3 substrate, one-carbon homologs.

Scheme 2.7. Unsuccessful synthesis of one-carbon thioether substrate.



2.4 Expression of Tylosin Module 3 β -Processing Domains.

With TylKR3 substrate mimics **2.4** and **2.5** in hand, we sought to express and purify the KR and DH domains of Tyl module 3. By sequence alignment to structurally characterized domains^{8,41-43}, the sequence boundaries of the KR and DH were determined. Initial efforts to recombinantly express the mono-domain TylKR3 were hampered by poor expression levels and protein aggregation. Strategies to alleviate these issues included an increase of rare tRNA codons (Rosetta cell line), optimization of codon selection (synthetic TylKR3 gene), toxic protein-compatible expression hosts (pLysS cell line), appending a fusion protein (attempted with SUMO, mOCR, and GST), chaperone coexpression (GroEL-GroES) and truncations of both N- and C-termini. Disappointingly, these techniques failed to improve expression of soluble non-aggregated TylKR3 and forced us to abandon the expression of the mono-domain construct. As the TylKR3 was recalcitrant to purification, our collaborators at the University of Michigan (Greg Dodge, Dr. Janet L. Smith) constructed a plasmid encoding the TylDH3-KR3 di-domain including a portion of linker between the KR and ACP domains (residues 957-1682 of tylosin PKS module 3). The didomain was stable upon purification, and used in further analysis. The molecular weight of the recombinant proteins determined by SDS-

PAGE was 76 kDa and found to be 76,265 by mass spectrometry, both consistent with the calculated value (76,511 Da).

2.5 Enzymatic Analysis of TyIDH3-KR3.

2.5.1 Analysis of ketoreductase activity

We initially attempted to characterize the activity of the TyIKR3 domain with substrates **2.4** and **2.5** in the presence of NADPH using LC-MS/MS analysis with an internal standard for rigorous quantitation and synthetic standards for product identification. Overnight incubation of the TyIDH3-KR3 di-domain with **2.4** and **2.5** afforded the D-configured reduction products **2.7** and **2.9** in relatively minor amounts, consistent with the B-type KR domain, along with the dehydration products **2.10** and **2.11** as the major species. NAC thioester **2.4** provided **2.7:2.10** in ratio of 1:22 while NAC thioether **2.5** furnished **2.9:2.11** in a ratio of 1:102 (**Figure 2.4**, panels **A** and **B**). However, the KR acted very slowly, as the total conversion in each case was less than 2% of input substrate. The combination of slow KR conversion and low KR:DH product ratio suggests that the ketoreductase product can efficiently shuttle to the dehydratase in absence of ACP tethering. It further suggests that the chemically reversible dehydration reaction is unidirectional with TyIDH3 since an unexpectedly high amount of dehydration product was formed from a freely diffusible reduction product. Unfortunately, we were unable to kinetically characterize TyIKR3 due to the slow substrate turnover.

2.5.2 Analysis of dehydratase activity

We next examined the ability of TyIDH3-KR3 to process DH substrates **2.6**, **2.7**, **2.8**, and **2.9**. Each substrate (1 mM) was individually incubated overnight with 10 μ M TyIDH3-KR3 and the reactions were analyzed by LC-MS/MS as before. The D-alcohols **2.7** and **2.9** led to nearly quantitative formation of *trans*-olefin products **2.10** and **2.11**, respectively (**Figure 2.4**, panels **C** and **D**) whereas L-alcohols **2.6** and **2.8** were not turned over by the enzyme. This further corroborates the bioinformatic prediction that the

preceding B-type TylKR3 should produce D-alcohols and is consistent with empirical observations that D-alcohols yield *trans*-olefins.^{44,45} Based on the enhanced activity of TylDH3 relative to TylKR3 we performed a large-scale incubation of **2.7** and **2.9**, and isolated **2.10** and **2.11** in 67 and 98% yield, respectively after column chromatography. The product identities were unequivocally confirmed by ¹H and ¹³C-NMR spectroscopy and exhibited nearly identical diagnostic ¹³C chemical shifts of ~147 and ~133 ppm and a ³J_{HH} coupling constant of ~ 16 Hz.

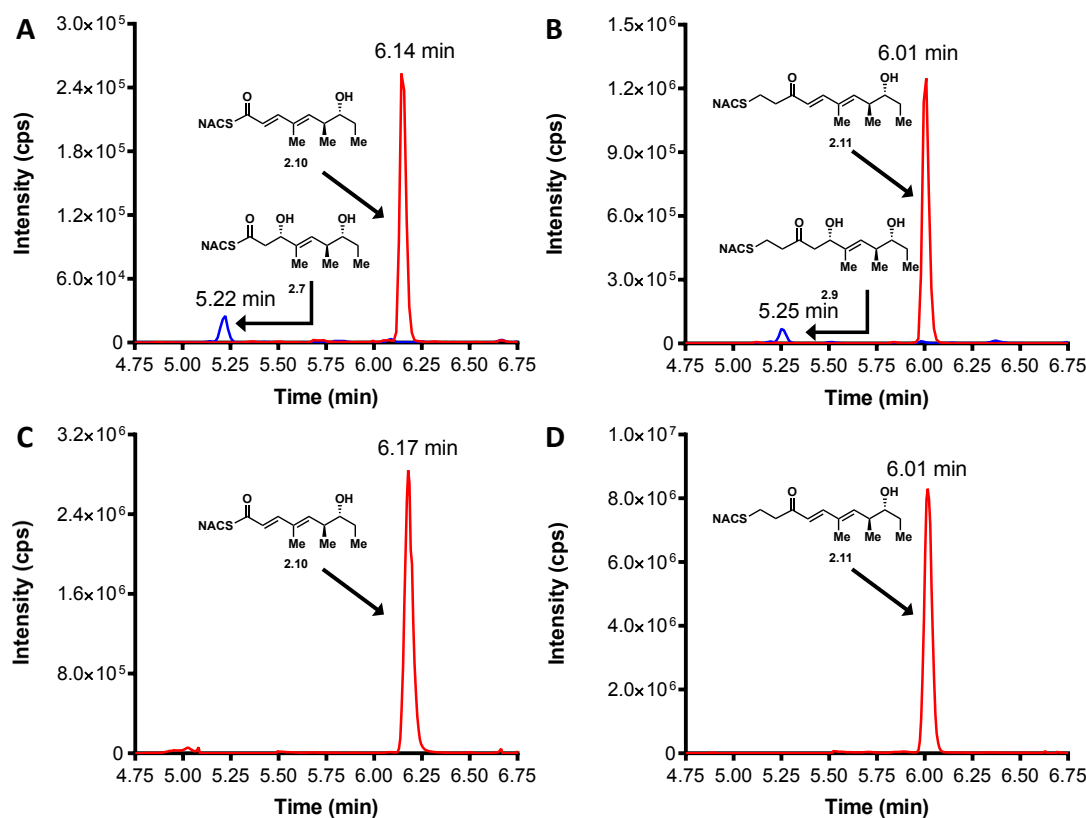
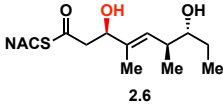
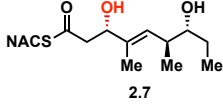
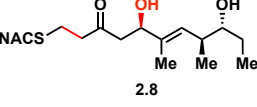
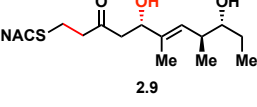
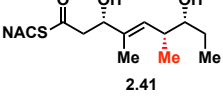
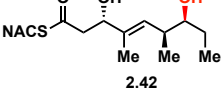
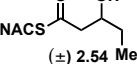


Figure 2.4. LC-MS/MS traces of *in vitro* ketoreduction and dehydration reactions. Overnight incubation conducted with KR substrates **2.4** (panel **A**) and **2.5** (panel **B**) and TyIDH3-KR3 in the presence of NADPH. The identity of the β -hydroxy products (shown in blue) was confirmed by co-injection with authentic standards. Incubation with synthetic **2.7** (panel **C**) and **2.9** (panel **D**) resulted in sole formation of dehydration products **2.10** and **2.11** (trace shown in red), respectively. Panels **A** and **C** blue trace represents MRM (m/z 340 \rightarrow 184) and red trace represents MRM (m/z 300 \rightarrow 181). Panels **B** and **D** blue trace represents MRM (m/z 368 \rightarrow 212) red trace represents MRM (m/z 328 \rightarrow 151).)

The enhanced activity of TyIDH3 domain enabled characterization by steady-state kinetic analysis. The velocity remained linear up to 10 minutes reaction time and was also linear with respect to TyIDH3-KR3 concentration from 0.25 to 1 μ M. The initial rates, v_0 at a given $[S]$ were thus determined by single-time point stopped-time incubations at 8

minutes with 0.5 μM TyIDH3-KR3. Due to the limited solubility of substrates **6b** and **7b** we were unable to reach saturation, consequently the plots of initial velocity versus $[S]$ were fit by linear regression analysis to determine the specificity constants ($k_{\text{cat}}/K_{\text{M}}$). Thioester **2.7** and thioether **2.9** displayed specificity constants of 908 ± 30 and $410 \pm 20 \text{ min}^{-1} \text{ M}^{-1}$, respectively (**Table 2.1** and **Figure 2.5** (panels **A** and **B**)). The modest 2.5-fold difference in $k_{\text{cat}}/K_{\text{M}}$ indicates thioethers are well tolerated, validating their use as stabilized forms of substrates otherwise prone to nonproductive, intramolecular cyclization.

Table 2.1. Steady-state kinetic analysis of TyIDH3 substrates.

cmpd#	DH Substrate	$k_{\text{cat}}/K_{\text{M}}, \text{min}^{-1} \text{ M}^{-1}$
2.6		$<10^{\text{a}}$
2.7		980 ± 30
2.8		$<10^{\text{a}}$
2.9		410 ± 20
2.41		22 ± 2
2.42		72 ± 6
(\pm) 2.54		$<10^{\text{a}}$

^abelow the limit of detection (LOD) of products in LC-MS/MS.

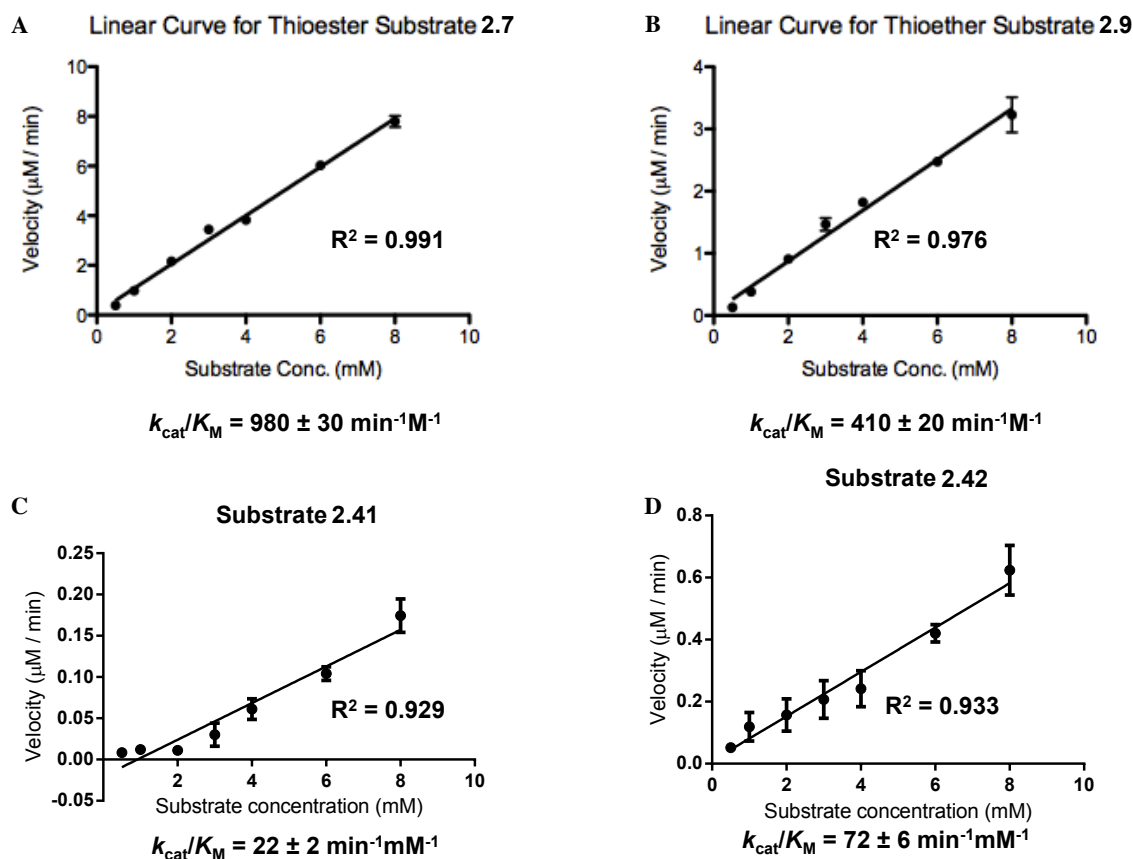


Figure 2.5. Linear regression analysis of TyIDH3KR3 kinetic data with substrates **2.7**, **2.9**, **2.41**, and **2.42**. The kinetic plots of thioester **2.7**, thioether **2.9**, thioester **2.41** and thioester **2.42** are shown in panels **A**, **B**, **C** and **D**, respectively. Represented data is the result of duplicate LC-MS/MS data normalized with controls lacking enzyme. Specificity constants (k_{cat}/K_M) for each substrate are displayed below the corresponding plot.

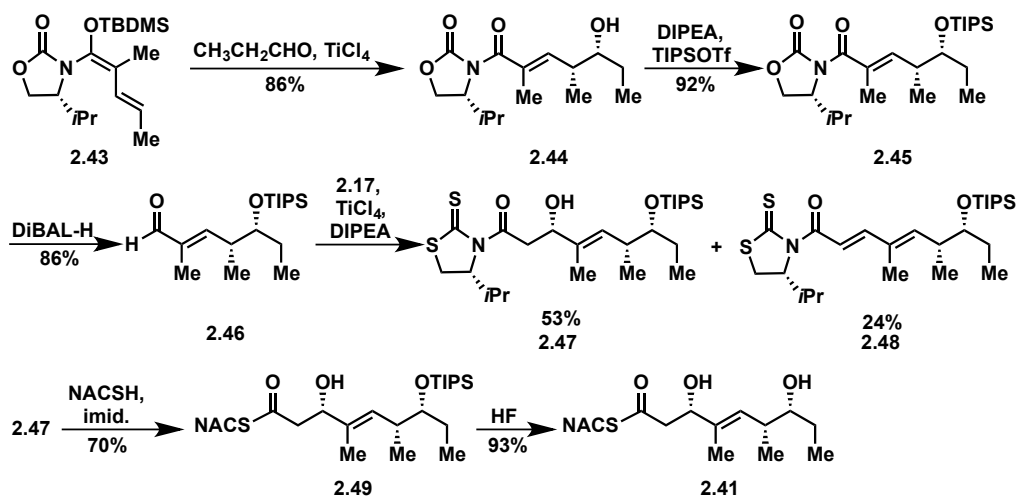
2.6 Synthesis and Activity of Epimeric DH Substrates

To explore the impact of remote stereocenters on processing by TyIDH3 we synthesized full-length tetraketide NAC thioesters **2.41** and **2.42**, epimeric at the ϵ - and ζ -stereocenters, respectively (**Schemes 2.8** and **2.9**). The syntheses closely followed that of previous TyIDH3 substrates except in regards to the use of Hosokawa's modified vinylogous aldol conditions for obtaining syn-aldol products.⁴⁶ The serendipitous

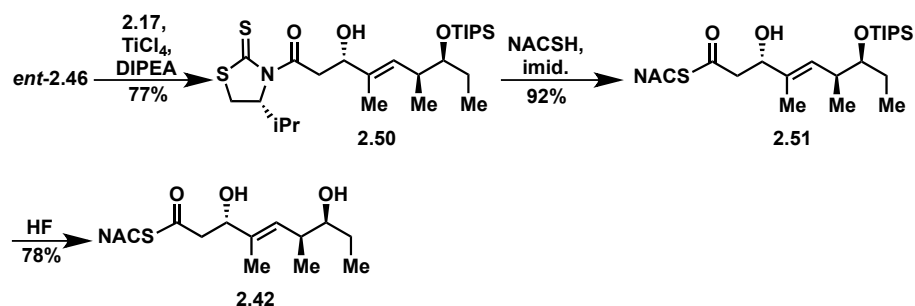
formation of dehydration product **2.48** during the extended aldol reaction served to provide a route to the dehydration product (**2.53**) for an authentic LC-MS/MS standard (Scheme 2.10).

With the epimers in hand, we kinetically evaluated the TyIDH3 in a similar manner as we had done with **2.7** and **2.9**. The specificity constant for **2.41** was $22 \pm 2 \text{ min}^{-1} \text{ M}^{-1}$, which is 45-fold less than **2.7** (Table 1, Figure 2.5 (panel C)). Although **2.41** only differs from **2.7** via inversion of the ϵ -methyl group, we expect the trisubstituted olefin may enhance the 1,3-allylic ($A^{1,3}$) strain and more severely impact the side chain conformation, potentially contributing to the drastic attenuation in k_{cat}/K_M . Boddy and co-workers also invoked $A^{1,3}$ strain to rationalize substrate tolerance in their work on PKS thioesterases.⁴⁷ We next evaluated the ζ -epimer **2.42**, whose specificity constant was $72 \pm 6 \text{ min}^{-1} \text{ M}^{-1}$, approximately 14-fold less than **2.7** (Figure 2.5 (panel D)). Since inversion of the ζ -stereocenter is not expected to significantly alter the substrate conformation, we speculate that the ζ -hydroxyl group may be important for substrate recognition that is otherwise dominated by hydrophobic interactions of this nonpolar substrate. To complete our substrate specificity studies, we also evaluated diketide (\pm)-**2.54**, but it was not processed, highlighting the significance of using full-length substrates.²⁹

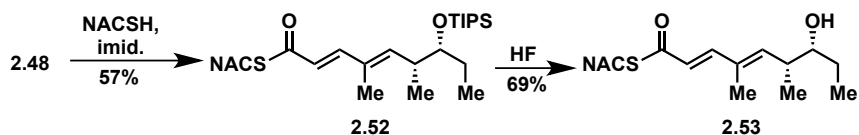
Scheme 2.8. Synthetic route towards dehydratase substrate **2.41**.



Scheme 2.9. Synthesis of substrate **2.42**.



Scheme 2.10. Synthetic route towards authentic product standard **2.53**.



2.7. Tylosin Module 3 Summary

The use of full-length, diffusible tetraketide probes allowed for systematic analysis of the module 3 processing domains of tylosin: TylKR3 and TylDH3. The TylKR3 domain was weakly active and produced D-alcohols stereoselectively, further confirming the accuracy of existing bioinformatic approaches.^{17,23} In contrast, the TylDH3 domain proved robust in its production of *trans*-olefins allowing for the chemoenzymatic synthesis of dehydration products. Dehydratase substrate specificity in relation to each stereocenter was independently determined through steady-state kinetic analysis via LC-MS/MS detection revealing unpredicted biases for the native substrate. TylDH3 did not tolerate β -stereochemistry inversion, and epimerization of distal stereocenters attenuated the activity by 14-45 fold when compared to the native substrate. This finding was rationalized through recognition of allylic A^{1,3} strain within the molecule and the potential electrostatic and/or hydrogen bonding interactions of the distal hydroxyl moiety. The distant elements of the substrate were necessary for activity as truncated substrate (\pm)-**2.54** was not dehydrated by TylDH3. Additionally, thioethers proved to be stable

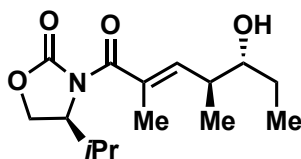
thioester surrogates.

This work highlights the *in vitro* use of di-domains in the study of cryptic processes as potential solutions for insoluble and/or unreactive domains. The ACP domain has been largely assumed to control the flow of intermediates throughout the reductive progression of domains towards the ultimate module product.⁴⁸⁻⁵⁰ Unexpectedly, we discovered that tylosin module 3 funnels diffusible substrates from ketoreductase to dehydratase independent of ACP tethering. The exact mechanism of this observed phenomenon remains to be determined and could involve the proximity of the KR product exit and DH substrate entrance, thereby increasing the local concentration of DH substrate. Alternatively, a conformational change prior to or upon substrate release from the ketoreductase may draw the two catalytic sites together, leading to the observed shuttling process. Our results are consistent with structures of the pikromycin module 5 in which the ACP localization was determined by the tethered acyl group.^{51,52}

The finding that the distal stereochemical fidelity of preceding modules can be closely regulated by dehydratase activity via a stringently stereospecific process may have far-reaching implications in the fields of natural product isolation and synthetic biology. Specifically, this research directly supports the hypothesis that tightly controlled relative and absolute polyketide stereochemistry may not necessitate the action of exquisitely stereoselective domains but, instead, be the consequence of iterative, stereospecific checkpoints or gatekeeper domains. Stalled chain intermediates have been previously shown to be hydrolyzed by downstream TE domains, freeing a non-productive, immature polyketide acid and phosphopantetheine-ACP arm for productive product formation.⁵³⁻⁵⁵ Interestingly, our work suggests that the dehydratase domain, which removes stereochemical information via elimination of water, can additionally enrich the final product optical purity. As the dehydratase-catalyzed syn-elimination of water is the only β -processing domain to require a specific, two-centered tetrahedral substrate conformation, it may be naturally sensitive to the local stereochemical features of the substrate.

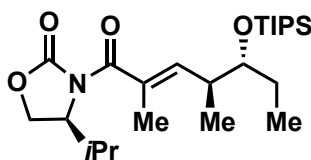
2.8 Chemistry experimental section

General Chemistry Procedures. All chemical reagents were used as provided unless explicitly indicated otherwise. Tetrahydrofuran (THF) and dichloromethane (CH₂Cl₂) were purified via passage through alumina columns. All reactions were performed under anhydrous argon atmosphere using oven-dried (150 °C) glassware. Reaction mixtures were stirred magnetically using oven-dried magnetic stir bars. Compound purification via flash chromatography utilized silica gel (300–400 mesh) in the indicated solvent system. TLC was performed using 250 μ m, F₂₅₄ silica gel plates and visualized UV and *para*-anisaldehyde stain. A Rudolph Autopol III polarimeter at the indicated temperature using the sodium D line (λ = 589 nm) unless otherwise specified and reported as follows: $[\alpha]_D^{temp}$ = rotation (*c* g/100 mL, solvent). ¹H and ¹³C NMR spectra were recorded on a Bruker 400 spectrometer at 400 Hz for ¹H NMR and at 100 Hz for ¹³C NMR. Chemical shifts are reported in ppm based on an internal standard of residual CHCl₃ (7.26 ppm in ¹H NMR and 77.16 in ¹³C NMR). Proton chemical data are reported in the following format: chemical shift (ppm) (multiplicity (s = singlet, d = doublet, t = triplet, q = quartet, quin = quintet, sextet = sextet, sept = septet, m = multiplet, br = broad peak), *J* = coupling constant (Hz), integration). High-resolution mass spectra (HRMS) were obtained on a Bruker BioTOF II ESI-TOF/MS using either PEG or PPG standards as high-resolution calibrants.



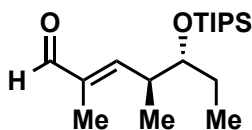
(S)-3-((4S,5R,E)-5-Hydroxy-2,4-dimethylhept-2-enoyl)-4-isopropylloxazolidin-2-one (2.14). Freshly distilled propionaldehyde⁵⁶ (4.93 mL, 68.3 mmol, 2.00 equiv) in anhydrous CH₂Cl₂ (120 mL) was placed in dry ice-acetone bath (-78 °C) and allowed to equilibrate. To the cooled solution was added TiCl₄ (3.77 mL, 34.2 mmol, 1 equiv). To the resulting yellow reaction mixture was slowly added the vinylketene silyl *N,O*-acetal **2.13**³¹ (11.6 g, 34.2 mmol, 1.00 equiv) as a solution in CH₂Cl₂ (45 mL). The reaction

quickly adopted a dark red hue. Following completion of addition, the reaction mixture was transferred to a dry ice-MeCN bath (-40 °C) and stirred for 21 h. The reaction mixture was quenched upon treatment with saturated aqueous Rochelle's salt, followed by saturated aqueous sodium bicarbonate solutions at -40 °C. The cloudy, white mixture was allowed to warm to room temperature and stirred for 1 h. The resulting biphasic solution was separated and the aqueous layer was extracted with CH₂Cl₂ (3 × 75.0 mL) and EtOAc (3 × 75.0 mL). The combined organic solutions were dried over Na₂SO₄, filtered, and concentrated under reduced pressure. The resulting crude oil was dry-loaded onto silica column and purified by flash chromatography (30% EtOAc/hexanes) to afford the title compound (8.76 g, 30.9 mmol, 90%) as a viscous, slightly yellow oil. TLC: R_f = 0.20 (20% EtOAc/hexanes); $[\alpha]_D^{23}$ = 28.3 (c 1.00, CHCl₃); ¹H NMR (CDCl₃, 400 MHz) δ 5.82 (d, J = 10.4 Hz, 1H), 4.58 (dt, J = 8.8, 4.8 Hz, 1H), 4.34 (t, J = 8.8 Hz, 1H), 4.18 (dd, J = 7.2, 7.6 Hz, 1H), 3.32–3.25 (m, 1H), 3.08 (br s, 1H), 2.63–2.52 (m, 1H), 2.38–2.28 (m, 1H), 1.94 (s, 3H), 1.76–1.64 (m, 1H), 1.44 (app. sept, J = 7.6 Hz, 1H), 1.01 (t, J = 7.2 Hz, 3H), 0.98 (d, J = 7.2 Hz, 3H), 0.95–0.89 (m, 6H); ¹³C NMR (CDCl₃, 100 MHz) δ 171.7, 154.7, 142.5, 131.2, 76.7, 63.6, 58.3, 39.9, 28.6, 26.8, 18.0, 16.3, 15.4, 14.1, 10.1; HRMS (ESI-TOF) m/z : $[M + Na]^+$ Calcd for C₁₅H₂₄NO₄Na 306.1676, found 306.1673.



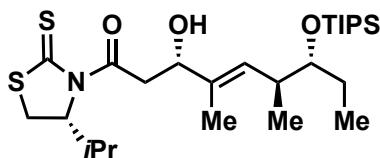
(S)-3-((4S,5R,E)-2,4-Dimethyl-5-((triisopropylsilyl)oxy)-hept-2-enoyl)-4-isopropylloxazolidin-2-one (2.15). A solution containing the aldol adduct **2.14** (0.889 g, 3.14 mmol, 1.00 equiv) in CH₂Cl₂ (24.0 mL) was cooled in an ice-water bath. To the chilled, colorless solution was added *i*-Pr₂NEt (0.655 mL, 3.76 mmol, 1.20 equiv) followed by TIPSOTf (1.01 mL, 3.76 mmol, 1.20 equiv). The resulting solution was stirred at 0° C for 1 h and transferred to a refrigerator (3-5° C) for 24 h. The clear yellow solution was quenched upon addition of saturated aqueous NaHCO₃ solution (12.0 mL) at 0° C, and

allowed to warm to room temperature over 20 min. The biphasic mixture was separated, and the aqueous layer was extracted with CH₂Cl₂ (4 × 20.0 mL). The combined organic layers were dried (Na₂SO₄), filtered, and concentrated under reduced pressure. The product residue was purified by flash chromatography (10% EtOAc/hexanes) to afford the title compound (1.3805 g, 3.14 mmol, quant.) as a transparent, colorless oil. TLC: R_f = 0.68 (20% EtOAc/hexanes); $[\alpha]_D^{21}$ = 29.5 (c 1.00, CHCl₃); ¹H NMR (CDCl₃, 400 MHz) δ 6.19 (dd, J = 9.6, 1.2 Hz, 1H), 4.50 (ddd, J = 9.2, 5.6, 4.4 Hz, 1H), 4.29 (t, J = 8.8 Hz, 1H), 4.14 (dd, J = 9.2, 6.0 Hz, 1H), 3.73 (ddd, J = 5.2, 2.4, 7.6 Hz, 1H), 2.72 (ddq, 9.6, 6.8, 2.4 Hz, 1H), 2.42–2.30 (m, 1H), 1.92 (d, J = 1.2 Hz, 3H), 1.63–1.48 (m, 2H), 1.10–1.04 (m, 24H), 0.90 (t, J = 7.2 Hz, 6H), 0.86 (t, J = 7.6 Hz, 3H); ¹³C NMR (CDCl₃, 100 MHz) δ 172.4, 153.8, 141.1, 130.6, 77.8, 63.4, 58.4, 37.0, 28.3, 18.5, 18.4, 18.0, 16.7, 15.1, 13.7, 13.2, 10.5; HRMS (ESI-TOF) m/z : $[M + Na]^+$ Calcd for C₂₄H₄₅NO₄Na 462.3010, found 462.3019.



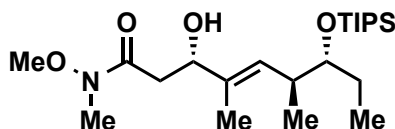
(4*S*,5*R*,*E*)-2,4-Dimethyl-5-((triisopropylsilyl)oxy)hept-2-enal (2.16). A solution of imide **2.15** (3.185 g, 7.24 mmol, 1.00 equiv) in anhydrous dichloromethane (229 mL) was equilibrated in dry ice-acetone bath (-78 °C) under argon atmosphere. To the stirred solution was added DIBAL-H (1.49 M in toluene, 9.73 mL, 14.5 mmol, 2.00 equiv) in a dropwise fashion over 2 min. The reaction mixture was allowed to stir at -78 °C for 14 min then quenched upon successive addition of MeOH (15.0 mL) and saturated aqueous sodium potassium tartrate (15.0 mL). The resulting mixture was allowed to warm to room temperature and stirred vigorously for 14 h. The biphasic solution was separated and the aqueous layer was extracted with CH₂Cl₂ (3 × 100 mL). Combined organic extracts were dried over Na₂SO₄, filtered and concentrated under vacuum. The crude oil was purified by flash chromatography (10% EtOAc/hexanes) furnishing the title compound (1.98 g, 6.34 mmol, 88%) as a clear, colorless oil. TLC: R_f = 0.52 (10% EtOAc/hexanes); $[\alpha]_D^{23}$ =

−4.3 (*c* 1.00, CHCl₃); ¹H NMR (CDCl₃, 400 MHz) δ 9.40 (s, 1H), 6.59 (d, *J* = 10.0 Hz, 1H), 3.78 (app. quin, *J* = 4.0 Hz, 1H), 2.89 (ddq, *J* = 10.0, 6.8, 3.2 Hz, 1H), 1.76 (s, 3H), 1.65–1.54 (m, 1H), 1.41 (app. sept, *J* = 7.6 Hz, 1H), 1.12 (d, *J* = 7.2 Hz, 3H), 1.08 (s, 21H), 0.86 (t, *J* = 7.6 Hz, 3H); ¹³C NMR (CDCl₃, 100 MHz) δ 195.8, 156.8, 139.1, 77.4, 37.7, 28.6, 18.4, 16.9, 13.1, 9.9, 9.6; HRMS (ESI-TOF) *m/z*: [M + Na]⁺ Calcd for C₁₈H₃₆O₂SiNa 335.2377, found 335.2372.

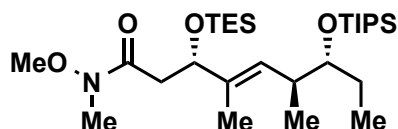


(3*S*,6*S*,7*R*,*E*)-3-Hydroxy-1-((*R*)-4-isopropyl-2-thioxo-thiazolidin-3-yl)-4,6-dimethyl-7-((triisopropylsilyl)-oxy)non-4-en-1-one (2.18). A CH₂Cl₂ (19.6 mL) solution of acetylthiazolidinone **2.17** (1.07 g, 5.26 mmol, 1.70 equiv) was cooled to −40 °C (dry ice-MeCN) under inert, argon atmosphere. To the chilled, yellow solution was added TiCl₄ (0.611 mL, 5.57 mmol, 1.80 equiv) resulting in a sudden color change to bright orange. The reaction mixture was stirred for 30 min. Slow addition of freshly distilled *i*PrNEt⁵⁶ (0.970 mL, 5.57 mmol, 1.80 equiv) over 3 min caused a dramatic color change to blood red. The enolate solution was stirred for 2 h 12 min while maintaining an external temperature of −40 °C. The reaction was cooled to −78 °C and aldehyde **2.16** (0.967 g, 3.09 mmol, 1.00 equiv) was slowly added over the course of 1 min as a solution in CH₂Cl₂ (3.87 mL) and stirred for 5 h. The resulting red-orange mixture was quenched via addition of saturated aqueous NH₄Cl (10.0 mL) at −78 °C. The biphasic solution was allowed to warm to room temperature and the layers were separated. The aqueous layer was extracted with CH₂Cl₂ (3 × 15 mL) and the combined organic layers were dried over Na₂SO₄, filtered and concentrated under reduced pressure. The resulting clear, golden oil was purified by flash chromatography (20% EtOAc/hexanes) affording the title compound (1.29 g, 2.50 mmol, 81%) as a bright yellow, viscous oil. TLC: *R_f* = 0.29 (20% EtOAc/hexanes); [α]_D²² = −219.0 (*c* 1.00, CHCl₃); ¹H NMR (400 MHz, CDCl₃) δ 5.51 (d, *J* = 9.6 Hz, 1H), 5.15 (app. t, *J* = 6.8 Hz, 1H), 4.58 (dd, *J* = 8.8, 3.2 Hz, 1H), 3.66 (dt, *J* =

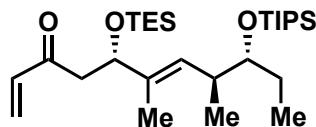
6.4, 3.2 Hz, 1H), 3.56–3.44 (m, 3H), 3.03 (d, J = 11.6 Hz, 1H), 2.63–2.55 (m, 1H), 2.38 (app. sextet, J = 7.2 Hz, 1H), 1.68 (s, 3H), 1.52–1.40 (m, 2H), 1.07 (s, 24H), 0.99 (d, J = 2.4, 3H), 0.98 (d, J = 2.4, 3H), 0.85 (t, J = 7.2 Hz, 3H); ^{13}C NMR (CDCl_3 , 100 MHz) δ 203.1, 173.0, 135.2, 129.1, 77.7, 73.4, 71.7, 44.3, 36.6, 31.0, 30.8, 27.6, 19.3, 18.5, 17.9, 16.9, 13.2, 12.6, 10.5; HRMS (ESI-TOF) m/z : $[\text{M} + \text{Na}]^+$ Calcd for $\text{C}_{26}\text{H}_{49}\text{NO}_3\text{S}_2\text{SiNa}$ 538.2815, found 538.2815.



(3*S*,6*S*,7*R*,*E*)-3-Hydroxy-*N*-methoxy-*N*,4,6-trimethyl-7-((triisopropylsilyl)oxy)non-4-enamide (2.19). To a bright yellow CH_2Cl_2 (2.00 mL) solution of acyl thiazolidinethione **2.18** (0.203 g, 0.390 mmol, 1.00 equiv) was added imidazole (0.133 g, 1.95 mmol, 5.00 equiv) followed by $\text{HN}(\text{OMe})\text{Me}\cdot\text{HCl}$ (95.0 mg, 0.980 mmol, 2.50 equiv). A catalytic amount of DMAP (one grain) was added to the final mixture. The reaction was stirred 20 h at room temperature and quenched via addition of saturated aqueous NH_4Cl (2.00 mL). The biphasic mixture was separated and the aqueous layer was extracted with CH_2Cl_2 (4 \times 10.0 mL). The combined organic layers were dried over Na_2SO_4 , filtered and concentrated under reduced pressure. The crude residue was purified by flash chromatography (30% EtOAc/hexanes) providing the title compound (0.155 g, 0.372 mmol, 96%) as a slightly yellow, clear, viscous oil. TLC: R_f = 0.34 (40% EtOAc/hexanes); $[\alpha]_D^{21}$ = -35.1 (c 1.00, CHCl_3); ^1H NMR (400 MHz, CDCl_3) δ 5.49 (d, J = 9.6 Hz, 1H), 4.45 (dd, J = 8.0, 4.4 Hz, 1H), 3.69 (s, 3H), 3.68–3.63 (m, 1H), 3.20 (s, 3H), 2.68–2.56 (m, 3H), 1.69 (s, 1H), 1.47 (dq, J = 7.6, 6.8 Hz, 2H), 1.07 (s, 21H), 0.99 (d, J = 6.8 Hz, 3H), 0.85 (t, J = 7.6 Hz, 3H); ^{13}C NMR (CDCl_3 , 100 MHz) δ 173.9, 135.4, 128.5, 77.8, 73.4, 61.4, 37.2, 36.6, 32.0, 27.4, 18.4, 16.8, 13.1, 12.6, 10.5; HRMS (ESI-TOF) m/z : $[\text{M} + \text{Na}]^+$ Calcd for $\text{C}_{22}\text{H}_{45}\text{NO}_4\text{SiNa}$ 438.3010, found 438.3009.

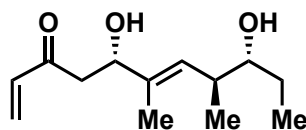


(3*S*,6*S*,7*R*,*E*)-*N*-Methoxy-*N*,4,6-trimethyl-3-((tri-ethylsilyl)oxy)-7-((triisopropylsilyl)oxy)non-4-enamide (2.20). To a reaction flask containing β -hydroxy amide **2.19** (0.345 g, 0.829 mmol, 1.00 equiv) dissolved in CH_2Cl_2 (15 mL) in ice-water bath (0 °C) was added 2,6-lutidine (0.387 mL, 3.32 mmol, 4.00 equiv). The resulting basic solution was supplemented with TESOTF (0.375 mL, 1.66 mmol, 2.00 equiv) and stirred for 1.5 h. The reaction was terminated via the sequential addition of MeOH (3 mL) followed by saturated aqueous NaHCO_3 (5.00 mL) at 0 °C. The biphasic mixture was warmed to room temperature, separated, and the aqueous fractions were extracted with CH_2Cl_2 (4 \times 10.0 mL). The combined organic fractions were dried over anhydrous sodium sulfate, filtered and concentrated under reduced pressure. The resulting crude oil was purified by flash chromatography (10% EtOAc/hexanes) affording the title compound (0.411 g, 0.776 mmol, 94%) as a clear, slightly yellow oil. TLC: R_f = 0.61 (20% EtOAc/hexanes); $[\alpha]_D^{23}$ = -20.6 (c 1.00, CHCl_3); ^1H NMR (400 MHz) δ 5.45 (d, J = 9.6 Hz, 1H), 4.58 (dd, J = 8.8, 4.4 Hz, 1H), 3.70 (s, 3H), 3.65 (dt, J = 6.8, 2.8 Hz, 1H), 3.17 (s, 3H), 2.94–2.80 (m, 1H), 2.56 (ddq, J = 9.6, 6.8, 2.8 Hz, 1H), 2.31 (dd, J = 14.0, 4.4 Hz, 1H), 1.64 (s, 3H), 1.52–1.39 (m, 2H), 1.08 (s, 21H), 0.96 (d, J = 6.8 Hz, 3H), 0.91 (t, J = 8.0 Hz, 9H), 0.85 (t, J = 7.6 Hz, 3H), 0.56 (q, J = 8.0 Hz, 6H); ^{13}C NMR (CDCl_3 , 100 MHz) δ 172.3, 136.8, 128.0, 78.0, 75.5, 61.5, 39.7, 36.6, 32.1, 27.6, 18.4, 16.7, 13.1, 11.7, 10.8, 7.0, 4.9; HRMS (ESI-TOF) m/z : $[\text{M} + \text{Na}]^+$ Calcd for $\text{C}_{28}\text{H}_{59}\text{NO}_4\text{Si}_2\text{Na}$ 552.3875, found 552.3882.



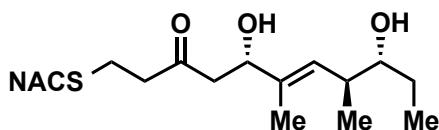
(5*S*,8*S*,9*R*,*E*)-6,8-Dimethyl-5-((triethylsilyl)oxy)-9-((triisopropylsilyl)oxy)undeca-1,6-dien-3-one (2.21). A reaction vessel containing Weinreb amide **2.20** (0.237 g, 0.448 mmol, 1.00 equiv) in THF (32.0 mL) was placed in ice-water bath (0 °C) and allowed to equilibrate. To the chilled, clear solution was added solution of vinylmagnesium bromide

(1.0 M in THF, 1.44 mL, 1.44 mmol, 3.20 equiv). The reaction mixture was stirred at 0 °C for 4 h. An additional aliquot of vinylmagnesium bromide (0.450 mL, 0.450 mmol, 1.00 equiv) was added and the reaction mixture was stirred for 1 h prior to quenching with saturated aqueous NH₄Cl (10.0 mL). The biphasic mixture was allowed to warm to room temperature, separated and the aqueous layer was extracted with CH₂Cl₂ (3 × 15.0 mL). The combined organic layers were dried over Na₂SO₄, filtered and concentrated under reduced pressure. The resulting crude oil was purified by flash chromatography (5% EtOAc/hexanes) yielding the title compound (0.192 g, 0.387 mmol, 86%) as a clear, colorless oil. TLC: *R*_f = 0.38 (5% EtOAc/hexanes); [α]_D²² = −20.7 (*c* 0.978, CHCl₃); ¹H NMR (400 MHz) δ 6.36 (dd, *J* = 17.6, 10.8 Hz, 1H), 6.20 (d, *J* = 17.6 Hz, 1H), 5.82 (d, *J* = 10.8 Hz, 1H), 5.43 (d, *J* = 9.2 Hz, 1H), 4.54 (dd, *J* = 8.4, 4.4 Hz, 1H), 3.64 (dt, *J* = 6.9, 2.6 Hz, 1H), 2.94 (dd, *J* = 14.0, 8.5 Hz, 1H), 2.63–2.42 (m, 2H), 1.63 (s, 3H), 1.52–1.35 (m, 2H), 1.08 (s, 21H), 0.95 (d, *J* = 6.8, 3H), 0.89 (t, *J* = 8.0 Hz, 9H), 0.85, (t, *J* = 7.4 Hz, 3H), 0.54 (q, *J* = 8.0 Hz, 6H); ¹³C NMR (CDCl₃, 100 MHz) δ 199.6, 137.6, 136.5, 128.5, 128.1, 77.9, 75.6, 47.0, 36.6, 27.6, 18.4, 13.1, 11.6, 10.8, 7.0, 6.0, 4.9; HRMS (ESI-TOF) *m/z*: [M + Na]⁺ Calcd for C₂₈H₅₆O₃Si₂Na 519.3660, found 519.3647.



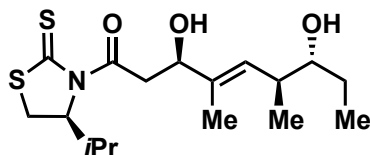
(5*S*,8*S*,9*R*,*E*)-5,9-Dihydroxy-6,8-dimethylundeca-1,6-dien-3-one (2.22). To a polypropylene tube (15 mL, BD Falcon™) containing silylether **2.21** (29.8 mg, 0.0600 mmol, 1.00 equiv) was added MeCN (3.00 mL) and magnetic stir bar. The mixture was stirred in ice-water bath (0 °C) until a homogenous solution was obtained. A solution of 48% aqueous HF–MeCN (11:89, 8.36 mL) was slowly added to the reaction vessel. The resulting clear solution was stirred vigorously for 1 h and placed in a refrigerator (4 °C) for 15 h. The reaction was quenched at 0 °C via dropwise addition of a saturated aqueous NaHCO₃ solution until the pH was 7. The neutralized solution was extracted with EtOAc (4 × 15.0 mL). All organic fractions were combined, dried over Na₂SO₄, filtered and concentrated under reduced pressure. The crude residue was purified by flash column

chromatography (5% MeOH/CH₂Cl₂) affording the title compound (13.3 mg, 0.586 mmol, 98%) as a clear, colorless oil. TLC: R_f = 0.30 (5% MeOH/CH₂Cl₂); $[\alpha]_D^{21}$ = -37.2 (c 0.26, CHCl₃); ¹H NMR (400 MHz) δ 6.37 (dd, J = 17.6, 10.3 Hz, 1H), 6.26 (dd, J = 17.7, 1.0 Hz, 1H), 5.90 (dd, J = 11.4, 1.0 Hz, 1H), 5.38 (d, J = 9.9 Hz, 1H), 4.52 (dd, J = 7.3, 4.7 Hz, 1H), 3.32 (ddd, J = 8.4, 6.4, 3.6 Hz, 1H), 2.99 (br s, 1H), 2.86–2.80 (m, 2H), 2.53–2.41(m, 1H), 1.69 (d, J = 1.2 Hz, 3H), 1.62–1.53 (m, 2H), 1.45–1.33 (m, 1H), 0.97 (t, J = 7.4 Hz, 3H), 0.96 (d, J = 6.8 Hz, 3H); ¹³C NMR (CDCl₃, 100 MHz) δ 201.0, 137.6, 136.9, 129.5, 128.4, 77.0, 73.0, 44.6, 38.1, 27.1, 17.2, 13.0, 10.2; HRMS (ESI-TOF) m/z : $[M + Na]^+$ Calcd for C₁₃H₂₂O₃Na 249.1461, found 249.1466.



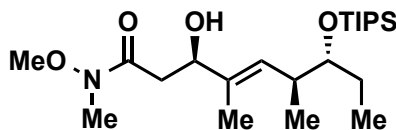
***N*-(2-(((5*S*,8*S*,9*R*,*E*)-5,9-Dihydroxy-6,8-dimethyl-3-oxoundec-6-en-1-yl)thio)ethyl)-acetamide (2.9).** A reaction flask containing vinyl ketone **2.22** (3.9 mg) in THF (5.0 mL) was supplemented with *N*-acetylcysteamine (2.0 μ L, 0.019 mmol, 1.1 equiv). To the resulting clear solution was added a catalytic amount of Cs₂CO₃ and the resulting reaction mixture was stirred for 5 h at ambient temperature under argon atmosphere. The reaction was quenched upon addition of a saturated, aqueous NH₄Cl solution (5.0 mL). The biphasic mixture was separated and the aqueous layer was extracted with EtOAc (8 \times 10 mL). The combined organic fractions were dried over Na₂SO₄, filtered and concentrated under reduced pressure. The crude residue was purified by flash chromatography with a small CuSO₄-impregnated silica gel plug (2.0 cm thick) on top (eluent = 10% MeOH/CH₂Cl₂) furnishing the title compound (5.9 mg, 0.017 mmol, quant.) as a colorless, translucent oil. TLC: R_f = 0.13 (5% MeOH/CH₂Cl₂); $[\alpha]_D^{21}$ = -24.9 (c 0.38, CHCl₃); ¹H NMR (400 MHz) δ 6.11 (s, 1H), 5.36 (d, J = 9.9 Hz, 1H), 4.48 (dd, J = 8.5, 3.4 Hz, 1H), 3.43 (app. q, J = 6.1 Hz, 2H), 3.37–3.24 (m, 1H), 2.86–2.58 (m, 8H), 2.49–2.39 (m, 1H), 1.99 (s, 3H), 1.66 (d, J = 1.0 Hz, 3H), 1.61–1.52 (m, 1H), 1.44–1.32 (m, 1H), 0.99–0.93 (m, 6H); ¹³C NMR (CDCl₃, 100 MHz) δ 209.4, 170.5, 137.5, 128.4,

77.1, 73.1, 48.2, 43.8, 38.7, 38.0, 32.2, 27.2, 25.2, 23.4, 17.2, 13.0, 10.2; HRMS (ESI-TOF) m/z : $[M + Na]^+$ Calcd for $C_{17}H_{31}NO_4SNa$ 368.1866, found 368.1872.

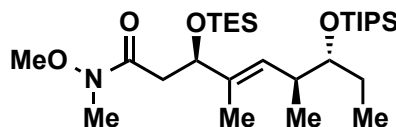


(3R,6S,7R,E)-3-Hydroxy-1-((S)-4-isopropyl-2-thioxo-thiazolidin-3-yl)-4,6-dimethyl-7-((triisopropylsilyl)-oxy)non-4-en-1-one (2.24). A reaction vessel containing thiazolidinethione **2.23** (91.9 mg, 0.452 mmol, 1.50 equiv) in CH_2Cl_2 (3.00 mL) was cooled in ice-water bath (0 °C). To the chilled, bright yellow solution was added $TiCl_4$ (55.0 μ L, 0.503 mmol, 1.67 equiv) resulting in a color change to red-orange. The reaction was stirred for 5 min, then placed in dry ice–acetone bath (-78 °C) and allowed to equilibrate. To the chilled reaction mixture was added freshly distilled iPr_2NEt (87.6 μ L, 0.503 mmol, 1.67 equiv) dropwise over 4 min causing a sudden color change to blood red. The solution was stirred at -78 °C for 2 h. To the enolate solution was added aldehyde **2.16** (94.0 mg, 0.301 mmol, 1.00 equiv) as a solution in anhydrous CH_2Cl_2 (11.00 mL) over the course of 6 min. The reaction mixture was stirred at -78 °C for an additional 6 h and quenched upon addition of saturated, aqueous NH_4Cl (5.00 mL). The biphasic solution was warmed to ambient temperature, separated and the aqueous layer extracted with dichloromethane (4 \times 10.0 mL). The combined, organic fractions were dried over Na_2SO_4 , filtered and concentrated under reduced pressure. Purification by flash chromatography (20% EtOAc/hexanes) provided the title compound (0.106 mg, 0.205 mmol, 68%) as a yellow, viscous oil. TLC: R_f = 0.31 (20% EtOAc/hexanes); $[\alpha]_D^{22}$ = 217.2 (c 1.00, $CHCl_3$); 1H NMR (400 MHz) δ 5.51 (d, J = 9.5 Hz, 1H), 5.15 (t, J = 6.5 Hz, 1H), 4.58 (d, J = 9.3 Hz, 1H), 3.65 (br s, 1H), 3.56–3.38 (m, 3H), 3.03 (d, J = 11.5 Hz, 1H), 2.58 (br, 1H), 2.45–2.32 (m, 1H), 1.67 (s, 3H), 1.54–1.35 (m, 2H), 1.07 (app. s, 24H), 0.97 (t, J = 6.0 Hz, 6H), 0.84 (t, J = 7.0 Hz, 3H); ^{13}C NMR ($CDCl_3$, 100 MHz) δ 203.1, 173.0, 135.1, 129.3, 77.7, 77.4, 73.5, 71.7, 44.2, 36.6, 31.0, 27.7, 19.3, 18.5, 18.0, 17.0, 13.2, 12.4, 10.4; HRMS (ESI-TOF) m/z : $[M + Na]^+$ Calcd for $C_{26}H_{49}NO_3S_2SiNa$

538.2815, found 538.2821.

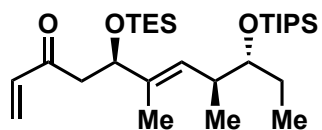


(3R,6S,7R,E)-3-Hydroxy-N-methoxy-N,4,6-tri-methyl-7-((triisopropylsilyl)oxy)non-4-enamide (2.25). To a reaction vessel containing acyl thiazolidinethione **2.24** (0.298 g, 0.578 mmol) in CH₂Cl₂ (3.00 mL) was sequentially added imidazole (0.197 g, 2.89 mmol, 5.00 equiv) and HN(OMe)Me•HCl (0.141 g, 1.45 mmol, 2.50 equiv). The reaction mixture was stirred at ambient temperature under argon atmosphere for 16 h and quenched upon addition of a saturated, aqueous NH₄Cl (4.00 mL). The biphasic solution was separated and the aqueous layer was extracted with CH₂Cl₂ (3 × 7.00 mL). Combined organic fractions were dried over Na₂SO₄, filtered, concentrated under reduced pressure and purified by flash chromatography (40% EtOAc/hexanes) yielding the title compound (0.208 g, 0.501 mmol, 87%) as a slightly yellow, clear oil. TLC: *R_f* = 0.37 (40% EtOAc/hexanes); $[\alpha]_D^{23} = 26.3$ (*c* 1.00, CHCl₃); ¹H NMR (400 MHz) δ 5.48 (d, *J* = 9.6 Hz, 1H), 4.47–4.41 (m, 1H), 3.67 (s, 3H), 3.66–3.60 (m, 2H), 3.19 (s, 3H), 2.69–2.51 (m, 3H), 1.67 (s, 3H), 1.52–1.36 (m, 2H), 1.06 (s, 21H), 0.99 (d, *J* = 6.9 Hz, 3H), 0.84 (t, *J* = 7.4 Hz, 3H); ¹³C NMR (CDCl₃, 100 MHz) δ 173.9, 135.4, 129.8, 77.8, 73.6, 61.4, 37.3, 36.6, 32.0, 27.6, 18.4, 17.0, 13.1, 12.3, 10.4; HRMS (ESI-TOF) *m/z*: [M + Na]⁺ Calcd for C₂₂H₄₅NO₄SiNa 438.3010, found 438.3010.



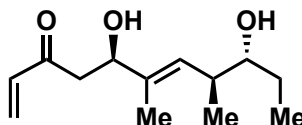
(3R,6S,7R,E)-N-Methoxy-N,4,6-trimethyl-3-((tri-ethylsilyl)oxy)-7-((triisopropylsilyl)oxy)non-4-enamide (2.26). To a flask containing β-hydroxy amide **2.25** (79.0 mg, 0.190 mmol) under argon atmosphere in an ice-water bath (0 °C) was added CH₂Cl₂ (3.5 mL). The resulting clear solution was supplemented with 2,6-lutidine (89.0 μL, 0.761

mmol, 4.00 equiv) and TESOTf (86.0 μ L, 0.380 mmol, 2.00 equiv). The reaction mixture was stirred at 0 $^{\circ}$ C for 2.5 h and quenched upon sequential addition of MeOH (2.00 mL) and saturated, aqueous NaHCO₃ (2.00 mL). The biphasic solution was warmed to ambient temperature and the layers were separated. The aqueous layer was extracted with CH₂Cl₂ (3 \times 10.0 mL) and the combined organic fractions were dried over Na₂SO₄, filtered and concentrated under reduced pressure. The crude residue was purified by flash chromatography (10-20% EtOAc/hexanes) affording the title compound (89.3 mg, 0.169 mmol, 89%) as a transparent, clear oil. TLC: R_f = 0.58 (20% EtOAc/hexanes); $[\alpha]_D^{22}$ = 9.7 (c 1.00, CHCl₃); ¹H NMR (400 MHz) δ 5.45 (d, J = 9.5 Hz, 1H), 4.59 (dd, J = 8.8, 4.5 Hz, 1H), 3.70 (s, 3H), 3.61 (dt, J = 6.5, 2.8 Hz, 1H), 3.16 (s, 3H), 2.99–2.80 (m, 1H), 2.60–2.50 (m, 1H), 2.31 (dd, J = 13.9, 4.3 Hz, 1H), 1.64 (d, J = 1.1 Hz, 3H), 1.49–1.34 (m, 2H), 1.07 (s, 21H), 1.00 (d, J = 6.9 Hz, 3H), 0.91 (t, J = 7.9 Hz, 9H), 0.82 (t, J = 7.4 Hz, 3H), 0.56 (q, J = 7.9 Hz, 6H); ¹³C NMR (CDCl₃, 100 MHz) δ 136.7, 128.2, 77.8, 75.6, 61.4, 39.5, 36.7, 32.1, 27.5, 18.5, 16.5, 13.1, 11.4, 10.7, 6.9, 4.9 (missing amide carbonyl carbon); HRMS (ESI-TOF) m/z : [M + Na]⁺ Calcd for C₂₈H₅₉NO₄Si₂Na 552.3875, found 552.3905.



(5R,8S,9R,E)-6,8-Dimethyl-5-((triethylsilyl)oxy)-9-((triisopropylsilyl)oxy)undeca-1,6-dien-3-one (2.27). To a reaction vessel containing Weinreb amide **2.26** (37.6 mg, 0.0710 mmol) under argon atmosphere was added THF (5.00 mL). The resulting clear solution was cooled with ice-water bath (0 $^{\circ}$ C). A solution of vinylmagnesium bromide (1.00 M) (0.224 mL, 0.224 mmol, 3.16 equiv) was added to the stirred solution. After 3 h, the reaction was quenched at 0 $^{\circ}$ C via addition of saturated, aqueous NH₄Cl (5.00 mL) and allowed to warm to ambient temperature. The biphasic solution was separated and the aqueous layer was repeatedly extracted with EtOAc (3 \times 10 mL). The combined organic layers were dried over Na₂SO₄, filtered and concentrated under vacuum. Purification of the crude residue by flash chromatography (5% EtOAc/hexanes) furnished

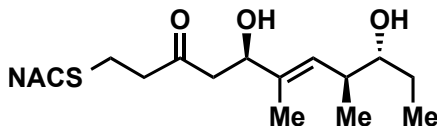
the title compound (32.7 mg, 0.658 mmol, 93%) as a clear, light yellow oil. TLC: R_f = 0.45 (5% EtOAc/hexanes); $[\alpha]_D^{22}$ = 7.6 (c 1.00, CHCl_3); ^1H NMR (400 MHz) δ 6.35 (dd, J = 17.6, 10.5 Hz, 1H), 6.19 (d, J = 17.6 Hz, 1H), 5.81 (d, J = 10.5 Hz, 1H), 5.42 (d, J = 9.6 Hz, 1H), 4.55 (dd, J = 8.3, 4.7 Hz, 1H), 3.69–3.52 (m, 1H), 2.94 (dd, J = 14.0, 8.4 Hz, 1H), 2.58–2.47 (m, 2H), 1.62 (s, 3H), 1.50–1.30 (m, 2H), 1.07 (s, 21H), 0.99 (d, J = 6.9 Hz, 3H), 0.89 (t, J = 7.9 Hz, 9H), 0.81 (t, J = 7.4 Hz, 3H), 0.54 (q, J = 7.9 Hz, 6H); ^{13}C NMR (CDCl_3 , 100 MHz) δ 199.4, 137.6, 136.4, 128.4 (2), 77.8, 75.8, 46.9, 36.6, 27.6, 18.4, 16.6, 13.2, 11.3, 10.6, 7.0, 4.9; HRMS (ESI-TOF) m/z : $[\text{M} + \text{Na}]^+$ Calcd for $\text{C}_{28}\text{H}_{56}\text{NO}_3\text{Si}_2\text{Na}$ 519.3660, found 519.3674.



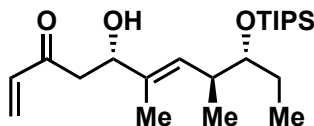
(5R,8S,9R,E)-5,9-Dihydroxy-6,8-dimethylundeca-1,6-dien-3-one (2.28). Disilylether **2.27** (10.9 mg, 0.220 mmol) was transferred to a small polypropylene tube (15 mL, BD FalconTM) and cooled via ice-water bath (0 °C). Compound **2.27** was dissolved in MeCN

(1.00 mL) and to the resulting clear solution was added a solution of 48% HF–MeCN (11:89, 3.2 mL). The reaction mixture was placed in a refrigerator (4 °C) for 19 h and quenched via addition of an aqueous, saturated NH_4Cl until the mixture was neutralized ($\text{pH} = 7$). Extraction of the reaction mixture with EtOAc (4×15.0 mL), drying over Na_2SO_4 , filtration and concentration under reduced pressure gave a crude product residue. Purification by flash chromatography (50% EtOAc/hexanes) provided the title compound (4.97 mg, 0.220 mmol, quant.) as a cloudy, colorless oil. TLC: R_f = 0.33 (50% EtOAc/hexanes); $[\alpha]_D^{21}$ = 25.6 (c 0.87, CHCl_3); ^1H NMR (400 MHz) δ 6.37 (dd, J = 17.6, 10.4 Hz, 1H), 6.26 (d, J = 17.6 Hz, 1H), 5.90 (d, J = 10.4 Hz, 1H), 5.37 (d, J = 10.0 Hz, 1H), 4.53 (dd, J = 8.4, 4.0 Hz, 1H), 3.34–3.27 (m, 1H), 2.88 (dd, J = 8.4, 16.8 Hz, 1H), 2.80 (dd, J = 16.8, 4.4 Hz, 1H), 2.52–2.38 (m, 1H), 1.69 (s, 3H), 1.61–1.51 (m, 1H), 1.43–1.31 (m, 1H), 0.97 (d, J = 6.8 Hz, 3H), 0.97 (t, J = 7.6 Hz, 3H); ^{13}C NMR (CDCl_3 , 100 MHz) δ 200.8, 137.4, 136.8, 129.5, 129.0, 77.1, 73.2, 44.7, 38.1, 27.2, 17.2, 12.6, 10.2;

HRMS (ESI-TOF) m/z : $[M + Na]^+$ Calcd for $C_{13}H_{22}O_3Na$ 249.1461, found 249.1463.

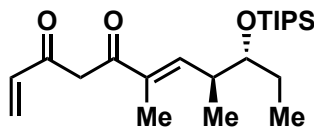


***N*-(2-(((5*R*,8*S*,9*R*,*E*)-5,9-Dihydroxy-6,8-dimethyl-3-oxoundec-6-en-1-yl)thio)ethyl)-acetamide (2.8).** To a small round bottom flask containing vinyl ketone **2.28** (26.0 mg, 0.115 mmol) in THF (9.00 mL) under argon atmosphere was added *N*-acetylcysteamine (14.6 μ L, 0.138 mmol, 1.20 equiv). A catalytic amount of CS_2CO_3 was added to the reaction mixture and the solution was stirred at ambient temperature for 11 h. The reaction was concentrated under reduced pressure and purified by flash chromatography (10% MeOH/ CH_2Cl_2 , 1.00 cm plug of $CuSO_4$ -silica on top) yielding the title compound (21.4 mg, 0.0620 mmol, 54%) as a colorless, cloudy oil. TLC: R_f = 0.46 (10% MeOH/ CH_2Cl_2); $[\alpha]_D^{22}$ = 5.9 (c 0.59, $CHCl_3$); 1H NMR (400 MHz) δ 6.17 (s, 1H), 5.36 (d, J = 10.0 Hz, 1H), 4.48 (dd, J = 8.1, 3.5 Hz, 1H), 3.43 (q, J = 6.3 Hz, 2H), 3.33–3.26 (m, 1H), 2.87 (br, 1H), 2.80–2.74 (m, 4H), 2.74–2.58 (m, 4H), 2.49–2.38 (m, 1H), 1.99 (s, 3H), 1.81 (s, 1H), 1.65 (s, 3H), 1.61–1.50 (m, 1H), 1.36 (dq, J = 14.1, 7.4 Hz, 1H), 0.96 (d, J = 7.4 Hz, 3H), 0.95 (t, J = 7.7 Hz, 3H); ^{13}C NMR ($CDCl_3$, 100 MHz) δ 209.1, 170.5, 137.4, 128.9, 77.4, 73.2, 48.4, 43.6, 38.7, 38.0, 32.2, 27.3, 25.2, 23.4, 17.3, 12.6, 10.2; HRMS (ESI-TOF) m/z : $[M + Na]^+$ Calcd for $C_{17}H_{31}NO_4SNa$ 368.1866, found 368.1873.



(5*S*,8*S*,9*R*,*E*)-5-Hydroxy-6,8-dimethyl-9-((triisopropylsilyl)-oxy)undeca-1,6-dien-3-one (2.29). To a reaction vessel containing disilylether **2.21** (39.3 mg, 0.0792 mmol) in a mixture of tetrahydrofuran (1.98 mL) and deionized water (0.296 mL) was added TFA (15.6 μ L, 0.210 mmol, 2.65 equiv). The acidic solution was stirred for 2.5 h at ambient temperature and carefully neutralized upon addition of a saturated, aqueous $NaHCO_3$

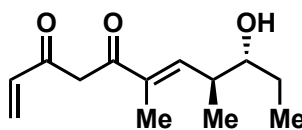
solution. The biphasic solution was separated and the aqueous layer repeatedly extracted with EtOAc (4 × 7.00 mL). The combined organic layers were dried over Na₂SO₄, filtered and concentrated under reduced pressure. The crude product was purified by flash column chromatography (10% EtOAc/hexanes) producing the title compound (29.5 mg, 0.0771 mmol, 97%) as a light yellow, clear oil. TLC: R_f = 0.25 (10% EtOAc/hexanes); $[\alpha]_D^{24}$ = -23.0 (c 1.00, CHCl₃); ¹H NMR (400 MHz) δ 6.37 (dd, J = 17.7, 10.4 Hz, 1H), 6.25 (d, J = 16.6 Hz, 1H), 5.89 (d, J = 10.4 Hz, 1H), 5.48 (d, J = 9.6 Hz, 1H), 4.52 (dd, J = 9.1, 2.8 Hz, 1H), 3.65 (dt, J = 6.2, 3.3 Hz, 1H), 2.87 (dd, J = 16.8, 9.2 Hz, 1H), 2.75 (dd, J = 16.8, 3.1 Hz, 1H), 2.62–2.54 (m, 1H), 1.68 (d, J = 1.3 Hz, 3H), 1.54–1.40 (m, 2H), 1.07 (s, 21H), 0.97 (d, J = 6.9 Hz, 3H), 0.85 (t, J = 7.5 Hz, 3H); ¹³C NMR (CDCl₃, 100 MHz) δ 201.1, 136.9, 135.3, 129.2, 128.9, 77.8, 73.3, 44.8, 36.6, 27.6, 18.5, 16.9, 13.2, 12.5, 10.5; HRMS (ESI-TOF) m/z : [M + Na]⁺ Calcd for C₂₂H₄₂O₃SiNa 405.2795, found 405.2795.



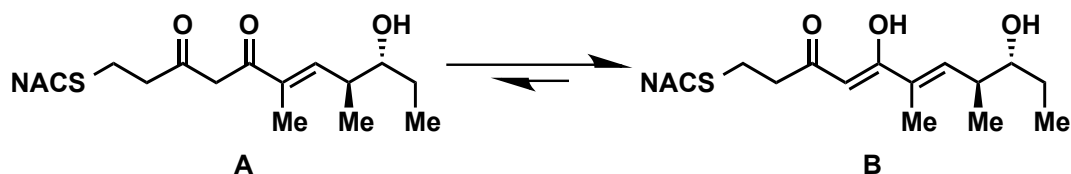
(8*S*,9*R*,*E*)-6,8-Dimethyl-9-((triisopropylsilyl)oxy)undeca-1,6-diene-3,5-dione (2.30).

To a small flask containing β -hydroxy ketone **2.29** (80.0 mg, 0.209 mmol) in EtOAc (10.0 mL) was added IBX (0.390 g, 0.627 mmol, 3.00 equiv, 45% w/w). The white, cloudy solution was rapidly stirred and heated at reflux for 2 h. The slightly yellow solution was cooled to ambient temperature and concentrated under reduced pressure. The resulting concentrated solution was purified by flash chromatography (5% EtOAc/hexanes) affording the title compound (72.4 mg, 0.190 mmol, 92%) as a red-orange oil. TLC: R_f = 0.36 (5% EtOAc/hexanes); $[\alpha]_D^{21}$ = -47.2 (c 1.00, CHCl₃); ¹H NMR (400 MHz) δ 15.46 (s, 1H), 6.71 (dd, J = 9.9, 1.0 Hz, 1H), 6.25 (dd, J = 17.2, 2.0 Hz, 1H), 6.17 (dd, J = 9.9, 17.2 Hz, 1H), 5.89 (s, 1H), 5.64 (dd, J = 9.9, 2.0 Hz, 1H), 3.75 (ddd, J = 7.8, 4.6, 3.6 Hz, 1H), 2.81–2.72 (m, 1H), 1.87 (d, J = 1.1 Hz, 3H), 1.63–1.52 (m, 1H), 1.49–1.37 (m, J = 14.9, 7.4 Hz, 1H), 1.09–1.07 (m, 24H), 0.86 (t, J = 7.5 Hz,

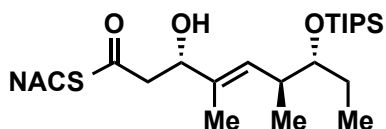
3H); ^{13}C NMR (CDCl_3 , 100 MHz) δ 193.1, 176.5, 143.0, 134.4, 133.3, 124.5, 96.6, 77.6, 37.8, 28.4, 18.4, 16.9, 13.2, 11.9, 10.0; HRMS (ESI-TOF) m/z : $[\text{M} + \text{Na}]^+$ Calcd for $\text{C}_{22}\text{H}_{40}\text{O}_3\text{SiNa}$ 403.2639, found 403.2646.



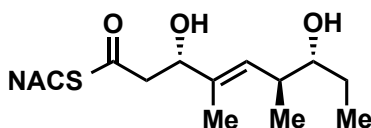
(8*S*,9*R*,*E*)-9-Hydroxy-6,8-dimethylundeca-1,6-diene-3,5-dione (2.31). To a polypropylene tube (15 mL, BD FalconTM) containing silylether **22** (72.4 mg, 0.140 mmol) was added MeCN (1.23 mL). The clear solution was equilibrated in ice-water bath (0 °C) for 10 min. A pre-chilled solution of 48% HF–MeCN (11:89, 9.84 mL) was slowly added to the rapidly stirred solution. The resulting slightly yellow solution was placed in refrigerator (4 °C) for 40 h. The reaction mixture was quenched via slow neutralization with aqueous, saturated NaHCO_3 solution at 0 °C. The aqueous layer was extracted with EtOAc (5 \times 20.0 mL) and the combined organic layers were concentrated under reduced pressure. The product was placed under high vacuum for 2 h furnishing the title compound (42.6 mg, 0.190 mmol, quant.) as a viscous, yellow oil. TLC: R_f = 0.20 (20% EtOAc/hexanes); $[\alpha]_D^{22} = -51.2$ (c 1.00, CHCl_3); (Compound **2.31** was found to exist entirely in the enol form (not drawn)) ^1H NMR (400 MHz) δ 15.54 (br s, 1H), 6.59 (dd, J = 10.0, 0.96 Hz, 1H), 6.28 (dd, J = 17.2, 2.4 Hz, 1H), 6.21 (dd, J = 17.2, 9.5 Hz, 1H) 5.90 (s, 1H), 5.66 (dd, J = 9.5, 2.4 Hz, 1H), 3.49 (dt, J = 8.8, 4.6 Hz, 1H), 2.73–2.60 (m, 1H), 1.89 (d, J = 1.0 Hz, 3H), 1.60–1.49 (m, 1H), 1.43 (dq, J = 14.2, 7.5 Hz, 1H), 1.08 (d, J = 6.7 Hz, 3H), 0.97 (t, J = 7.4 Hz, 3H); ^{13}C NMR (CDCl_3 , 100 MHz) δ 192.1, 177.7, 141.6, 135.1, 133.3, 125.0, 96.9, 76.9, 39.2, 27.9, 16.8, 12.2, 10.2; HRMS (ESI-TOF) m/z : $[\text{M} + \text{Na}]^+$ Calcd for $\text{C}_{13}\text{H}_{20}\text{O}_3\text{Na}$ 247.1305, found 247.1310.



***N*-(2-(((8*S*,9*R*,*E*)-9-Hydroxy-6,8-dimethyl-3,5-dioxoundec-6-en-1-yl)thio)ethyl)acetamide (**2.5**).** To a round bottom flask containing the vinyl ketone **2.31** (12.3 mg, 0.0550 mmol) in THF (10.0 mL) was added *N*-acetylcysteamine (6.40 μ L, 0.0600 mmol, 1.10 equiv) as a solution in anhydrous THF (64.0 μ L). The reaction mixture was supplemented with a catalytic amount of Cs_2CO_3 and stirred at ambient temperature for 4.5 h. The bright yellow, transparent solution was quenched via addition of aqueous, saturated NH_4Cl (5.00 mL) and the resulting biphasic solution was separated. The aqueous layer was repeatedly extracted with EtOAc (5×10.0 mL). Combined organic fractions were dried over anhydrous sodium sulfate, filtered and concentrated under reduced pressure. The crude residue was purified by flash chromatography (5% MeOH/ CH_2Cl_2) providing the title compound (7.2 mg, 0.021 mmol, 38%) as a viscous, bright orange oil. TLC: R_f = 0.30 (5% MeOH/ CH_2Cl_2); $[\alpha]_D^{21} = -30.0$ (c 0.46, CHCl_3); (Compound **2.5** existed in a $\sim 3:1$ mixture of enol (**B**) and keto (**A**) tautomers, respectively) ^1H NMR (400 MHz) δ 15.58 (s, 0.75H), 6.66–6.56 (m, 1H), 6.09 (br, 0.25H), 5.96 br, 0.75H), 5.80 (br s, 0.75H), 3.96 (d, $J = 14.7$ Hz, 0.25H), 3.79 (d, $J = 14.7$ Hz, 0.25H), 3.61–3.36 (m, 3H), 2.87–2.80 (m, 2H), 2.80–2.74 (m, 0.50H), 2.72–2.62 (m, 4.5H), 1.98–2.02 (m, 3H), 1.85 (d, $J = 1.2$ Hz, 2.25H), 1.81 (d, $J = 1.2$ Hz, 0.75H), 1.60–1.48 (m, 1H), 1.47–1.37 (m, 1H), 1.09 (d, $J = 6.9$ Hz, 0.75H), 1.06 (dd, $J = 6.8$ Hz, 2.25H), 1.00–0.93 (m, 3H); (Only the major (enol) tautomer **B** carbon shifts are recorded) ^{13}C NMR (CDCl_3 , 100 MHz) δ 194.8, 183.7, 170.4, 141.2, 132.2, 96.6, 76.9, 39.7, 39.1, 38.6, 32.2, 27.9, 27.2, 23.4, 16.8, 12.4, 10.2; HRMS (ESI-TOF) m/z : $[\text{M} + \text{Na}]^+$ Calcd for $\text{C}_{17}\text{H}_{29}\text{NO}_4\text{SSi}$ 366.1710, found 366.1716.

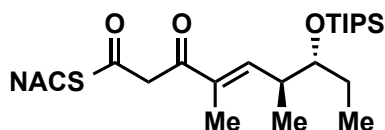


***S*-(2-Acetamidoethyl) (3*S*,6*S*,7*R*,*E*)-3-hydroxy-4,6-di-methyl-7-((triisopropylsilyl)-oxy)non-4-enethioate (2.32).** A reaction vessel containing thiazolidinethione **2.18** (0.142 g, 0.276 mmol) in CH₂Cl₂ (2.00 mL) under argon atmosphere was added imidazole (56.4 mg, 0.828 mmol, 3.00 equiv). To the clear, yellow solution was added *N*-acetylcysteamine (32.3 μL, 0.304 mmol, 1.10 equiv) and the resulting reaction mixture was stirred at ambient temperature for 14 h. The crude reaction mixture was purified by flash chromatography (5% MeOH/CH₂Cl₂) affording the title compound (0.119 g, 0.251 mmol, 91%) as a transparent, slightly yellow oil. TLC: *R_f* = 0.32 (5% MeOH/CH₂Cl₂); $[\alpha]_D^{22} = -15.0$ (*c* 1.00, CHCl₃); ¹H NMR (400 MHz) δ 5.82 (s, 1H), 5.49 (d, *J* = 9.7 Hz, 1H), 4.49 (d, *J* = 8.4 Hz, 1H), 3.65 (br s, 1H), 3.45 (q, *J* = 5.9 Hz, 2H), 3.05 (t, *J* = 6.2 Hz, 2H), 2.85 (dd, *J* = 15.0, 9.2 Hz, 1H), 2.79–2.64 (m, 1H), 2.63–2.51 (m, 1H), 2.34 (br s, 1H), 1.97 (s, 3H), 1.65 (s, 3H), 1.54–1.36 (m, 2H), 1.07 (s, 21H), 0.96 (d, *J* = 6.9 Hz, 3H), 0.84 (t, *J* = 7.3 Hz, 3H); ¹³C NMR (CDCl₃, 100 MHz) δ 199.1, 170.5, 134.9, 129.6, 77.7, 74.4, 49.8, 39.6, 36.6, 29.0, 27.6, 23.4, 18.5, 17.0, 13.2, 12.2, 10.4; HRMS (ESI-TOF) *m/z*: [M + Na]⁺ Calcd for C₂₄H₄₇NO₄SSiNa 496.2887, found 494.2896.

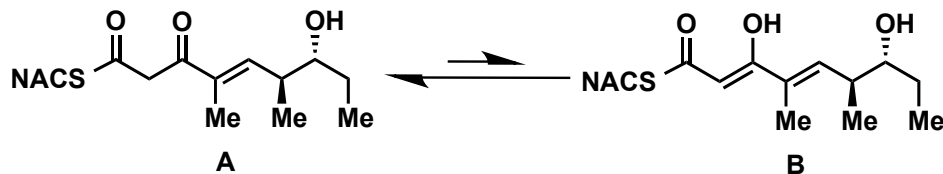


***S*-(2-Acetamidoethyl) (3*S*,6*S*,7*R*,*E*)-3,7-dihydroxy-4,6-dimethylnon-4-enethioate (2.7).** A solution of silylether **2.32** (33.4 mg, 0.0706 mmol) in MeCN (3.55 mL) in a polypropylene tube (15 mL, BD Falcon™) was cooled in ice-water bath (0 °C). To the reaction mixture was added a chilled solution of 48% HF–MeCN (11:89, 10.6 mL) and the resulting combined solution was transferred to a refrigerator for 15 h. The reaction mixture was neutralized via slow addition of a saturated, aqueous NaHCO₃ solution at 0 °C. The clear solution was extracted with EtOAc (3 × 25.0 mL). The combined organic layers were dried over Na₂SO₄, filtered and concentrated under vacuum. Flash column

chromatography (10% MeOH/CH₂Cl₂) of the crude residue produced the title compound (14.1 mg, 0.0445 mmol, 63%) as a colorless, clear oil. TLC: R_f = 0.44 (10% MeOH/CH₂Cl₂); $[\alpha]_D^{22}$ = -6.0 (c 0.51, CHCl₃); ¹H NMR (400 MHz) δ 6.16 (br s, 1H), 5.38 (d, J = 9.9 Hz, 1H), 4.46 (br s, 1H), 3.52–3.35 (m, 2H), 3.33–3.22 (m, 1H), 3.11–2.96 (m, 3H), 2.87 (dd, J = 14.7, 7.5 Hz 1H), 2.79 (dd, J = 14.5, 4.0 Hz 1H), 2.49–2.39 (m, 1H), 1.96 (s, 3H), 1.67 (s, 3H), 1.62–1.53 (m, 1H), 1.45–1.31 (m, 1H), 1.01–0.88 (m, 6H); ¹³C NMR (CDCl₃, 100 MHz) δ 199.0, 170.7, 137.2, 128.9, 77.1, 74.0, 49.3, 39.3, 38.1, 29.3, 27.2, 23.3, 17.2, 13.1, 10.1; HRMS (ESI-TOF) m/z : $[M + Na]^+$ Calcd for C₁₅H₂₇NO₄SNa 340.1553, found 340.1565.

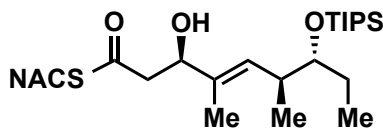


***S*-(2-Acetamidoethyl) (6*S*,7*R*,*E*)-4,6-dimethyl-3-oxo-7-((triisopropylsilyl)oxy)non-4-enethioate (2.33).** To a small round bottom flask was added β -hydroxythioester **2.32** (20.7 mmol, 0.0437 mmol) in EtOAc (2.00 mL). The colorless solution was diluted with additional EtOAc (3.00 mL) and IBX (81.8 mg, 0.131 mmol, 3.00 equiv, 45% w/w) was added. The white suspension was refluxed for 1 h. After cooling to ambient temperature, the reaction mixture was filtered through a celite pad (3.00 cm) and concentrated under reduced pressure affording the crude title compound as a yellow oil which was taken to the next step without further purification. TLC: R_f = 0.45 (5% MeOH/CH₂Cl₂).



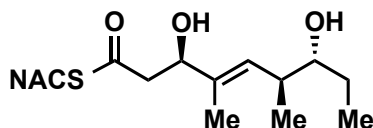
***S*-(2-Acetamidoethyl) (6*S*,7*R*,*E*)-7-hydroxy-4,6-dimethyl-3-oxonon-4-enethioate (2.4).** The crude silylether **2.33** (20.6 mg, 0.0437 mmol) was transferred as an acetonitrile

solution (0.200 mL) to a polypropylene tube (15 mL, BD Falcon™) and cooled via ice-water bath (0 °C). To the pre-chilled solution was added a 48% HF–MeCN (11:89, 2.50 mL). The reaction mixture was placed in a refrigerator (4 °C) for 24 h. TLC analysis of the reaction mixture indicated incomplete conversion and an additional portion of HF solution (freshly prepared and identical to above, 1.00 mL) was added to the reaction mixture at 0 °C. After an additional 12 h at 4 °C, the reaction mixture was neutralized at 0 °C via addition of aqueous, saturated NaHCO₃. The reaction mixture was extracted with EtOAc (4 × 25.0 mL). The combined organic fractions were dried over Na₂SO₄, filtered and concentrated under reduced pressure. The crude product was purified by column chromatography (5% MeOH/CH₂Cl₂) yielding the title compound (11.8 mg, 0.0374 mmol, 86% from **24**) as a slightly yellow oil. TLC: R_f = 0.25 (5% MeOH/CH₂Cl₂); $[\alpha]_D^{21}$ = –35.8 (c 0.79, CHCl₃); (Compound **26** exists as in equilibrium of **A** and **B** (~3:1)) ¹H NMR (400 MHz) δ 12.71 (br s, 0.25H), 6.65 (d, J = 9.8 Hz, 0.75H), 6.58 (d, J = 10.1 Hz, 0.25H), 6.24 (s, 0.75H), 6.05 (s, 0.25H), 5.66 (s, 0.25H), 4.08 (d, J = 15.0 Hz, 0.75H), 3.90 (d, J = 15.0 Hz, 0.75H), 3.59–3.33 (m, 3H), 3.13–3.00 (m, 2H), 2.74–2.59 (m, 1H), 2.02–1.91 (m, 3H), 1.85–1.78 (s, 3H), 1.58–1.34 (m, 2H), 1.09 (d, J = 6.8 Hz, 2.25H), 1.04 (d, J = 6.8 Hz, 0.75H), 1.00–0.90 (m, 3H); (Carbon shifts only given for major tautomer) ¹³C NMR (CDCl₃, 100 MHz) δ 193.8, 193.5, 170.9, 147.7, 137.3, 76.9, 53.2, 39.5, 39.2, 29.5, 28.3, 23.2, 16.8, 11.7, 10.3; HRMS (ESI-TOF) m/z : $[M + Na]^+$ Calcd for C₁₅H₂₅NO₄SSi 338.1397, found 338.1398.



***S*-(2-Acetamidoethyl) (3*R*,6*S*,7*R*,*E*)-3-hydroxy-4,6-di-methyl-7-((triisopropylsilyl)-oxy)non-4-enethioate (**2.34**).** To a reaction vessel containing acyl thiazolidinethione **2.24** (66.0 mg, 0.128 mmol) in CH₂Cl₂ (2.00 mL) was sequentially added imidazole (26.0 mg, 0.384 mmol, 3.00 equiv) and *N*-acetylcysteamine (16.0 μ L, 0.154 mmol, 1.20 equiv). The

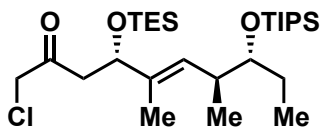
transparent, yellow solution was stirred vigorously under argon atmosphere at ambient temperature for 15 h. The reaction was quenched upon addition of aqueous, saturated NH_4Cl (3.00 mL) and the biphasic solution was separated. The aqueous layer was extracted with CH_2Cl_2 (3×10.0 mL). The combined organic layers were dried over Na_2SO_4 , filtered, concentrated under reduced pressure and purified by flash chromatography (5% $\text{MeOH}/\text{CH}_2\text{Cl}_2$) using a small plug of CuSO_4 -impregnated silica gel (1.00 cm) on top furnished the title compound (59.0 mg, 0.125 mmol, 97%) as a colorless oil. TLC: $R_f = 0.35$ (5% $\text{MeOH}/\text{CH}_2\text{Cl}_2$); $[\alpha]_D^{22} = -7.4$ (c 1.00, CHCl_3); ^1H NMR (400 MHz) δ 5.94 (br s, 1H), 5.48 (d, $J = 9.7$ Hz, 1H), 4.49 (dd, $J = 9.2, 3.4$ Hz, 1H), 3.71–3.56 (m, 1H), 3.44 (q, $J = 6.1$ Hz, 2H), 3.13–2.94 (m, 2H), 2.85 (dd, $J = 15.0, 9.2$ Hz, 1H), 2.71 (dd, $J = 14.9, 3.6$ Hz, 1H), 2.55 (ddd, $J = 9.9, 6.8, 3.2$ Hz, 1H), 2.47 (br, 1H), 1.96 (s, 3H), 1.64 (d, $J = 1.1$ Hz, 3H), 1.52–1.30 (m, 2H), 1.06 (s, 21H), 0.98 (d, $J = 6.9$ Hz, 3H), 0.82 (t, $J = 7.4$ Hz, 3H); ^{13}C NMR (CDCl_3 , 100 MHz) δ 199.0, 170.6, 134.9, 129.7, 77.7, 74.5, 49.8, 39.5, 36.5, 28.9, 27.7, 23.3, 18.4, 17.0, 13.1, 12.0, 10.4; HRMS (ESI-TOF) m/z : $[\text{M} + \text{Na}]^+$ Calcd for $\text{C}_{24}\text{H}_{47}\text{NO}_4\text{SSiNa}$ 496.2887, found 496.2881.



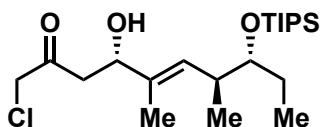
***S*-(2-Acetamidoethyl) (3*R*,6*S*,7*R*,*E*)-3,7-dihydroxy-4,6-dimethylnon-4-enethioate (2.6).**

The silylether **2.34** (40.0 mg, 0.0845 mmol) was deprotected in a manner analogous to the production of diol **6b** affording the title compound (21.5 mg, 0.678 mmol, 80%) as a clear, colorless oil. TLC: $R_f = 0.43$ (10% $\text{MeOH}/\text{CH}_2\text{Cl}_2$); $[\alpha]_D^{22} = 18.2$ (c 1.00, CHCl_3); ^1H NMR (400 MHz) δ 6.19 (br s, 1H), 5.34 (d, $J = 10.0$ Hz, 1H), 4.50 (t, $J = 6.6$ Hz, 1H), 3.48 (app. dq, $J = 12.4, 6.2$ Hz, 1H), 3.42–3.31 (m, 1H), 3.30–3.24 (m, 1H), 3.04 (t, $J = 6.2$ Hz, 2H), 2.83 (dd, $J = 6.6, 3.1$ Hz, 2H), 2.62 (br s, 1H), 2.49–2.39 (m, 1H), 1.96 (s, 3H), 1.69 (d, $J = 1.1$ Hz 3H), 1.63–1.52 (m, 1H), 1.43–1.31 (m, 1H), 0.96 (t, $J = 7.3$ Hz,

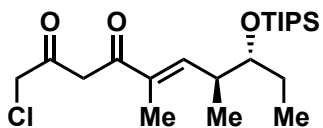
3H), 0.96 (d, $J = 6.7$ Hz, 3H); ^{13}C NMR (CDCl_3 , 100 MHz) δ 198.6, 170.7, 137.2, 129.9, 77.1, 74.5, 49.7, 39.4, 38.2, 29.3, 27.2, 23.3, 17.2, 12.2, 10.1; HRMS (ESI-TOF) m/z : $[\text{M} + \text{Na}]^+$ Calcd for $\text{C}_{15}\text{H}_{27}\text{NO}_4\text{SiNa}$ 340.1553, found 340.1554.



(4*S*,7*S*,8*R*,*E*)-1-Chloro-5,7-dimethyl-4-((triethylsilyl)oxy)-8-((triisopropylsilyl)oxy)dec-5-en-2-one (2.35). To a flask containing Weinreb amide **2.20** (0.134 g, 0.252 mmol, 1.00 equiv) in THF (4.00 mL) was added ClCH_2I (55.0 μL , 0.756 mmol, 3.00 equiv). The clear solution was cooled to -78°C (dry ice–acetone bath). To the cold solution was added MeLi (1.4M in Et_2O , 0.388 mL, 0.559 mmol, 2.20 equiv) over 35 min. The reaction mixture was stirred at -78°C for 2 h 10 min. The reaction was quenched by addition of aqueous saturated NH_4Cl (5.00 mL). The biphasic mixture was warmed to ambient temperature, separated and the aqueous layer was extracted with Et_2O (4×10 mL). The combined organic layers were dried over Na_2SO_4 , filtered and concentrated under reduced pressure. The crude material was purified by flash chromatography (5% EtOAc /hexanes) affording the title compound (0.102 g, 0.197 mmol, 78%) as a colorless oil. TLC: $R_f = 0.31$ (5% EtOAc /hexanes); $[\alpha]_D^{22} = -27.2$ (c 0.35, CHCl_3); ^1H NMR (400 MHz) δ 5.48 (d, $J = 9.6$ Hz, 1H), 4.50 (dd, $J = 8.4, 3.6$ Hz, 1H), 4.19 (d, $J = 16$ Hz, 1H), 4.13 (d, $J = 16$ Hz, 1H), 3.67–3.61 (m, 1H), 2.86 (dd, $J = 13.6, 8.8$ Hz, 1H), 2.59–2.51 (m, 1H), 2.47 (dd, $J = 14.0, 4.0$ Hz, 1H), 1.61 (s, 3H), 1.53–1.35 (m, 2H), 1.08 (s, 21H), 0.96 (d, $J = 6.8$ Hz, 3H), 0.91 (t, $J = 8.0$ Hz, 9H), 0.84 (t, $J = 7.6$ Hz, 3H), 0.56 (q, $J = 8.0$ Hz, 6H); ^{13}C NMR (CDCl_3 , 100 MHz) δ 200.9, 135.9, 128.7, 77.9, 75.6, 50.1, 47.2, 36.5, 27.8, 18.4, 16.9, 13.1, 11.7, 10.8, 6.96, 4.81; HRMS (ESI-TOF) m/z : $[\text{M} + \text{Na}]^+$ Calcd for $\text{C}_{27}\text{H}_{55}\text{ClO}_3\text{Si}_2\text{Na}$ 541.3270, found 541.3250.

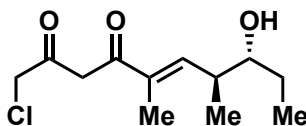


(4*S*,7*S*,8*R*,*E*)-1-Chloro-4-hydroxy-5,7-dimethyl-8-((triisopropylsilyl)oxy)dec-5-en-2-one (2.36). To a flask containing the silyl ether **2.35** (47.1 mg, 0.0908 mmol, 1.00 equiv) in THF–H₂O (6.7:1, 4.18 mL) was added dropwise TFA (17.9 μ L, 0.241 mmol, 2.65 equiv). The mixture was vigorously stirred at ambient temperature for 2 h. The reaction was quenched upon slow addition of aqueous saturated NaHCO₃ until the solution was neutral (pH = 7.0). The reaction was diluted with EtOAc–H₂O (1:1, 20.0 mL) and the biphasic solution was separated. The aqueous layer was extracted with EtOAc (4 \times 20.0 mL). The combined organic layers were dried over Na₂SO₄, filtered and concentrated under reduced pressure. The crude product residue was purified by flash chromatography (20% EtOAc/hexanes) affording the title compound (34.2 mg, 0.0844 mmol, 93%) as a faintly yellow viscous oil. TLC: R_f = 0.39 (20% EtOAc/hexanes); $[\alpha]_D^{22}$ = –23.7 (c 0.41, CHCl₃); ¹H NMR (400 MHz) δ 5.50 (d, J = 9.6 Hz, 1H), 4.51 (dd, J = 9.7, 2.8 Hz, 1H), 4.18 (d, J = 15.7 Hz, 1H), 4.13 (d, J = 15.6 Hz, 1H), 3.68–3.61 (m, 1H), 2.87 (dd, J = 16.4, 9.6 Hz, 1H), 2.70 (dd, J = 16.4, 3.2 Hz, 1H), 2.62–2.52 (m, 1H), 1.66 (d, J = 1.2 Hz, 3H), 1.55–1.36 (m, 2H), 1.07 (s, 21H), 0.97 (d, J = 7.2 Hz, 3H), 0.85 (t, J = 7.2 Hz, 3H); ¹³C NMR (CDCl₃, 100 MHz) δ 202.5, 135.2, 129.3, 77.7, 73.5, 49.1, 45.5, 36.5, 27.7, 18.5, 17.1, 13.15, 12.3, 10.4; HRMS (ESI-TOF) m/z : $[M + Na]^+$ Calcd for C₂₁H₄₁ClO₃SiNa 427.2406, found 427.2436.

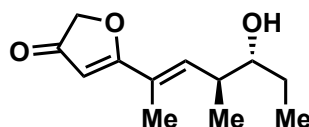


(7*S*,8*R*,*E*)-1-Chloro-5,7-dimethyl-8-((triisopropylsilyl)oxy)dec-5-ene-2,4-dione (2.37). A flask containing alcohol **2.36** (39.0 mg, 0.0960 mmol, 1.00 equiv) dissolved in EtOAc (10.0 mL) was heated to reflux (77 °C) for 48 min. The reaction was removed from heat and allowed to cool to ambient temperature. The mixture was concentrated under reduced pressure. The crude product residue was purified by flash chromatography (5%

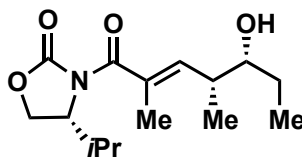
EtOAc/hexanes) affording the title compound (30.5 mg, 0.076 mmol, 79%) as a red-orange viscous oil. TLC: R_f = 0.40 (5% EtOAc/hexanes); $[\alpha]_D^{22}$ = -43.5 (c 0.43, CHCl_3); ^1H NMR (400 MHz) δ 15.3 (s, 1H), 7.81 (d, J = 9.6 Hz, 1H), 6.12 (s, 1H), 4.07 (s, 2H), 3.73–3.72 (m, 1H), 2.81–2.71 (m, 1H), 1.86 (s, 3H), 1.64–1.52 (m, 1H), 1.49–1.37 (m, 1H), 1.11–1.06 (m, 24H), 0.86 (t, J = 7.6 Hz, 3H); ^{13}C NMR (CDCl_3 , 100 MHz) δ 188.0, 186.1, 143.6, 131.3, 94.1, 45.0, 37.8, 28.4, 18.4, 16.8, 13.14, 13.13, 12.1, 9.8; HRMS (ESI-TOF) m/z : $[\text{M} + \text{Na}]^+$ Calcd for $\text{C}_{21}\text{H}_{39}\text{ClO}_3\text{SiNa}$ 425.2249, found 425.2226.



(7*S*,8*R*,*E*)-1-chloro-8-hydroxy-5,7-dimethyldec-5-ene-2,4-dione (2.38). To a polypropylene tube containing the silyl ether **2.37** (16.4 mg, 0.0410 mmol, 1.00 equiv) was added MeCN (0.300 mL). The faintly yellow solution was cooled to 0 °C (ice–water bath) and an HF–MeCN (11:89, 48% aqueous HF–MeCN, 2.11 mL) was slowly added to the solution. The reaction was placed in a refrigerator (4 °C) for 32 h. The reaction was quenched upon slow addition of aqueous saturated NH_4Cl (until pH = 7). The resulting mixture was allowed to warm to ambient temperature and supplemented with EtOAc (5.00 mL). The biphasic solution was separated and the aqueous layer was extracted with EtOAc (5 \times 10.0 mL). The combined organic layers were dried over Na_2SO_4 , filtered and concentrated under reduced pressure affording the title compound (9.80 mg, 0.0398 mmol, 98%) as a yellow oil. TLC: R_f = 0.11 (10% EtOAc/hexanes); $[\alpha]_D^{22}$ = -35.8 (c 0.59, CHCl_3); ^1H NMR (400 MHz) δ 15.26 (br s, 1H), 6.68 (dd, J = 10.0, 1.2 Hz, 1H), 6.09 (s, 1H), 4.08 (s, 2H), 3.52–3.46 (m, 1H), 2.72–2.62 (m, 1H), 1.88 (d, J = 1.6 Hz, 3H), 1.59–1.50 (m, 1H), 1.46–1.38 (m, 1H), 1.07 (d, J = 6.8 Hz, 3H), 0.97 (t, J = 7.6 Hz, 3H); ^{13}C NMR (CDCl_3 , 100 MHz) δ 189.3, 184.7, 142.3, 132.1, 94.5, 77.4, 45.3, 39.2, 27.9, 16.7, 12.4, 10.2; HRMS (ESI-TOF) m/z : $[\text{M} + \text{Na}]^+$ Calcd for $\text{C}_{12}\text{H}_{19}\text{ClO}_3\text{Na}$ 269.0915, found 269.0900.



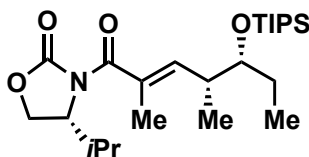
5-((4*S*,5*R*,*E*)-5-Hydroxy-4-methylhept-2-en-2-yl)furan-3(2*H*)-one (2.40). To a flask containing chloromethyl ketone **2.38** (9.80 mg, 0.0398 mmol, 1.00 equiv) in THF (5.00 mL) was added *N*-acetylcysteamine (5.00 μ L, 0.0438 mmol, 1.10 equiv). To the solution was added Cs_2CO_3 (13.0 mg, 0.0398 mmol, 1.00 equiv) portionwise over 10 min. The reaction mixture was stirred at ambient temperature for 1.5 h. The reaction was quenched by addition of aqueous saturated NH_4Cl (5.00 mL) and the resulting biphasic mixture was separated. The aqueous layer was extracted with EtOAc (4 \times 20 mL). The combined organic layers were dried over Na_2SO_4 , filtered and concentrated under reduced pressure. The crude product was purified by flash chromatography (30% EtOAc/hexanes) yielding the title compound (3.80 mg, 0.0103 mmol, 26%) as a bright yellow oil. TLC: 0.45 (30% EtOAc/hexanes; ^1H NMR (400 MHz) δ 6.59 (dd, J = 10.0, 1.2 Hz, 1H), 5.63 (s, 1H), 4.55 (s, 2H), 3.50–3.42 (m, 1H), 2.74–2.64 (m, 1H), 1.93 (d, J = 1.2 Hz, 3H), 1.59–1.48 (m, 1H), 1.46–1.37 (m, 1H), 1.08 (d, J = 6.8 Hz, 3H), 0.98 (t, J = 7.2 Hz, 3H); HRMS (ESI-TOF) m/z : $[\text{M} + \text{Na}]^+$ Calcd for $\text{C}_{12}\text{H}_{18}\text{O}_3\text{Na}$ 233.1148, found 233.1172.



(*R*)-3-((4*R*,5*R*,*E*)-5-Hydroxy-2,4-dimethylhept-2-enoyl)-4-isopropylloxazolidin-2-one (2.44). This procedure is adapted from that of Hosokawa and coworkers.⁴⁶ To a reaction vessel containing *ent*-**2.43**⁵⁷ (0.720 g, 2.12 mmol, 1.50 equiv) in CH_2Cl_2 (42.0 mL) under argon atmosphere was added freshly distilled propionaldehyde⁵⁶ (0.102 mL, 1.41 mmol, 1.00 equiv). The resulting solution was cooled to -78°C (dry ice–acetone). TiCl_4 (0.621 mL, 5.65 mmol, 4.00 equiv) was added, in one portion, to the chilled solution. The reaction mixture immediately developed a dark blue hue. The reaction was stirred at -78°C for 17 h and quenched via addition saturated aqueous NaHCO_3 (10.0 mL) and saturated aqueous potassium sodium tartrate (10.0 mL). The biphasic solution was

warmed to ambient temperature, separated and the aqueous layer was extracted with CH₂Cl₂ (3 × 20 mL). The combined organic layers were dried over Na₂SO₄, filtered and concentrated under reduced pressure. Purification by flash chromatography (30% EtOAc/hexanes) furnished the title compound (0.344 g, 1.21 mmol, 86%) as a colorless, clear oil. TLC: *R*_f = 0.26 (30% EtOAc/hexanes); $[\alpha]_D^{22} = -65.2$ (*c* 1.00, CHCl₃); ¹H NMR (400 MHz) δ 5.92 (d, *J* = 10.8 Hz, 1H), 4.56 (dt, *J* = 9.6, 5.0 Hz, 1H), 4.33 (t, *J* = 9.0 Hz, 1H), 4.18 (dd, *J* = 8.9, 5.6 Hz, 1H), 3.55 (dt, *J* = 8.8, 4.2 Hz, 1H), 2.76 – 2.64 (m, 1H), 2.40 – 2.27 (m, 1H), 1.94 (d, *J* = 1.3 Hz, 3H), 1.63–1.51 (m, 1H), 1.45–1.31 (m, 1H), 1.03 (d, *J* = 6.8 Hz, 3H), 0.98 (t, *J* = 7.3 Hz, 3H), 0.93 (d, 5.5 Hz, 3H), 0.91 (d, 5.7 Hz, 3H); ¹³C NMR (CDCl₃, 100 MHz) δ 171.9, 154.3, 142.5, 130.6, 77.4, 63.6, 58.3, 38.6, 28.5, 26.5, 18.0, 15.3, 14.3, 13.9, 10.8; HRMS (ESI-TOF) *m/z*: [M + Na]⁺ Calcd for C₁₅H₂₅NO₄Na 306.1678, found 306.1680.

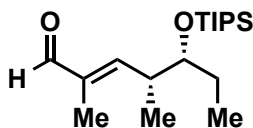
(*S*)-3-((4*S*,5*S*,*E*)-5-Hydroxy-2,4-dimethylhept-2-enoyl)-4-isopropylloxazolidin-2-one (*ent*-2.44). The title compound was synthesized in an analogous manner to its enantiomer and was identical with respect to ¹H-NMR and ¹³C-NMR spectra. $[\alpha]_D^{22} = 66.0$ (*c* 1.00, CHCl₃); HRMS (ESI-TOF) *m/z*: [M + Na]⁺ Calcd for C₁₅H₂₅NO₄Na 306.1678, found 306.1682.



(*R*)-3-((4*R*,5*R*,*E*)-2,4-Dimethyl-5-((triisopropylsilyl)oxy)-hept-2-enoyl)-4-isopropyl-oxazolidin-2-one (2.45). To a reaction flask containing aldol adduct **2.44** (0.260 g, 0.918 mmol) in CH₂Cl₂ (10.0 mL) under argon atmosphere in ice-water bath (0 °C) was added *i*Pr₂NEt (0.192 mL, 1.10 mmol, 1.20 equiv) followed by TIPSOTf (0.296 mL, 1.10 mmol, 1.20 equiv). The reaction was stirred at 0 °C for 19 h and quenched upon addition of an aqueous saturated NaHCO₃ (5.00 mL). The biphasic mixture was allowed to warm to ambient temperature and separated. The aqueous layer was extracted with CH₂Cl₂ (3 ×

20.0 mL) and the combined organic fractions were dried over Na₂SO₄, filtered and concentrated under reduced pressure. The crude residue was purified by flash chromatography (10% EtOAc/hexanes) affording the title compound (0.373 mg, 0.848 mmol, 92%) as a colorless oil. TLC: R_f = 0.32 (10% EtOAc/hexanes); $[\alpha]_D^{22}$ = -42.6 (c 1.00, CHCl₃); ¹H NMR (400 MHz) δ 6.04 (dd, J = 10.0, 1.4 Hz, 1H), 4.53–4.43 (m, 1H), 4.30 (t, J = 8.8 Hz, 1H), 4.17 (dd, J = 8.9, 5.4 Hz, 1H), 3.75 (q, J = 5.2 Hz, 1H), 2.72–2.59 (m, 1H), 2.46–2.34 (m, 1H), 1.92 (d, J = 1.4 Hz, 3H), 1.66–1.54 (m, 2H), 1.07 (s, 21H), 1.01 (d, J = 6.8 Hz, 3H), 0.92 (d, J = 7.2 Hz, 3H), 0.90 (d, J = 7.0 Hz, 3H), 0.88 (t, 7.5 Hz, 3H); ¹³C NMR (CDCl₃, 100 MHz) δ 172.2, 153.7, 142.3, 129.7, 76.2, 63.5, 58.6, 36.7, 28.3, 28.0, 18.4, 18.1, 15.1, 14.1, 13.8, 13.1, 9.1; HRMS (ESI-TOF) m/z : [M + Na]⁺ Calcd for C₂₄H₄₅NO₄SiNa 462.3010, found 462.2986.

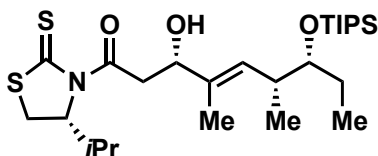
(*S*)-3-((4*S*,5*S*,*E*)-2,4-Dimethyl-5-((triisopropylsilyl)oxy)hept-2-enoyl)-4-isopropylloxazolidin-2-one (*ent*-2.45). The title compound was synthesized in an analogous manner to its enantiomer and was identical with respect to ¹H-NMR and ¹³C-NMR spectra. $[\alpha]_D^{22}$ = 45.1 (c 1.00, CHCl₃); HRMS (ESI-TOF) m/z : [M + Na]⁺ Calcd for C₂₄H₄₅NO₄SiNa 462.3010, found 462.3017.



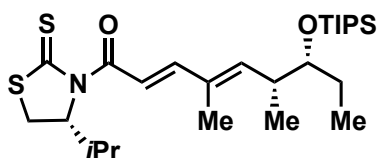
(4*R*,5*R*,*E*)-2,4-Dimethyl-5-((triisopropylsilyl)oxy)hept-2-enal (2.46). A flask containing acyl oxazolidinone **2.45** (0.373 g, 0.848 mmol) dissolved in CH₂Cl₂ (27 mL) under argon atmosphere was cooled to -78 °C (dry ice–acetone). To the chilled reaction mixture was added DIBAL-H (1.49 M in toluene, 1.14 mL, 1.70 mmol, 2.00 equiv) dropwise over two min. The reaction mixture was stirred at -78 °C for 13 min and quenched upon sequential addition of MeOH (10.0 mL) and saturated, aqueous potassium sodium tartrate solution (10.0 mL). The biphasic solution was allowed to warm to ambient temperature and separated. The aqueous layer was extracted with CH₂Cl₂ (3 × 15.0 mL) and the combined organic fractions were dried over Na₂SO₄, filtered and

concentrated under reduced pressure. The crude product was purified by flash chromatography (10% EtOAc/hexanes) to provide the title compound (0.229 g, 0.733 mmol, 86%) as a clear and colorless oil. TLC: R_f = 0.56 (10% EtOAc/hexanes); $[\alpha]_D^{22}$ = -17.7 (c 1.00, CHCl_3); ^1H NMR (400 MHz) δ 9.39 (s, 1H), 6.55 (d, J = 9.8 Hz, 1H), 3.79 (dt, J = 8.1, 4.4 Hz, 1H), 2.93 – 2.78 (m, 1H), 1.76 (s, 3H), 1.72–1.49 (m, 2H), 1.10–1.04 (s, 24H), 0.89 (t, J = 7.5 Hz, 3H); ^{13}C NMR (CDCl_3 , 100 MHz) δ 195.8, 158.7, 137.9, 76.4, 37.3, 27.9, 18.4, 13.6, 13.1, 9.52, 9.46; HRMS (ESI-TOF) m/z : $[\text{M} + \text{Na}]^+$ Calcd for $\text{C}_{18}\text{H}_{36}\text{O}_2\text{SiNa}$ 335.2377, found 335.2396.

(4*S*,5*S*,*E*)-2,4-Dimethyl-5-((triisopropylsilyl)oxy)hept-2-enal (ent-2.46). The title compound was synthesized in an analogous manner to its enantiomer and was identical with respect to ^1H -NMR and ^{13}C -NMR spectra. $[\alpha]_D^{23}$ = 18.5 (c 1.00, CHCl_3); HRMS (ESI-TOF) m/z : $[\text{M} + \text{Na}]^+$ Calcd for $\text{C}_{18}\text{H}_{36}\text{O}_2\text{SiNa}$ 335.2377, found 335.2375.



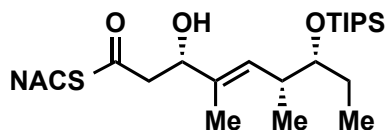
(3*S*,6*R*,7*R*,*E*)-3-Hydroxy-1-((*R*)-4-isopropyl-2-thioxo-thiazolidin-3-yl)-4,6-dimethyl-7-((triisopropylsilyl)oxy)non-4-en-1-one (2.47).



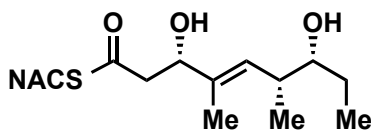
(2*E*,4*E*,6*R*,7*R*)-1-((*R*)-4-Isopropyl-2-thioxothiazolidin-3-yl)-4,6-dimethyl-7-((triisopropylsilyl)oxy)nona-2,4-dien-1-one (2.48). A reaction vessel containing acyl thiazolidinethione **2.17** (0.126 g, 0.620 mmol, 1.70 equiv) in CH_2Cl_2 (2.30 mL) under argon atmosphere was cooled to -40°C (dry ice–MeCN). The equilibrated solution was supplemented by TiCl_4 (72.0 μL , 0.657 mmol, 1.80 equiv) and stirred for 30 min. To the reaction was slowly added freshly distilled $i\text{Pr}_2\text{NEt}$ ⁵⁶ (0.114 mL, 0.657 mmol, 1.80

equiv). The blood red reaction mixture was stirred for 2 h and transferred to dry ice–acetone bath (-78 °C). A CH₂Cl₂ (1.30 mL) solution of aldehyde **S9** (0.114 g, 0.365 mmol, 1.00 equiv) was slowly added to the cooled solution over 12 min. After stirring for 4 h at -78 °C the reaction was quenched via addition of saturated aqueous NH₄Cl (5.00 mL). The biphasic mixture was warmed to ambient temperature and separated. The aqueous layer was extracted with CH₂Cl₂ (3 × 10.0 mL). Combined organic layers were dried over Na₂SO₄, filtered and concentrated under reduced pressure. The resulting crude oil was purified by flash chromatography (20% EtOAc/hexanes) to give both the aldol adduct **S10** (99.3 mg, 0.192 mmol, 53%) as a thick, bright yellow oil, and the dehydration product **S11** (44.4 mg, 0.0893 mmol, 24%) as a viscous, yellow oil. For **2.47**: TLC: *R_f* = 0.25 (20% EtOAc/hexanes); $[\alpha]_D^{22} = -189.2$ (*c* 1.00, CHCl₃); ¹H NMR (400 MHz) δ 5.49 (d, *J* = 9.6 Hz, 1H), 5.16 (t, *J* = 7.0 Hz, 1H), 4.56 (d, *J* = 9.3 Hz, 1H), 3.65 (dt, *J* = 6.6, 4.7 Hz, 1H), 3.53 (dd, *J* = 7.7, 3.7 Hz, 1H), 3.51–3.47 (m, 1H), 3.40 (dd, *J* = 17.4, 9.6 Hz, 1H), 3.03 (d, *J* = 11.5 Hz, 1H), 2.60–2.48 (m, 2H), 2.38 (app. sextet, *J* = 6.7 Hz, 1H), 1.67 (s, 3H), 1.61–1.46 (m, 2H), 1.09–1.03 (m, 24H), 0.99 (d, *J* = 7.0 Hz, 3H), 0.96 (d, *J* = 0.68 Hz, 3H), 0.86 (t, *J* = 7.4 Hz, 3H); ¹³C NMR (CDCl₃, 100 MHz) δ 203.1, 173.1, 134.0, 131.4, 77.3, 73.6, 71.6, 44.2, 36.0, 31.0, 30.8, 27.8, 19.2, 18.5, 18.0, 15.2, 13.2, 12.2, 9.4; HRMS (ESI-TOF) *m/z*: [M + Na]⁺ Calcd for C₂₆H₄₉NO₃S₂SiNa 538.2815, found 538.2841.

For **2.48**: TLC: *R_f* = 0.70 (20% EtOAc/hexanes); $[\alpha]_D^{22} = -207.8$ (*c* 0.23, CHCl₃); ¹H NMR (400 MHz) δ 7.37 (d, *J* = 15.2 Hz, 1H), 7.32 (d, *J* = 15.3 Hz, 1H), 5.97 (d, *J* = 9.9 Hz, 1H), 5.07 (ddd, *J* = 8.2, 5.6, 2.6 Hz, 1H), 3.72 (dt, *J* = 6.9, 4.6 Hz, 1H), 3.50 (dd, *J* = 11.4, 8.1 Hz, 1H), 3.09 (dd, *J* = 11.4, 2.6 Hz, 1H), 2.74–2.64 (m, 1H), 2.54–2.41 (m, 1H), 1.82 (d, *J* = 1.1 Hz, 3H), 1.64–1.47 (m, 2H), 1.09–1.03 (m, 24H), 1.00 (d, *J* = 6.9 Hz, 6H), 0.86 (t, *J* = 7.5 Hz, 3H); ¹³C NMR (CDCl₃, 100 MHz) δ 202.6, 167.5, 150.4, 147.3, 132.5, 118.1, 72.4, 37.4, 30.9, 30.7, 28.0, 19.2, 18.5, 18.4, 17.4, 14.8, 13.2, 12.7, 9.3; HRMS (ESI-TOF) *m/z*: [M + Na]⁺ Calcd for C₂₆H₄₇NO₂S₂SiNa 520.2710, found 520.2713.

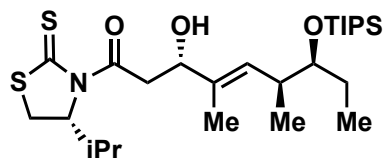


***S*-(2-Acetamidoethyl) (3*S*,6*R*,7*R*,*E*)-3-hydroxy-4,6-di-methyl-7-((triisopropylsilyl)-oxy)non-4-enethioate (2.49).** To a flask containing acyl thiazolidinethione **2.47** (50.5 mg, 0.0979 mmol) under argon atmosphere was added CH₂Cl₂ (3.00 mL). A superstoichiometric amount of imidazole (20.0 mg, 0.294 mmol, 3.00 equiv) was added to the rapidly stirred, yellow mixture at ambient temperature. A slight excess of *N*-acetylcysteamine (11.5 μL, 0.108 mmol, 1.10 equiv) was added to the reaction solution. After stirring at ambient temperature for 13.5 h, the mixture was concentrated under vacuum and purified by column chromatography (5% MeOH/CH₂Cl₂, 1.00 cm thick CuSO₄-SiO₂) affording the title compound (32.3 mg, 0.682 mmol, 70%) as a clear, colorless wax. TLC: *R_f* = 0.30 (5% MeOH/CH₂Cl₂); [α]_D²³ = -2.5 (*c* 1.00, CHCl₃); ¹H NMR (400 MHz) δ 5.80 (br s, 1H), 5.48 (d, *J* = 9.6 Hz, 1H), 4.48 (dd, *J* = 9.4, 3.0 Hz, 1H), 3.64 (dt, *J* = 6.8, 4.7 Hz, 1H), 3.46 (app. dq, *J* = 6.6, 1.8 Hz, 1H), 3.06 (q, *J* = 6.3 Hz, 1H), 2.84 (dd, *J* = 15.0, 9.5 Hz, 1H), 2.70 (dd, *J* = 15.0, 3.2 Hz, 1H), 2.56–2.46 (m, 1H), 1.97 (s, 3H), 1.65 (d, *J* = 1.2 Hz, 3H), 1.62–1.41 (m, 2H), 1.06 (s, 21H), 0.95 (d, *J* = 6.8 Hz, 3H), 0.85 (t, *J* = 7.4 Hz, 3H); ¹³C NMR (CDCl₃, 100 MHz) δ 199.2, 170.5, 133.8, 131.7, 77.4, 74.5, 49.7, 39.6, 36.0, 29.0, 27.8, 23.4, 18.5, 15.2, 13.2, 12.0, 9.3; HRMS (ESI-TOF) *m/z*: [M + Na]⁺ Calcd for C₂₄H₄₇NO₄SSiNa 496.2887, found 496.2887.



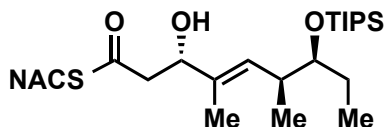
***S*-(2-Acetamidoethyl) (3*S*,6*R*,7*R*,*E*)-3,7-dihydroxy-4,6-dimethylnon-4-enethioate (2.41).** A polypropylene tube (15.0 mL, BD FalconTM) containing silylether **2.49** (32.3 mg, 0.682 mmol) dissolved in MeCN (3.40 mL) was placed in ice-water bath (0 °C) and allowed to equilibrate. To the chilled reaction vessel was added a solution of 48% HF–MeCN (11:89, 8.90 mL). The reaction mixture was transferred to a refrigerator (4 °C) for 48 h and quenched at 0 °C via careful neutralization by saturated aqueous NaHCO₃. The

resulting mixture was extracted with EtOAc (4 × 25.0 mL). The combined organic layers were dried over Na₂SO₄, filtered and concentrated under reduced pressure. The crude product residue was purified by column chromatography (10% MeOH/CH₂Cl₂) furnishing the title compound (20.2 mg, 0.0630 mmol, 93%) as a clear, colorless oil. TLC: R_f = 0.26 (10% MeOH/CH₂Cl₂); $[\alpha]_{365}^{22}$ = 5.0 (c 1.47, CHCl₃); ¹H NMR (400 MHz) δ 6.23 (br s, 1H), 5.35 (d, J = 9.7 Hz, 1H), 4.45 (dd, J = 7.8, 4.8 Hz, 1H), 3.41 (app. hept, J = 7.5 Hz, 2H), 3.34–3.28 (m, 1H), 3.08–2.95 (m, 2H), 2.82 (dd, J = 14.8, 8.2 Hz, 1H), 2.75 (dd, J = 14.8, 4.7 Hz, 1H), 2.47 (dq, J = 12.8, 6.4 Hz, 1H), 1.95 (s, 3H), 1.65 (s, 3H), 1.56–1.43 (m, 1H), 1.35–1.22 (m, 1H), 0.96 (d, J = 6.8 Hz, 3H), 0.92 (t, 7.4 Hz, 3H); ¹³C NMR (CDCl₃, 100 MHz) δ 198.7, 170.8, 135.7, 129.8, 77.2, 74.1, 49.8, 39.4, 37.8, 29.0, 27.1, 23.3, 15.7, 12.4, 10.6; HRMS (ESI-TOF) m/z : $[M + Na]^+$ Calcd for C₁₅H₂₇NO₄SN 340.1553, found 340.1547.



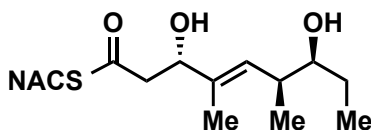
(3*S*,6*S*,7*S*,*E*)-3-Hydroxy-1-((*R*)-4-isopropyl-2-thioxo-thiazolidin-3-yl)-4,6-dimethyl-7-((triisopropylsilyl)-oxy)non-4-en-1-one (2.50). To a reaction flask containing acyl thiazolidinethione **2.17** (88.8 mg, 0.437 mmol, 1.70 equiv) under argon atmosphere was added CH₂Cl₂ (2.50 mL). The yellow solution was placed in dry ice–MeCN bath (–40 °C) and allowed to equilibrate. To the chilled solution was added TiCl₄ (50.7 μ L, 0.463 mmol, 1.80 equiv) and the resulting orange solution was stirred for 30 min. An aliquot of freshly distilled *i*Pr₂NEt (80.6 μ L, 0.463 mmol, 1.80 equiv) was slowly added to the reaction mixture and the blood red solution was stirred at –40 °C for 2 h. The reaction was transferred to a dry ice–acetone bath (–78 °C) and supplemented with a CH₂Cl₂ (0.400 mL) solution of aldehyde *ent*-**2.46** (80.3 mg, 0.257 mmol, 1.00 equiv) in a dropwise fashion. The resulting reaction mixture was stirred at –78 °C for 1 h 45 min and quenched upon addition of aqueous saturated NH₄Cl (7.00 mL). The biphasic mixture was warmed to ambient temperature and separated. The aqueous layer was extracted with

CH₂Cl₂ (3 × 15 mL) and the combined organic layers were dried over Na₂SO₄, filtered and concentrated under reduced pressure. The crude product residue was purified by flash chromatography (20% EtOAc/hexanes) affording the title compound (0.102 g, 0.198 mmol, 77%) as a bright yellow oil. TLC: *R_f* = 0.38 (20% EtOAc/hexanes); $[\alpha]_D^{22} = -199.5$ (*c* 1.00, CHCl₃); ¹H NMR (400 MHz) δ 5.50 (d, *J* = 9.6 Hz, 1H), 5.15 (d, *J* = 6.8 Hz, 1H), 4.55 (dd, *J* = 9.4, 2.2 Hz, 1H), 3.68 (q, *J* = 4.8 Hz, 1H), 3.57–3.51 (m, 1H), 3.51–3.47 (m, 1H), 3.41 (dd, *J* = 17.4, 9.5 Hz, 1H), 3.03 (d, *J* = 11.5 Hz, 1H), 2.58–2.48 (m, 1H), 2.39 (app. sextet, *J* = 6.8 Hz, 1H), 1.67 (s, 3H), 1.61–1.49 (m, 2H), 1.10–1.03 (m, 24H), 0.99 (d, *J* = 6.9 Hz, 3H), 0.94 (d, *J* = 6.8 Hz, 3H), 0.86 (t, *J* = 7.4 Hz, 3H); ¹³C NMR (CDCl₃, 100 MHz) δ 203.1, 173.0, 134.1, 131.1, 77.3, 73.2, 71.7, 44.3, 35.9, 31.0, 30.8, 27.9, 19.3, 18.4, 17.9, 15.1, 13.2, 12.7, 9.4; HRMS (ESI-TOF) *m/z*: [M + Na]⁺ Calcd for C₂₆H₄₉NO₃S₂SiNa 538.2815, found 538.2830.

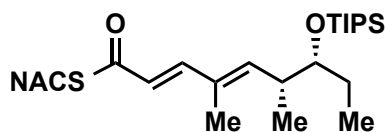


***S*-(2-Acetamidoethyl) (3*S*,6*S*,7*S*,*E*)-3-hydroxy-4,6-dimethyl-7-((triisopropylsilyl)oxy)non-4-enethioate (2.51).** To a flask containing aldol adduct **2.50** (42.0 mg, 0.0814 mmol) dissolved in CH₂Cl₂ (3.00 mL) under argon atmosphere was added imidazole (17.0 mg, 0.250, 3.07 equiv). To the stirred reaction mixture was added *N*-acetylcysteamine (9.50 μL, 0.0893 mmol, 1.10 equiv) and the resulting solution was stirred at ambient temperature for 7 h. The reaction mixture was quenched upon addition of a saturated, aqueous NH₄Cl (5.00 mL) and the biphasic solution was separated. The aqueous layer was extracted with CH₂Cl₂ (4 × 15.0 mL) and the combined organic layers were dried over Na₂SO₄, filtered and concentrated under reduced pressure. Crude product residues were purified by flash chromatography (5% MeOH/CH₂Cl₂) providing the title compound (35.3 mg, 0.746 mmol, 92%) as a clear, colorless oil. TLC: *R_f* = 0.23 (5% MeOH/CH₂Cl₂); $[\alpha]_D^{22} = -9.4$ (*c* 1.00, CHCl₃); ¹H NMR (400 MHz) δ 5.85 (br s, 1H), 5.48 (d, *J* = 9.6 Hz, 1H), 4.47 (dd, *J* = 9.0, 3.5 Hz, 1H), 3.76–3.60 (m, 1H), 3.45 (q, *J* = 6.2 Hz, 2H), 3.05 (dt, *J* = 5.3, 3.0 Hz, 2H), 2.82 (dd, *J* = 15.0, 9.0 Hz, 1H), 2.73 (dd, *J* =

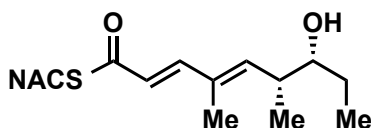
15.0, 3.7 Hz, 1H), 2.58–2.44 (m, 1H), 1.97 (s, 3H), 1.65 (s, 3H), 1.60–1.46 (m, 2H), 1.06 (s, 21H), 0.92 (d, $J = 6.8$ Hz, 3H), 0.85 (t, $J = 7.4$ Hz, 3H); ^{13}C NMR (CDCl_3 , 100 MHz) δ 199.1, 170.5, 133.9, 131.4, 77.4, 74.3, 49.8, 39.6, 35.9, 29.0, 27.8, 23.4, 18.4, 15.1, 13.2, 12.2, 9.3; HRMS (ESI-TOF) m/z : $[\text{M} + \text{Na}]^+$ Calcd for $\text{C}_{24}\text{H}_{47}\text{NO}_4\text{SSiNa}$ 496.2887, found 496.2881.



***S*-(2-Acetamidoethyl) (3*S*,6*S*,7*S*,*E*)-3,7-dihydroxy-4,6-dimethylnon-4-enethioate (2.42).** A large conical polypropylene tube (50.0 mL, BD FalconTM) containing silylether **2.51** (35.3 mg, 0.0746 mmol) dissolved in MeCN (3.75 mL) was placed in ice-water (0 °C) bath and allowed to equilibrate. To the chilled reaction vessel was added a solution of 48% HF–MeCN (11:89, 5.52 mL). The resulting clear solution was stored at 4 °C for 23 h and neutralized via addition of an aqueous saturated NaHCO_3 solution at 0 °C. The reaction mixture was extracted with EtOAc (4 \times 15.0 mL) and the combined organic fractions were dried over Na_2SO_4 , filtered and concentrated under reduced pressure. The crude residue was purified by flash column chromatography (10% MeOH/ CH_2Cl_2) yielding the title compound (18.5 mg, 0.0583 mmol, 78%) as a colorless oil. TLC: $R_f = 0.38$ (10% MeOH/ CH_2Cl_2); $[\alpha]_D^{23} = -25.0$ (c 0.62, CHCl_3); ^1H NMR (400 MHz) δ 6.19 (br s, 1H), 5.36 (d, $J = 9.7$ Hz, 1H), 4.46 (dd, $J = 8.2, 3.5$ Hz, 1H), 3.42 (q, $J = 6.1$ Hz, 2H), 3.38–3.29 (m, 1H), 3.09–2.95 (m, 2H), 2.83 (dd, $J = 14.8, 8.6$ Hz, 1H), 2.73 (dd, $J = 14.8, 3.8$ Hz, 1H), 2.48 (dq, $J = 13.3, 6.6$ Hz, 1H), 1.95 (s, 3H), 1.65 (s, 3H), 1.58–1.47 (m, 1H), 1.32 (dq, $J = 15.1, 7.8$ Hz, 1H), 0.94 (d, $J = 6.9$ Hz, 3H), 0.93 (t, $J = 7.2$ Hz, 3H); ^{13}C NMR (CDCl_3 , 100 MHz) δ 198.8, 170.8, 135.8, 129.7, 77.3, 74.2, 49.6, 39.4, 37.8, 29.0, 26.9, 23.3, 15.8, 12.5, 10.7; HRMS (ESI-TOF) m/z : $[\text{M} + \text{Na}]^+$ Calcd for $\text{C}_{15}\text{H}_{27}\text{NO}_4\text{SNa}$ 340.1553, found 340.1556.

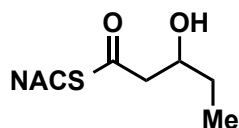


***S*-(2-Acetamidoethyl) (2*E*,4*E*,6*R*,7*R*)-4,6-dimethyl-7-((triisopropylsilyl)oxy)nona-2,4-dienethioate (2.52).** To a round bottom flask containing acyl thiazolidinethione **2.48** (44.2 mg, 0.0889 mmol) under argon atmosphere was added CH₂Cl₂ (3.00 mL). To the resulting clear solution was added DMAP (32.6 mg, 0.267 mmol, 3.00 equiv) followed by *N*-acetylcysteamine (10.4 μL, 0.098 mmol, 1.10 equiv). The resulting mixture was stirred at ambient temperature for 10 h and concentrated under reduced pressure. Purification of the crude residue by column chromatography (5% MeOH/CH₂Cl₂) yielded the title compound (23.1 mg, 0.0507 mmol, 57%) as a colorless wax. TLC: *R_f* = 0.38 (5% MeOH/CH₂Cl₂); $[\alpha]_D^{23}$ = 7.6 (*c* 1.00, CHCl₃); ¹H NMR (400 MHz) δ 7.25 (d, *J* = 15.3 Hz, 1H), 6.10 (d, *J* = 15.4 Hz, 1H), 6.01 (d, *J* = 9.8 Hz, 1H), 5.94 (br s, 1H), 3.72 (dt, *J* = 7.0, 4.6 Hz, 1H), 3.48 (app. q, *J* = 5.9 Hz, 2H), 3.12 (t, *J* = 6.3 Hz, 2H), 2.76–2.65 (m, 1H), 1.96 (s, 3H), 1.79 (s, 3H), 1.66–1.46 (m, 2H), 1.08–1.04 (m, 21H), 1.01 (d, *J* = 6.8 Hz, 3H), 0.87 (t, *J* = 7.5 Hz, 3H); ¹³C NMR (CDCl₃, 100 MHz) δ 190.7, 170.4, 148.9, 146.9, 131.4, 122.6, 40.2, 37.5, 28.5, 27.9, 23.4, 18.42, 18.37, 14.7, 13.1, 12.4, 9.3; HRMS (ESI-TOF) *m/z*: [M + Na]⁺ Calcd for C₂₄H₄₅NO₃SSiNa 478.2781, found 478.2780.



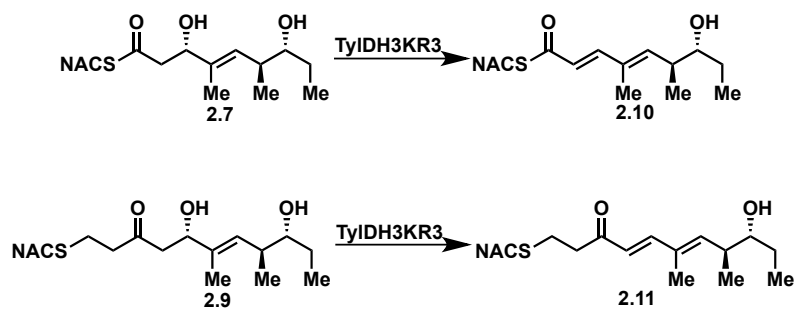
***S*-(2-Acetamidoethyl) (2*E*,4*E*,6*R*,7*R*)-7-hydroxy-4,6-dimethylnona-2,4-dienethioate (2.53).** A polypropylene tube (15.0 mL, BD Falcon™) containing silylether **2.52** (18.0 mg, 0.0395) dissolved in acetonitrile (4.15 mL) was equilibrated in ice-water bath (0 °C). To the chilled starting material was added a solution 48% HF–MeCN (11:89, 5.00 mL). The resulting acidified solution was stored at 4 °C for 48 h and quenched via addition of NaSO₄ at 0 °C. The reaction mixture was extracted with EtOAc (4 × 15.0 mL) and the combined organics were dried over Na₂SO₄. Filtration and concentration under reduced pressure gave the crude product residue. Purification by column chromatography (5%

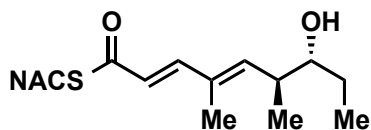
MeOH/CH₂Cl₂) provided the title compound (8.1 mg, 0.0271 mmol, 69%) as a cloudy, colorless oil. TLC: R_f = 0.28 (5% MeOH/CH₂Cl₂); $[\alpha]_D^{23}$ = 37.5 (c 0.52, CHCl₃); ¹H NMR (400 MHz) δ 7.26 (d, J = 15.5 Hz, 1H), 6.12 (d, J = 15.5 Hz, 1H), 5.94 (s, 1H), 5.87 (d, J = 10.1 Hz, 1H), 3.47 (q, J = 6.0 Hz, 2H), 3.39 (ddd, J = 9.2, 6.5, 3.4 Hz, 1H), 3.11 (t, J = 6.3 Hz, 2H), 2.63 (dt, J = 10.1, 6.6 Hz, 1H), 1.96 (s, 3H), 1.81 (d, J = 0.9 Hz, 3H), 1.61–1.49 (m, 1H), 1.41–1.27 (m, 1H), 1.06 (d, J = 6.7 Hz, 3H), 0.95 (t, J = 7.4 Hz, 3H); ¹³C NMR (CDCl₃, 100 MHz) δ 190.7, 170.4, 146.8, 146.6, 132.6, 123.1, 77.0, 40.1, 39.6, 28.5, 27.9, 23.4, 15.8, 12.6, 10.4; HRMS (ESI-TOF) m/z : [M + Na]⁺ Calcd for C₁₅H₂₅NO₃SSiNa 332.1447, found 322.1447. Upon literature analysis we discovered that this compound had been synthesized through a different route by Cane, DE and co-workers.⁵⁸ Our analytical data match that of the original report in all respects.



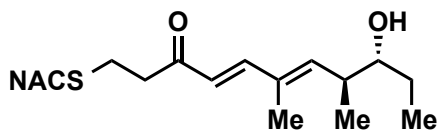
(±)-S-(2-Acetamidoethyl) 3-hydroxypentanethioate ((±)-2.54). The details for the synthesis of racemic diketide substrate **26** are included in a recently published manuscript by Yang Li, et al.²⁹

Scheme 2.11. Chemoenzymatic synthesis of diene products.





***S*-(2-Acetamidoethyl) (2*E*,4*E*,6*S*,7*R*)-7-hydroxy-4,6-di-methylnona-2,4-dienethioate (2.10).** To a small polypropylene conical tube (15 mL) containing sterile deionized water (0.630 mL) was added a concentrated Tris buffer solution (0.500 M Tris-HCl, 1.50 M NaCl, pH 8.0, 0.500 mL). The clear solution was vortexed to mix and β -hydroxy thioester **2.7** (3.17 mg, 0.0100 mmol) was added as a 50:50 DMSO-water stock solution (100 mM, 100 μ L) and mixed by inversion. Heterologously expressed TyLDH3KR3 (2.53 mg/mL stock solution, 1.52 mL, 3.85 mg, 50.3 nmol) was added to the buffered solution. The reaction mixture was capped and incubated at ambient temperature with shaking (250 rpm) for 26 h. The aqueous solution was extracted with EtOAc (3 \times 10.0 mL) followed by drying over Na₂SO₄, filtration and concentration under vacuum. The crude product residue was purified via flash chromatography (5% MeOH/CH₂Cl₂) affording the title compound (2.00 mg, 0.00667 mmol, 67%) as a cloudy, colorless oil. TLC: R_f = 0.32 (5% MeOH/CH₂Cl₂); Due to stability issues, an optical rotation was not obtained; ¹H NMR (400 MHz, CDCl₃) δ 7.29 (d, J = 15.6 Hz, 1H), 6.12 (d, J = 15.5 Hz, 1H), 5.96 (d, J = 10.1 Hz, 1H), 5.91 (br s, 1H), 3.52–3.39 (m, 3H), 3.12 (t, J = 6.3 Hz, 2H), 2.72–2.60 (m, 1H), 1.96 (s, 3H), 1.82 (s, 3H), 1.54–1.49 (m, 1H), 1.45–1.34 (m, 1H), 1.05 (d, J = 6.8 Hz, 3H), 0.96 (t, J = 7.4 Hz, 3H); ¹³C NMR (CDCl₃, 100 MHz) δ 190.7, 170.4, 146.6, 146.0, 133.5, 123.1, 77.0, 40.2, 39.2, 28.5, 27.8, 23.4, 17.0, 12.7, 10.2; HRMS (ESI-TOF) m/z : [M + Na]⁺ Calcd for C₁₅H₂₅NO₃SNa 322.1447, found 322.1451.



N-(2-(((4*E*,6*E*,8*S*,9*R*)-9-Hydroxy-6,8-dimethyl-3-oxoundeca-4,6-dien-1-yl)thio)ethyl)acetamide (2.11). β -Hydroxy ketone **2.9** (3.45 mg, 0.0100 mmol) was dehydrated in an analogous matter as the generation of dienoate **8** resulting in dienone **9** (3.17 mg, 0.00969 mmol, 97%). TLC: R_f = 0.30 (5% MeOH/CH₂Cl₂); Due to stability

issues, an optical rotation was not obtained; ^1H NMR (400 MHz) δ 7.17 (d, J = 16.7 Hz, 1H), 6.05 (d, J = 15.9 Hz, 1H), 5.89 (d, J = 10.0 Hz, 1H), 3.43–3.35 (m, 3H), 2.87–2.80 (m, 2H), 2.80–2.74 (m, 3H), 2.66–2.54 (m, 3H), 1.94 (s, 3H), 1.76 (s, 3H), 1.52–1.42 (m, 1H), 1.40–1.28 (m, 1H), 0.99 (d, J = 6.8 Hz, 3H), 0.90 (t, J = 7.4 Hz, 3H); ^{13}C NMR (CDCl_3 , 100 MHz) δ 198.8, 170.4, 148.7, 145.5, 133.9, 124.6, 77.0, 40.2, 39.2, 38.7, 32.3, 27.8, 26.1, 23.4, 17.1, 12.7, 10.2; HRMS (ESI-TOF) m/z : $[\text{M} + \text{Na}]^+$ Calcd for $\text{C}_{17}\text{H}_{29}\text{NO}_3\text{SNa}$ 350.1760, found 350.1762.

2.8 Biology experimental section

General biology procedures. All chemical reagents were purchased from Sigma-Aldrich and were used directly without further purification. *E. coli* BL21–AI cells were from Life Technologies. IPTG was acquired through Gold Biotechnology. L-(+)-Arabinose ($\geq 99\%$) was purchased through Sigma Aldrich. His60 Ni Superflow resin was purchased from Clontech Laboratories, Inc. OD_{600} was measured on an Eppendorf BioPhotometer. Sonication was carried out by Branson Sonifier 450. Gel filtration purification was performed on HiLoad 16/600 Superdex 200 pg column (GE). Protein mass spectrometry was carried out using an Agilent 6250 QTOF LC/MS. Kinetic LC–MS/MS was conducted with AB Sciex QTRAP 5500 mass spectrometer and Shimadzu LC system.

The TylKR3-DH3 didomain was ordered as codon-optimized synthetic DNA from Life Technologies. The synthetic DNA encoded the region 957-1682 from the ty lactone synthase module 3 polypeptide. The insert was cloned into pMCSG7 using ligation independent cloning (LIC). TylKr3-DH3 synthetic forward primer: 5'-**TACTTCCAATCCAATGCCCATCCGCTGCTGAGCG**-3'; TylKr3-DH3 synthetic reverse primer: 5'-**TTATCCACTTCCAATGTTAGTTGGTATCTTCCGGTGTACCAGGCG**-3' (LIC-overhangs in **bold**; inserted stop codon underlined). The insert was confirmed via sequencing.

Cloning and Expression of TylDH3-KR3 Construct

Initial efforts to recombinantly express the mono-domain TylKR3 were hampered by with poor expression levels and protein aggregation. Strategies to alleviate these issues included an increase of rare tRNA codons (Rosetta cell line), optimization of codon selection (synthetic TylKR3 gene), toxic protein-compatible expression hosts (pLysS cell line), appending a fusion protein (attempted with SUMO, mOCR, and GST), chaperone coexpression (GroEL-GroES) and truncations of both N- and C-termini. Disappointingly, these techniques failed to improve expression of soluble non-aggregated TylKR3 and forced us to abandon the expression of the mono-domain construct.

The *tylGII* region encoding TylDH3-KR3 didomain comprising residues 957-1682 was cloned into a pMCSG7 vector and transformed into *E. coli* BL21-AI cells containing the pRARE plasmid. A large TB media culture (0.5 L in 2.8 L Fernbach flask) was inoculated with as small amount of overnight culture (5 mL) and incubated at 37 °C, shaking at 250 RPM until OD₆₀₀ = 1.00–1.20. The culture was cooled to 20 °C and incubated with shaking (250 RPM) for 1 h. Cells were induced upon addition of IPTG (0.100 mM) and L-arabinose (1.00 g) and allowed to shake (250 RPM) at 20 °C for 19 h. The cell pellet was collected after centrifugation (4 °C, 5,000 x G, 30 min) and resuspended in lysis buffer (50 mM tricine, 50 mM (NH₄)₂SO₄, 100 mM urea, pH 8.5, 4 mL/g of pellet). The cells were lysed (3 x 2 min, 50% duty cycle, 40 % power, 4 °C) and centrifuged (4 °C, 28,600 x G, 45 min). The soluble protein was purified by sequential metal-immobilized affinity chromatography and size exclusion chromatography to afford approximately 9 mg of purified protein (18 mg / L) that was greater than 90% pure as judged by SDS-PAGE (**Figure 2.6**) and to be near the predicted calculated mass by mass spectrometry (**Figure 2.7**).

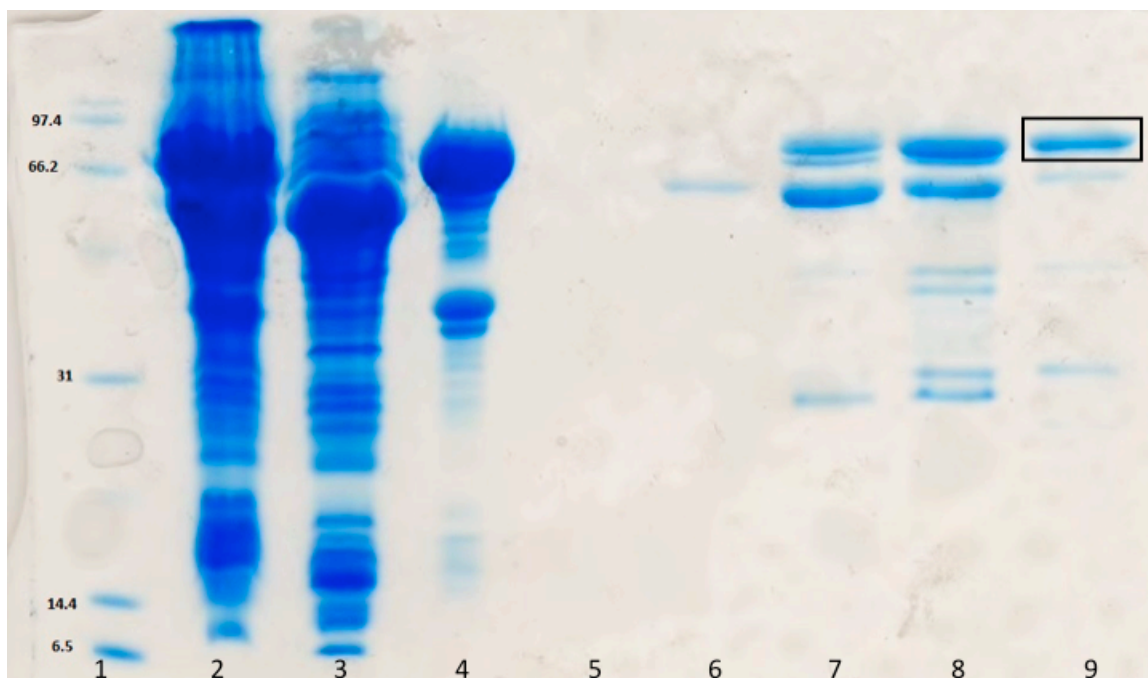


Figure 2.6. SDS-PAGE image of TyIDH3-KR3 purification. The ladder, cell lysate, insoluble pellet, soluble protein and serial nickel elution fractions are shown in lanes 1-9, respectively. The band corresponding to TyIDH3-KR3 is boxed.

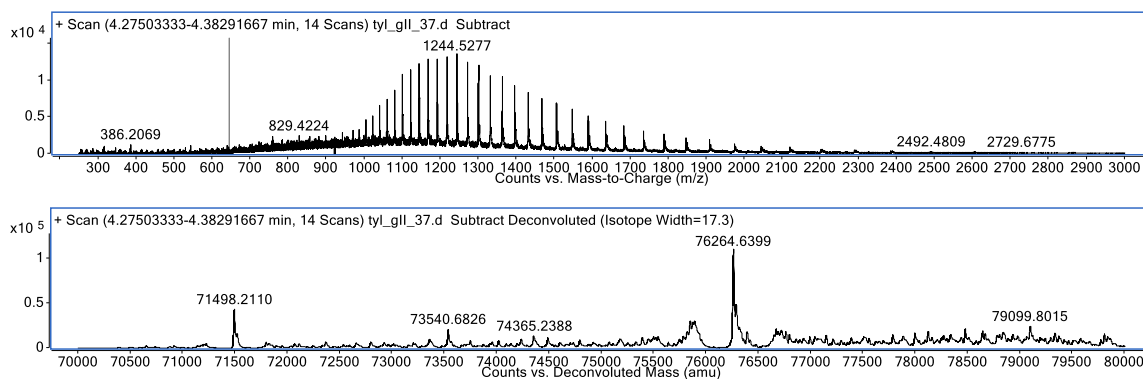


Figure 2.7. Mass spectrometry analysis of TyIDH3-KR3. The convoluted (raw) spectrum and deconvoluted are both displayed. TyIDH3-KR3 was found to have a mass of 76,264 Da. The spectrum was obtained using 0.5 mg/mL of recombinant TyIDH3-KR3 in 25% formic acid. (This mass was determined by Greg Dodge –University of Michigan)

Determination of TyIDH3-KR3 Ketoreductase Activity

A small eppendorf tube (1.5 mL, 100 μ L total volume) containing substrate **2.4** or **2.5** (1 mM), heterologously expressed TyIDH3-KR3 (5 μ M), NADPH (2 mM), Tris (50 mM), NaCl (150 mM) at pH 8.0 was incubated at ambient temperature for 15 h. The reaction was quenched upon addition of MeCN–H₂O (100 μ L) and brief centrifugation. A portion of the diluted reaction solution (60 μ L) was added to a HPLC vial and analyzed by LC-MS/MS (Table S4) employing a Kinetix reverse-phase C₁₈ column (50 mm \times 2.1 mm, 2.6 μ m, Phenomenex) operated at 0.4 mL min⁻¹ with a gradient between mobile phase A (H₂O) and mobile phase B (MeCN). The gradient program was 0 min, 5% B; 2 min, 5% B; 7 min, 55% B; 8 min, 70% B; 9 min, 70% B; 10.5 min, 5% B; 12 min, 5% B. Co-injection of standards **2.6**, **2.7**, and **2.10** for substrate **2.4** confirmed the identity of product traces. The standards **2.8**, **2.9**, and **2.11** were used for the analysis of the incubation of substrate **2.5**.

Table 2.2. LC-MS/MS analysis of analytes **2.6**, **2.7**, **2.10**, **2.8**, **2.9**, and **2.11**.

Analyte	HPLC retention	Transition
	time (min)	
2.6	5.19	340 \rightarrow 184
2.7	5.27	340 \rightarrow 184
2.10	6.17	300 \rightarrow 181
2.8	5.24	368 \rightarrow 212
2.9	5.30	368 \rightarrow 212
2.11	6.00	328 \rightarrow 151

Analysis of TyIDH3-KR3 Dehydratase Activity

Steady-State Analysis.

The enzymatic reactions were carried out in a total volume of 50 μ L under initial velocity conditions containing TyIDH3-KR3 (1 μ M), reaction buffer (50 mM Tris, 150 mM NaCl,

pH 8.0) and substrates **2.7** or **2.9** at variable concentrations (0.5, 1, 2, 3, 4, 6, 8 mM). The final DMSO concentration was held constant at 4%. After incubation at 25 °C for 8 min (the reaction found to be linear up to 10 min), 5 μ L of the reaction mixture was added to 495 μ L of 1:1 MeCN–reaction buffer (100-fold dilution). The resulting solution was vortexed, centrifuged and analyzed by 60 μ L of the diluted reaction solution was added to a HPLC vial with 10 μ L of internal standard (320 nM) and analyzed by LC-MS/MS (Table S4) employing a Kinetix reverse-phase C₁₈ column (50 mm \times 2.1 mm, 2.6 μ m, Phenomenex) operated at 0.4 mL min⁻¹ with a gradient between mobile phase A (H₂O) and mobile phase B (MeCN). The gradient program was 0 min, 5% B; 2 min, 5% B; 7 min, 55% B; 8 min, 70% B; 9 min, 70% B; 10.5 min, 5% B; 12 min, 5% B. Standard curves of enzymatic products **2.10** and **2.11** were generated by injecting the authentic standard at varying concentrations with a fixed concentration of an internal standard (**2.10** for the standard curve of **2.11** and **2.11** for the standard curve of **2.10**). The amount of enzymatic product formation at each time point was calculated by plotting the area ratio (analyte/internal standard) into the standard curve. Control reactions for each concentration of substrate were performed without the addition of enzyme. Each reaction was performed in duplicate. The specificity constants (K_M/k_{cat}) were determined by fitting the normalized v_0 vs $[S]$ plots to linear equations (**Figure S3** panels **A** and **B**).

Substrates **2.41** and **2.42** were analyzed in an analogous way using synthetic **2.53** as the product standard (**Figure 2.5** panels **C** and **D**). The LC-MS/MS trace of **2.53** is provided in **2.13**

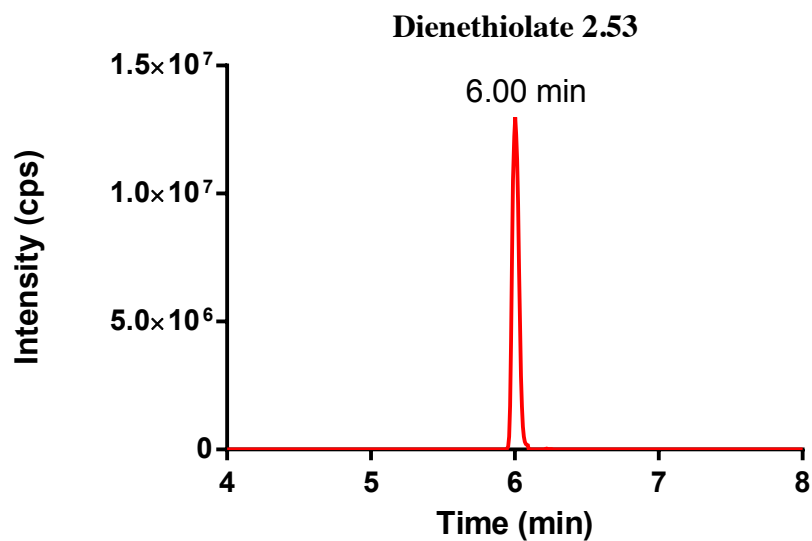


Figure 2.8. LC-MS/MS trace of dienethiolate **2.53**. The synthetic compound **2.53** was used to confirm the identity of the dehydration products arising from thioesters **2.41** and **2.42**. A standard curve for quantitative determination of specificity constants was generated from the synthetic compound.

Chapter 3: Curacin Module K Cryptic Dehydratase

3.1 Background on the natural product curacin

Curacin A, a mixed polyketide-nonribosomal peptide natural product isolated from the cyanobacteria *Moorea producens* (formerly *Lyngbya majuscula*) is a potent antiproliferative agent that arrests mitosis through the inhibition of tubulin polymerization.⁵⁹ Curacin A is biosynthesized via a nonribosomal peptide synthase-polyketide synthase pathway incorporating three malonyl-CoA units in a unique cyclopropyl moiety, one L-cysteine in a thiazoline cyclization reaction, and 7 units of malonyl-CoA through KS-catalyzed Claisen condensations (**Figure 3.1**). The curacin (Cur) biosynthetic pathway has provided a wealth of information about non-canonical enzymatic processes in polyketide biosynthesis including a GCN5-related *N*-acetyltransferase (GNAT)-like strategy for polyketide chain initiation, cyclopropane synthesis through β -branching and cryptic halogenation, and polyketide termination via off-loading of a terminal alkene⁶⁰⁻⁶² Moreover, the Cur pathway has yielded tremendous structural insight into this unprecedented PKS chemistry and three dimensional structures of fourteen proteins in the Cur pathway have been published.^{12,63-69}

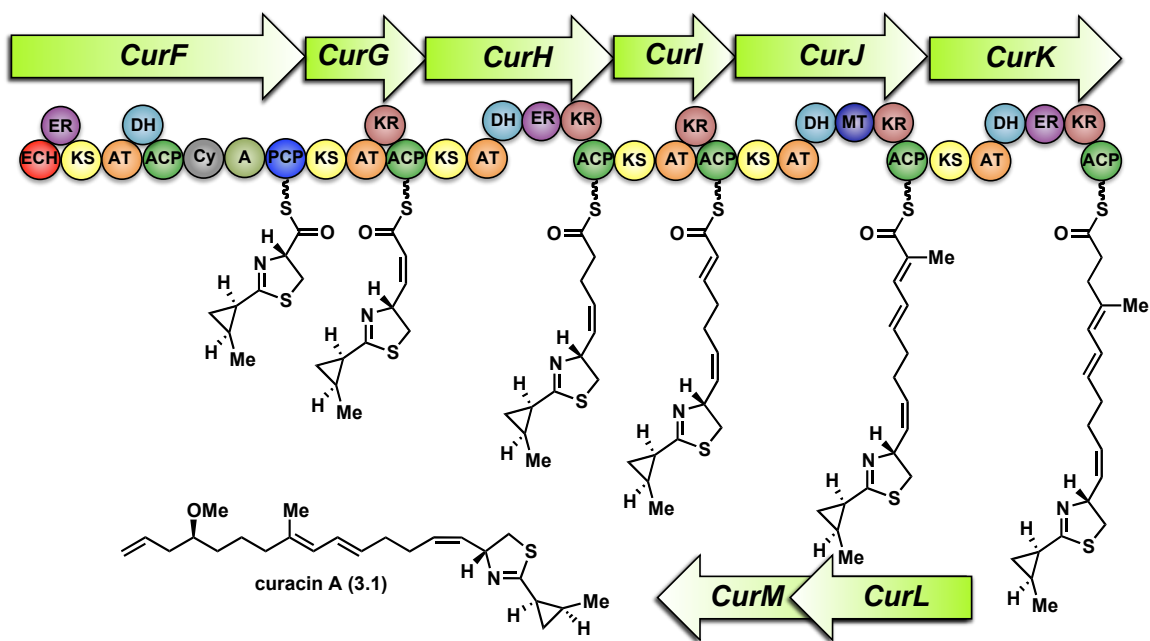


Figure 3.1. The curacin A biosynthetic pathway. Displayed are the detailed module products for CurF to CurK modules.

3.2 Chemical strategy and rationale

We selected the curacin biosynthetic pathway as a platform for studying dehydratase activity in PKSs. The pathway uniquely produces nearly every possible olefin substitution pattern (**Figure 3.1**). Additionally, curacin B and C constitute geometric isomers of A and suggest a degree of pathway flexibility in regards to olefin formation (**Figure 3.2**).⁷⁰ We were initially interested in the CurK dehydratase, catalyzing the last canonical dehydration in the pathway. The CurK ER reduces the product of dehydration, obscuring the olefin bond geometry of the intermediary unsaturated thioester. We wanted to probe the alkene to determine its identity (*E* or *Z*) as well as determine any substrate selectivity for the KR product. In so doing, we hoped to predict the cryptic KR stereochemistry in a fashion similar to the previous TyIDH3 study (**Chapter 2**).

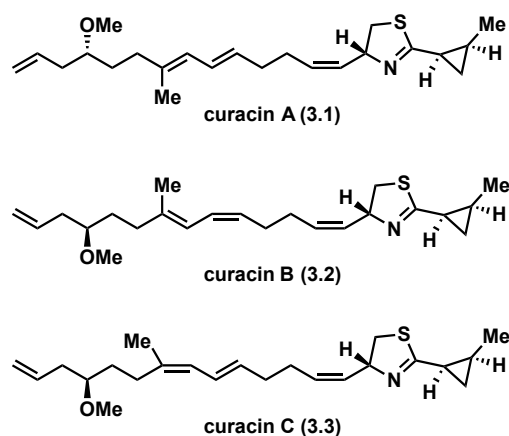


Figure 3.2. A comparison of natural curacin geometric isomers. Curacins B (**3.2**) and C (**3.3**) *E,Z* and *Z,E* isomers of the central diene moiety.

Due to the unique structure of the late-module CurK intermediates we chose to amend our previous synthetic strategy utilized in the synthesis of tylosin module 3 substrates and products. Specifically, we rationalized that due to the preference for thioesters exhibited by dehydratase domains in the tylosin pathway, there was no need to synthesize thioether CurK substrates. The complex distal components of the native substrate **3.4** (i.e. thiazoline and cyclopropyl moieties) persuaded us to truncate CurK substrates to ease their synthesis (**Figure 3.3**). As a result, we designed the target CurK DH substrates compounds **3.5** and **3.6**. We hoped to isolate the triene product **3.7** after incubation with the CurK DH.

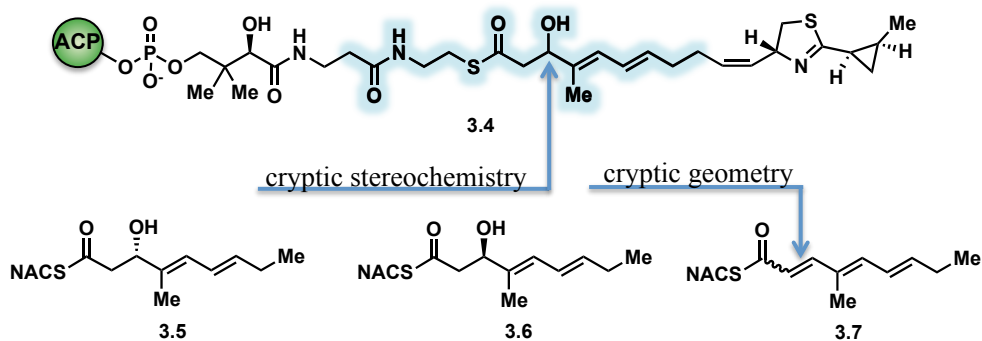


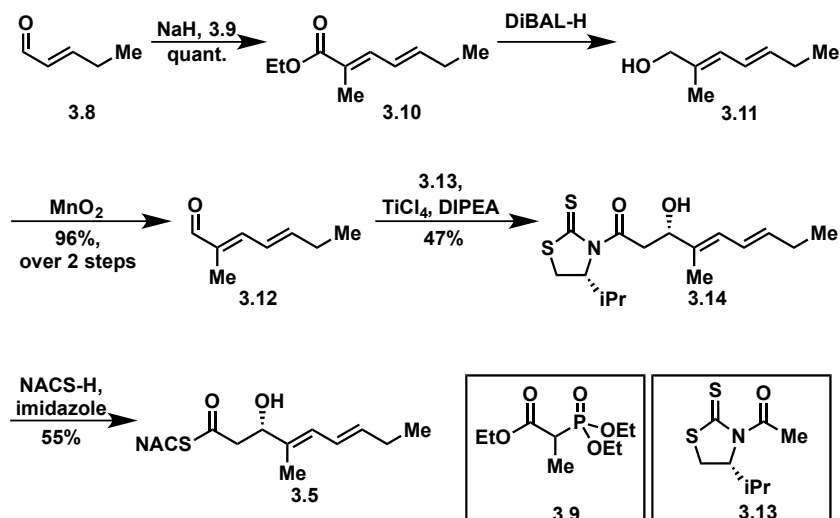
Figure 3.3. Curacin module K DH substrate and product design. The full ACP-loaded substrate **3.4** is highlighted in blue on the truncated region serving as the basis for synthetic substrate design. Enzymatic dehydratase substrates **3.5** and **3.6** were designed to reduce molecular complexity. The hypothetical triene product **3.7** is shown with ambiguous olefin geometry, as the CurK ER in curacin biosynthesis later reduces this moiety.

3.3 Synthesis of truncated CurK DH substrates

The synthesis of D-alcohol thioester substrate **3.5** commenced with commercially available *trans*-2-pentenal (**Scheme 3.1**). Addition of the aldehyde to a preformed enolate solution of Horner-Wadsworth-Emmons (HWE) reagent **3.9** quantitatively furnished dienoate **3.10**. The moderately volatile ester was fully reduced to the corresponding allylic alcohol **3.11** via action of excess DIBAL-H. MnO_2 was used to oxidize the crude **3.11** to the corresponding aldehyde **3.12** in an overall yield of 96% from *trans*-2-pentenal. The aldehyde **3.12** was found to be thermally unstable leading to a complex mixture upon attempted distillation. In light of this, aldehyde was **3.12** dried over 4 Å molecular sieves for (12 h) prior to submitting to the key acetate aldol reaction. In the event, the reaction with D-valine-derived Nagao thiazolidinethione **3.13** with titanium(IV) chloride as the Lewis acid cleanly produced aldol adduct **3.14** as a single diastereomer.^{32,33} The resulting thiazolidinethione was displaced by commercially available *N*-acetylcysteamine to form the desired truncated CurK dehydratase substrate **3.15**. The corresponding enantiomer (L-alcohol, **3.6**) was synthesized in a similar manner

from the common aldehyde **3.12** and the antipode of chiral auxiliary **3.13**.

Scheme 3.1. Synthetic route towards CurK DH substrate **3.5**.



3.4 CurK DH-catalyzed production and characterization of triene intermediate

Both substrates **3.5** and **3.6** (1 mM) were separately incubated overnight (12 h) with recombinant CurK DH (**Figure 3.4**). Both reaction mixtures were quenched via acetonitrile promoted protein precipitation and analyzed via low-resolution mass spectrometry. The D-alcohol substrate (**3.5**) was efficiently eliminated based on a new mass appearing at $m/z = 267.4$. No product formation was observed in the L-alcohol (**3.6**) mixture, indicating the reaction had occurred in a stereoselective fashion. This result matches the bioinformatic, amino acid sequence-based prediction that the CurK KR produces D-alcohols. The LC-MS/MS extracted ion chromatograms revealed that the CurK DH had the highest conversion of **3.5** to **3.7** (**Figure 3.5**, Panels **A** and **C**). Similar to the LRMS results, we found that substrate **3.6** showed no product formation when incubated with any the dehydratases in the pathway (**Figure 3.5**, Panel **B**). A time course study revealed that equilibrium between **3.5** and **3.7** was reached within one hour of incubation with CurK DH (5 μ M) (**Figure 3.5**, Panel **D**). Additionally, we were able to

test catalytic dyad mutants (H996F and D1169N) provided to us courtesy of Gregory Dodge (Dr. Janet L. Smith Lab, University of Michigan- Life Sciences Institute) and show they were catalytically inactive (H→F) or severely inhibited (D→N, <2% conversion over 12 h) with **3.5**.

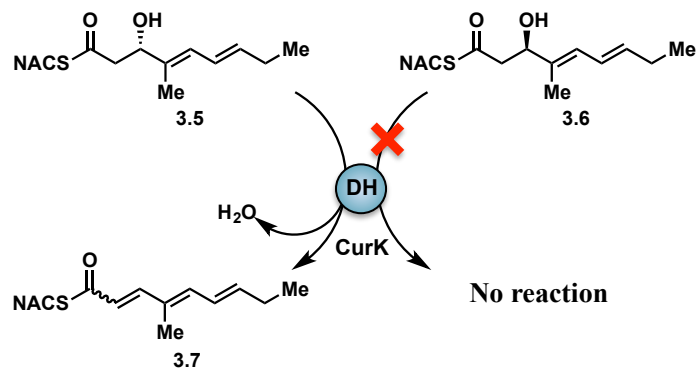


Figure 3.4. Graphical display of the stereoselective action of the CurK DH. Incubation with D-alcohol **3.5** resulted in conversion to dehydrated product **3.7** by LRMS. Conversely, the same enzyme failed to turnover L-alcohol **3.5**, yielding only starting material.

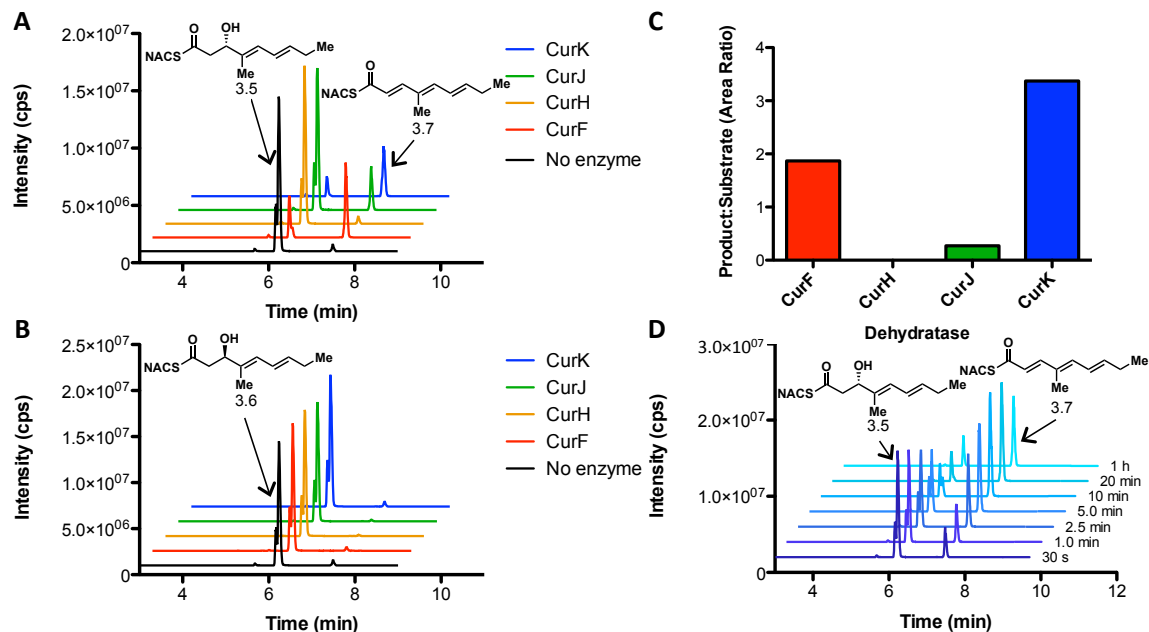


Figure 3.5. LC-MS/MS analysis of the incubation of **3.5** and **3.6** with the CurK DH. Panels **A** and **B** display the incubation of the curacin dehydratases for 12 h with substrates **3.5** and **3.6**, respectively. Panel **C** shows the area ratio of **3.7**:**3.5** for each dehydratase. Panel **D** displays the time course incubation of substrate **3.5** with CurK and formation of **3.7**. Extracted ion chromatograms were generated by scanning for MRM 268→121.

We were interested in investigating the triene product of the CurK DH more closely for its olefin bond geometry as well as obtaining a sample to serve as a standard for LC-MS/MS. A large amount of substrate **3.5** (10.0 mg, 35.0 μ mol) and CurK DH were incubated overnight. The crude mixture was extracted with ethyl acetate and the crude residue was purified by silica gel chromatography and the purified product was analyzed via ^1H NMR to determine the critical α , β J -coupling values. The J -values were found to be diagnostic of a *trans*-olefin (15.3 Hz) (**Figure 3.6**). This suggests that the frequently proposed empirical rule that the DH catalyzed elimination of D-alcohols typically results in *trans*-alkene geometry indeed holds true in the case of the CurK module.¹⁷

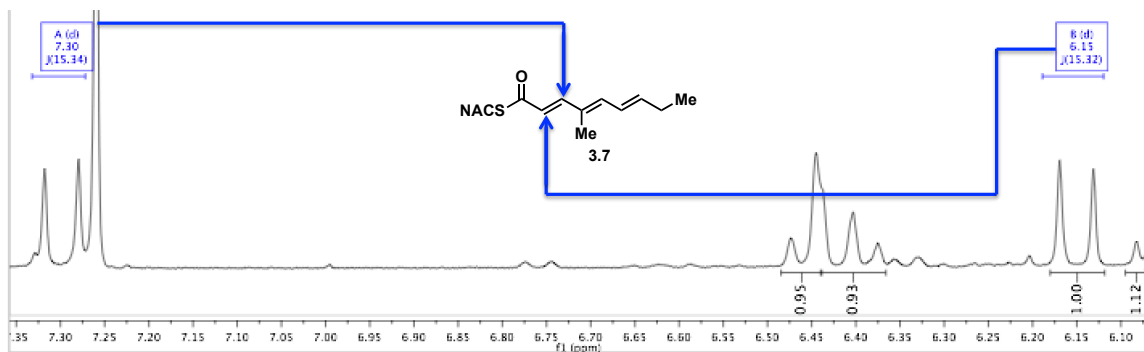


Figure 3.6. The diagnostic α , β -protons used to assign geometry in the CurK DH product. Correlating peaks are highlighted with blue. The J -coupling value is 15.3 Hz, indicative of a *trans*-olefin.

3.5 Quantitative Analysis of CurK DH-catalyzed dehydration

Next we investigated the kinetics of the CurK DH-catalyzed triene formation to compare with the previous TyIDH3 activity. With dehydrated product **3.7** in hand we were able to generate a standard curve for quantitative LC-MS/MS analysis. We chose synthetic dienoate **4.6** (See **Chapter 4** for synthetic details) as the internal standard given its molecular similarity to the product. A constant amount of internal standard (320 nM) was added to a range of concentrations of authentic product and the resulting mixture was analyzed via LC-MS/MS. We determined that the enzyme activity was linear up to 10 minutes and at a range of enzyme concentrations (10–250 nM) allowing us to set an enzymatic stop point at 4 minutes and 20 nM of enzyme for determining steady state enzyme kinetic parameters. By varying the substrate concentration from 0.25–6 mM we were able to obtain the area ratios (product/internal standard) that could be converted to concentrations (with the standard curve) necessary for generating kinetic plots. In so doing we were able to determine both the k_{cat} ($4319 \pm 1237 \text{ min}^{-1}$) and K_M ($12.0 \pm 4.68 \text{ mM}$) for the enzymatic dehydration of **3.5** via Michaelis-Menten analysis. (**Figure 3.7**) This results in a 396-fold increase in specificity constant ($360 \pm 84.3 \text{ min}^{-1} \text{ mM}^{-1}$) over the previously characterized TyIDH3 specificity constant ($908 \pm 30 \text{ min}^{-1} \text{ M}^{-1}$). Remarkably, this is determined with the severely truncated substrate **3.5**, suggesting that

the native substrate may be processed even more efficiently.

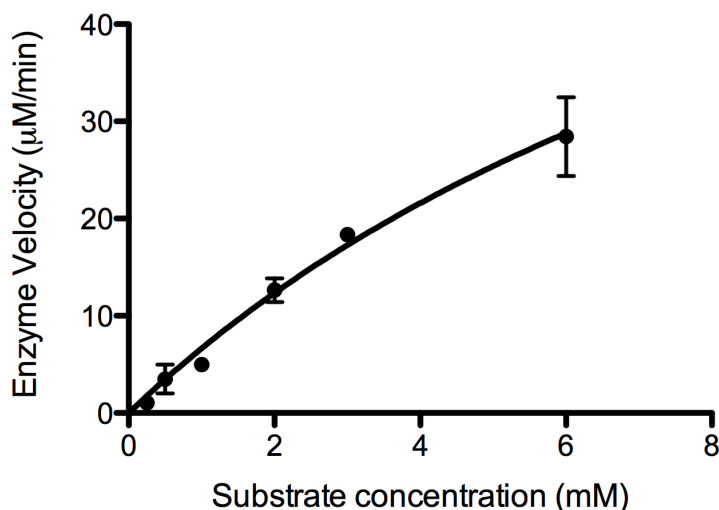
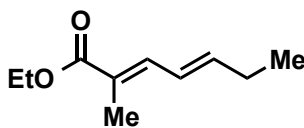


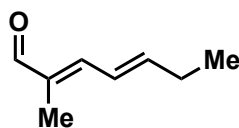
Figure 3.7. Michaelis-Menten analysis of substrate **3.5**. The points are derived through duplicate steady state analyses of CurK DH while varying substrate concentrations (0.25–6.0 mM). $R^2 = 0.974$.

3.6 Chemistry Experimental Section



Ethyl (2E,4E)-2-methylhepta-2,4-dienoate (3.10). A flask containing THF (36.0 mL) and triethyl 2-phosphonopropionate **3.9** (2.81 mL, 13.1 mmol, 1.10 equiv) was placed in ice-water cooling bath (0 °C). To the chilled mixture was added NaH (60% (w/w) in oil, 0.595 g, 14.9 mmol, 1.25 equiv) and stirred for 2 h. The enolate solution was supplemented with distilled *trans*-2-pentenal **3.8**⁵⁶ (1.16 mL, 11.9 mmol, 1.00 equiv) over 20 min. After stirring at 0 °C for 5.5 h, the reaction was quenched upon addition of H₂O (20.0 mL). The biphasic solution was separated and the aqueous layer was extracted

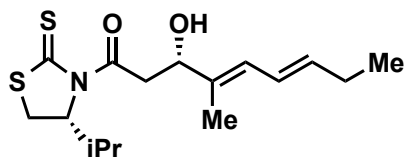
with diethyl ether (4×20.0 mL). The combined organic layers were dried over Na_2SO_4 , filtered and concentrated under reduced pressure. The crude product residue was purified by flash chromatography (5% Et_2O /pentane) affording the title compound (2.00 g, 11.9 mmol, quant.) slightly yellow oil (2.00 g, 11.9 mmol, quant.). TLC: $R_f = 0.22$ (2% Et_2O /pentane); ^1H NMR (CDCl_3 , 400 MHz) δ 7.16 (d, $J = 11.2$ Hz, 1H), 6.33 (dd, $J = 14.8, 11.2$ Hz, 1H), 6.11 (dt, $J = 15.2, 6.4$ Hz, 1H), 4.20 (q, $J = 7.2$ Hz, 2H), 2.21 (app. quint, $J = 7.2$ Hz, 2H), 1.93 (s, 3H), 1.30 (t, $J = 7.2$ Hz, 3H), 1.05 (t, $J = 7.6$ Hz, 3H); ^{13}C NMR (CDCl_3 , 100 MHz) δ 168.8, 144.6, 138.7, 125.3, 125.2, 60.6, 26.5, 14.5, 13.3, 12.7; HRMS (ESI-TOF) m/z : $[\text{M} + \text{Na}]^+$ Calcd for $\text{C}_{10}\text{H}_{16}\text{O}_2\text{Na}$ 191.1043, found 191.1039 ($\Delta = 2.0$ ppm).



(2E,4E)-2-Methylhepta-2,4-dienal (3.12). To a flask containing dienoate **3.9** (486 mg, 2.89 mmol, 1.00 equiv) was added CH_2Cl_2 (13.0 mL). The clear solution was cooled via ice-water bath (0°C). To the chilled reaction mixture was slowly added DIBAL-H (1M in hexanes, 6.93 mL, 6.93 mmol, 2.40 equiv). After 42 min the reaction was quenched via successive addition of MeOH (3.50 mL) and aqueous saturated sodium potassium tartrate (10.0 mL). The resulting biphasic mixture was stirred vigorously at room temperature for 14 h. The reaction mixture was diluted with H_2O (10.0 mL) and CH_2Cl_2 (10.0 mL). The biphasic mixture was separated and the aqueous layer was extracted with CH_2Cl_2 (3×12.0 mL). The combined organics were dried over NaSO_4 , filtered and concentrated under reduced pressure. The crude residue was carried to the next reaction without further purification. TLC: $R_f = 0.58$ (20% EtOAc /hexanes).

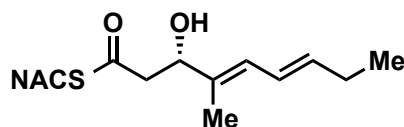
The crude alcohol **3.11** (2.89 mmol (assuming quantitative conversion for the preceding reduction)) was dissolved in CH_2Cl_2 (15.0 mL) and purged with argon atmosphere. To the reaction flask was added anhydrous MgSO_4 (1.04 g, 8.67 mmol, 3.00 equiv) followed by MnO_2 (88% activated, 1.76 g, 20.23 mmol, 7.00 equiv). The resulting gray solution

was vigorously stirred at ambient temperature for 24 h. The reaction mixture was filtered through celite pad (2.00 cm) and concentrated under reduced pressure. The crude residue was purified by flash chromatography (2% Et₂O/pentanes) affording the title compound (0.345 g, 2.77 mmol, 96% over 2 steps) as a colorless oil. TLC: R_f = 0.43 (10% Et₂O/pentane); ¹H NMR (CDCl₃, 400 MHz) δ 9.42 (s, 1H), 6.83 (d, J = 11.2 Hz, 1H), 6.52 (ddt, J = 14.8, 11.2, 1.6 Hz, 1H), 6.28 (dt, J = 14.8, 6.4 Hz, 1H), 2.32–2.23 (m, 2H), 1.84 (t, J = 0.8 Hz, 3H), 1.10 (t, J = 7.6 Hz, 3H); ¹³C NMR (CDCl₃, 100 MHz) δ 195.3, 149.5, 147.3, 136.2, 125.1, 26.7, 13.1, 9.5; HRMS (ESI-TOF) m/z : [M + Na]⁺ Calcd for C₈H₁₂ONa 147.0780; found 147.0794 (Δ = 9.5 ppm).

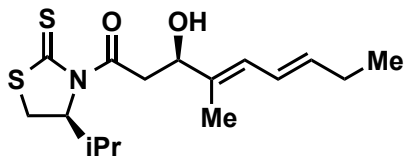


(S,4E,6E)-3-Hydroxy-1-((R)-4-isopropyl-2-thioxothiazolidin-3-yl)-4-methylnona-4,6-dien-1-one (3.14). To a flask acetyl thiazolidinethione **3.13** (0.484 g, 2.38 mmol, 1.60 equiv) was added CH₂Cl₂ (12.0 mL). The bright yellow solution was cooled via dry ice–MeCN (–40 °C). To the chilled solution was added TiCl₄ (0.277 mL, 2.53 mmol, 1.70 equiv) causing a color change to orange-red. The solution was stirred for 29 min prior to the slow addition of distilled *i*Pr₂NEt⁵⁶ (0.441 mL, 2.53 mmol, 1.70 equiv). After 2.25 h the blood-red solution was cooled via dry ice–acetone (–78 °C) and aldehyde **3.12** (dried overnight over 4 Å molecular sieves) (185.0 mg, 1.49 mmol, 1.00 equiv) was added to the solution over 1 min. The aldol reaction was stirred at –78 °C for 3.5 h and quenched by addition of saturated aqueous NH₄Cl (6.00 mL). The biphasic solution was separated and the aqueous layer was extracted with CH₂Cl₂ (4 × 10.0 mL). The combined organics were dried over Na₂SO₄, filtered and concentrated under reduced pressure. The crude mixture was purified via flash chromatography (30% EtOAc/hexanes)) affording the title compound (0.230 g, 0.703 mmol, 47%) as a bright yellow, viscous oil. TLC: R_f = 0.41 (30% EtOAc/hexanes)); $[\alpha]_D^{24}$ = –245.7 (*c* 1.00, CHCl₃); ¹H NMR (CDCl₃, 400 MHz) δ 6.24 (dd, J = 14.8, 10.8 Hz, 1H), 6.09 (d, J = 10.8 Hz, 1H), 5.76 (dt, J = 14.8, 6.8 Hz,

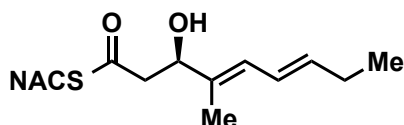
1H), 5.14 (t, $J = 6.8$ Hz, 1H), 4.61 (dd, $J = 8.8, 0.8$ Hz, 1H), 3.59–3.48 (m, 2H), 3.42 (dd, $J = 17.2, 9.2$ Hz, 1H), 3.03 (d, $J = 11.6$ Hz, 1H), 2.65 (br s, 1H), 2.37 (app. sext, $J = 6.4$ Hz, 1H), 2.13 (app. quint, $J = 7.2$ Hz, 2H), 1.77 (s, 3H), 1.08–0.97 (m, 9H); ^{13}C NMR (CDCl_3 , 100 MHz) δ 203.2, 172.9, 137.5, 135.2, 125.9, 124.9, 73.0, 71.7, 44.1, 31.0, 30.8, 26.2, 19.2, 18.0, 13.8, 13.0; HRMS (ESI-TOF) m/z : $[\text{M} + \text{Na}]^+$ Calcd for $\text{C}_{16}\text{H}_{25}\text{NO}_2\text{S}_2\text{Na}$ 350.1219; found 350.1207 ($\Delta = 3.4$ ppm).



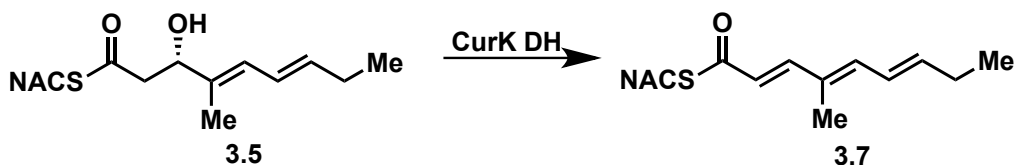
***S*-(2-Acetamidoethyl) (*S,4E,6E*)-3-hydroxy-4-methylnona-4,6-dienethioate (3.5).** The aldol adduct **3.14** (109.4 mg, 0.334 mmol, 1.00 equiv) and anhydrous dichloromethane (10.00 mL). The bright yellow solution was supplemented with *N*-acetylcysteamine (39.0 μL , 0.367 mmol, 1.10 equiv) and imidazole (14.7 mg, 0.216 mmol, 3.00 equiv). The reaction mixture was at ambient temperature for 21 h. The reaction mixture was evaporated by nitrogen stream and purified by flash chromatography (5% MeOH/ CH_2Cl_2). The title compound (52.4 mg, 0.184 mmol, 55%) was isolated as a clear, colorless oil. TLC: $R_f = 0.39$ (5% MeOH/ CH_2Cl_2); $[\alpha]_{\text{D}}^{24} = -20.8$ (c 0.52, CHCl_3); ^1H NMR (CDCl_3 , 400 MHz) δ 6.22 (dd, $J = 15.2, 10.4$ Hz, 1H), 6.07 (d, $J = 10.8$ Hz, 1H), 5.83 (br s, 1H), 5.76 (dt, $J = 15.2, 6.4$ Hz, 1H), 4.53 (dd, $J = 9.2, 3.6$ Hz, 1H), 3.48–3.40 (m, 2H), 3.05 (app. sext, $J = 8.0$ Hz, 2H), 2.84 (dd, $J = 15.2, 8.8$ Hz, 1H), 2.76 (dd, $J = 14.8, 4.0$ Hz, 1H), 2.48 (br, 1H), 2.13 (app. quint, $J = 7.2$ Hz, 2H), 1.96 (s, 3H), 1.75 (s, 3H), 1.01 (t, $J = 7.2$ Hz, 3H); ^{13}C NMR (CDCl_3 , 100 MHz) δ 199.0, 170.6, 138.0, 134.9, 126.3, 124.7, 74.0, 49.6, 39.5, 29.0, 26.1, 23.4, 13.8, 12.6; HRMS (ESI-TOF) m/z : $[\text{M} + \text{Na}]^+$ Calcd for $\text{C}_{14}\text{H}_{23}\text{NO}_3\text{SNa}$ 308.1291; found 308.1275 ($\Delta = 5.1$ ppm).



(*R*,4*E*,6*E*)-3-Hydroxy-1-((*S*)-4-isopropyl-2-thioxothiazolidin-3-yl)-4-methylnona-4,6-dien-1-one (*ent*-3.14). The title aldol adduct was obtained as a bright yellow oil (75%) following an analogous procedure as compound **3.14**, utilizing the L-valine derived Nagao's chiral auxiliary (*ent*-3.13). $[\alpha]_{\text{D}}^{24} = 233.2$ (*c* 1.00, CHCl_3). The product was identical in all remaining respects to its enantiomer, **3.14**.



***S*-(2-acetamidoethyl) (*R*,4*E*,6*E*)-3-hydroxy-4-methylnona-4,6-dienethioate (3.6).** The thioester substrate was synthesized from the precursor thiazolidinethione *ent*-3.13 in a similar manner to that of thioester **3.5**. The desired product was furnished as a slightly yellow, clear oil (24%). $[\alpha]_{\text{D}}^{24} = 17.1$ (*c* 1.00, CHCl_3). All remaining properties were identical to that of the enantiomeric thioester **3.5**.



***S*-(2-Acetamidoethyl) (2*E*,4*E*,6*E*)-4-methylnona-2,4,6-trienethioate (3.7).** To a small, conical tube (15.0 mL) was added autoclaved, deionized water (3.82 mL) and a small amount of 10X TRIS buffer solution (1.50 M NaCl, 0.500M Tris-HCl, pH 8.0) (0.600 mL). The reaction mixture was briefly vortexed. To the buffered solution was added a DMSO-H₂O (1:1) stock solution (50 mM) of the β -hydroxy thioester substrate **3.5** (0.700 mL, 10.0 mg, 35.0 μmol). The mixture was vortexed to mix and the CurK dehydratase (8.19 mg/mL, 0.684 mL, 5.60 mg, 0.160 μmol). The mixture was briefly inverted and covered with aluminum foil to shield it from light. The reaction mixture was shaken

overnight (200 rpm) at ambient temperature in the dark. The reaction mixture was extracted with EtOAc (4 × 10.0 mL) and the combined extracts were dried over sodium sulfate, filtered and concentrated under vacuum. The crude product extract was purified by flash chromatography (5% MeOH/CH₂Cl₂) affording the title compound (2.52 mg, 8.82 μmol, 25%) as a slightly yellow, clear oil (2.52 mg, 8.82 μmol, 25%). *R_f* = 0.35 (5% MeOH/CH₂Cl₂); ¹H NMR (CDCl₃, 400 MHz) δ 7.30 (d, *J* = 15.6 Hz, 1H), 6.46 (d, *J* = 11.2 Hz, 1H), 6.40 (app. t, *J* = 13.6 Hz, 1H), 6.15 (d, *J* = 15.2 Hz, 1H), 6.05 (dt, *J* = 13.6, 6.4 Hz, 1H), 5.98 (br s, 1H), 3.48 (q, *J* = 6.0 Hz, 2H), 3.12 (t, *J* = 6.4 Hz, 2H), 2.22 (app. quint, *J* = 6.8 Hz, 2H), 1.97 (s, 3H), 1.87 (s, 3H), 1.06 (t, *J* = 7.6 Hz, 3H); ¹³C NMR (CDCl₃, 100 MHz) δ 190.5, 170.6, 146.5, 143.6, 141.6, 131.2, 125.8, 122.8, 40.3, 28.5, 26.6, 23.4, 13.4, 12.5; HRMS (ESI-TOF) *m/z*: [M + Na]⁺ Calcd for C₁₄H₂₁NO₂SNa 290.1185; found 290.1208 (Δ = 7.9 ppm).

3.7 Biology Experimental Section

Generation of Standard Curve

A stock solution of the isolated triene product **3.7** (50 mM) in DMSO–H₂O (1:1), was serially diluted with buffered (5 mM Tris, 0.5 mM NaCl, pH 8.0) MeCN–H₂O (1:1) to the following concentrations: 1280, 640, 320, 160, 80, 40 and 20 nM. A small portion of each dilution (60 μL) was transferred to an HPLC vial containing the internal standard **4.6** (see **Chapter 4** for structure and synthesis) (320 nM, 10 μL). Samples were briefly mixed by pipetting and injected onto LC-MS/MS utilizing a Kinetix reverse-phase C₁₈ column (50 mm x 2.1 mm, 2.6 μm, Phenomenex[®]) operated at 0.4 mL min⁻¹ with a column temperature of 35 °C. LC–MS/MS was conducted with AB Sciex QTRAP 5500 mass spectrometer and Shimadzu LC system. The mobile phase A (0.1% formic acid in H₂O) and mobile phase B (MeCN) were run at the following gradient program: 0 min, 5% B; 2 min, 5% B; 7 min, 55% B; 8 min, 70% B; 9 min, 70% B; 10.5 min, 5% B; 12 min, 5% B, STOP. The monitored transitions and retention times are displayed in **Table 3.1**. Peak areas for the product and internal standard (**3.7** and **4.6**) were extracted via SCIEX

Analyst[®] software (**Table 3.2**). Area ratios (product/internal standard) were plotted in Microsoft Excel (**Figure 3.8**)

Table 3.1. CurK DH substrate, product and internal standard LC-MS/MS properties.

Analyte	HPLC retention time (min)	Transition
3.5 or 3.6	6.17	308→ 142
3.7	7.44	268→ 121
4.6	6.80	242→ 95

Table 3.2. CurK DH standard curve data.

Conc. 3.7 (nM)	Transition (g/mol)	Peak Area	Area Ratio (3.7/4.6)
0	268→ 121	7362.665	0.008408595
0	242→ 95	875611.851	
20	268→ 121	22332.363	0.025029893
20	242→ 95	892227.710	
40	268→ 121	31796.445	0.037390844
40	242→ 95	850380.513	
80	268→ 121	59521.288	0.078705923
80	242→ 95	756249.172	
160	268→ 121	107466.167	0.145652283
160	242→ 95	737826.866	
320	268→ 121	228634.211	0.300539582
320	242→ 95	760745.754	
640	268→ 121	425896.088	0.569489824
640	242→ 95	747855.484	
1280	268→ 121	730462.476	1.025132203
1280	242→ 95	712554.414	

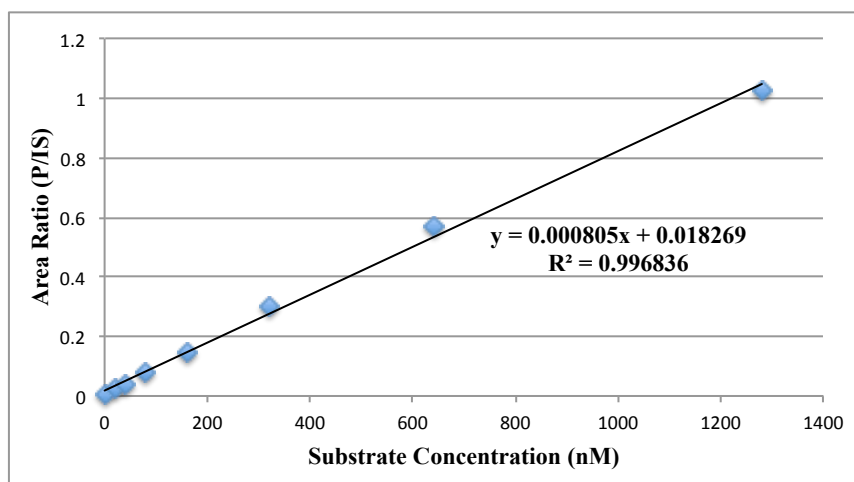


Figure 3.8. Standard curve of product **3.7**.

Quantification of CurK DH activity

Substrate **3.5** (0.25–6.0 mM) was incubated with recombinant CurK DH (20 nM) and reaction buffer (50 mM Tris, 150 mM NaCl, pH 8.0) in a total volume of 50 μ L at ambient temperature (24 $^{\circ}$ C). The reaction was quenched at 4 min time point via transfer of 5 μ L of the reaction mixture into 495 μ L of quench solution MeCN–H₂O (1:1). The quenched mixture was briefly vortexed and centrifuged to crash the protein. A portion of the resulting centrifuged solution (60 μ L) was transferred to a small HPLC vial and combined with the internal standard (10 μ L of a 320 nM solution of diene **4.6**), mixed and injected onto LC-MS/MS. The program was identical for that of the standard curve (*vida supra*). All experiments were performed in duplicate. Transitions and retention times are given in **Table 3.1**. The amount of enzymatic product formed at each substrate concentration was calculated by plotting the area ratio (analyte/internal standard) into the standard curve (**Table 3.3**). Each reaction was performed in duplicate. The calculated initial velocity at each substrate concentration was used to generate a Michaelis-Menten curve utilizing GraphPad Prism software (**Figure 3.7**).

Table 3.3 LC-MS/MS data for CurK DH substrate **3.5**.

Conc. 3.5 (nM)	Transition (g/mol)	Peak Area	Area Ratio (3.7/4.6)	Conc. 3.7 (nM)	Velocity (nM/min)	×100 (dil.)	Velocity (μM/min)
Blank	268→121	9949.448					
Blank	242→95	23056.428					
Blank	268→121	27593.916					
Blank	242→95	69868.674					
0.25	268→121	45799.656	0.0487	37.8	9.45	945.4	0.945
0.25	242→95	940210.259					
0.25	268→121	51390.985	0.0558	46.6	11.7	1166.1	1.166
0.25	242→95	920671.740					
0.50	268→121	153218.239	0.164	181.4	45.4	4535.9	4.536
0.50	242→95	932404.409					
0.50	268→121	88632.4536	0.0973	98.2	24.5	2455.3	2.455
0.50	242→95	910653.094					
1.00	268→121	154376.557	0.171	189.9	47.5	4746.6	4.747
1.00	242→95	902209.734					
1.00	268→121	177808.667	0.186	208.7	52.2	5217.6	5.218
1.00	242→95	954541.380					
2.00	268→121	359675.683	0.397	471.0	117.7	11774.6	11.775
2.00	242→95	905047.196					
2.00	268→121	425682.053	0.452	539.4	134.9	13485.8	13.486
2.00	242→95	940703.784					
3.00	268→121	587242.104	0.610	735.1	183.8	18378.3	18.378
3.00	242→95	962612.388					
3.00	268→121	551492.214	0.607	732.2	183.0	18304.5	18.305
3.00	242→95	907545.802					
6.00	268→121	1015127.87	1.03	1252.	313.0	31299.8	31.300
6.00	242→95	989286.137					
6.00	268→121	900205.392	0.841	1022.	255.6	25557.8	25.558
6.00	242→95	1070107.51					

Chapter 4: Curacin Module I and J Vinylogous Dehydration

4.1 Unusual architectural features of the curacin PKS

Previous analysis of the curacin gene cluster has revealed that expected dehydratases were missing from the PKS in modules G and I and the presence of an unpredicted and extraneous DH in module F (**Figure 4.1**).^{67,71} Neighboring curacin modules could accommodate for the missing eliminations through a process termed ‘domain stuttering’ (**Figure 4.2**).⁷² Stuttering entails an abnormal shuttling of the nascent polyketide chain directly from one ACP to the following module’s ACP. The substrate can then be eliminated by that module’s dehydratase and is loaded onto the ketosynthase within that same module. Normal chain elongation and β -processing occurs within the same module and the polyketide continues on to form the natural product. The expression and structures of all four dehydratases (F, H, J and K) have been previously reported.⁶⁷ The active site channels are surprisingly quite comparable giving few clues on the identity of their native substrates.

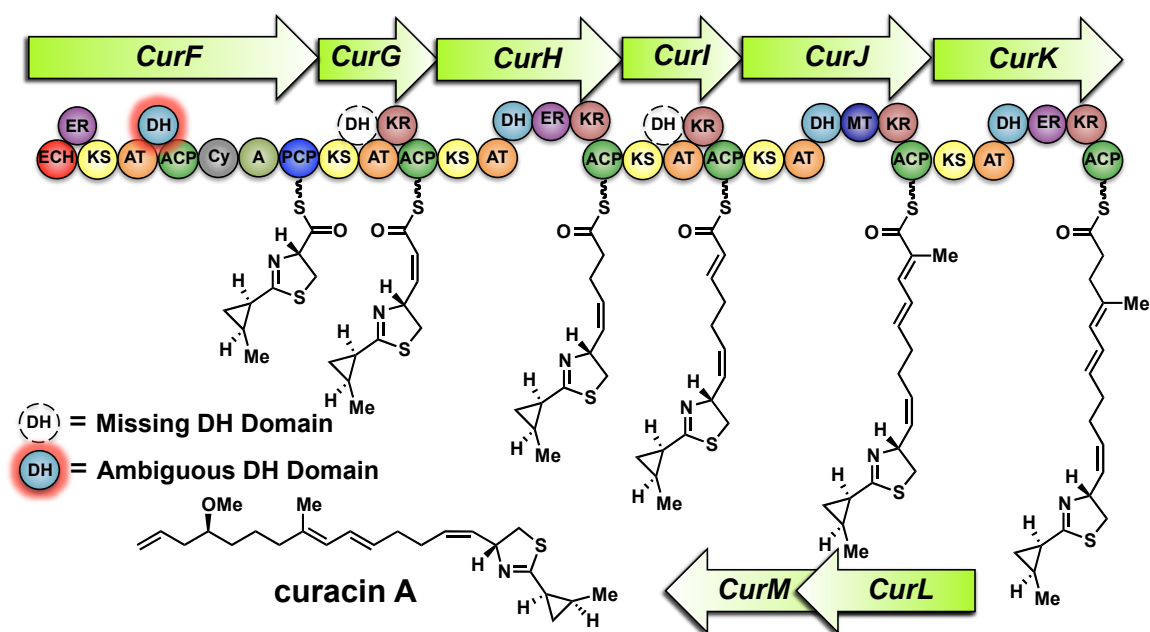


Figure 4.1. The curacin A biosynthetic pathway with proposed polyketide module intermediates. Missing dehydratase domains are shown with dotted lines in modules G and I. The module F dehydratase is shown highlighted in red.

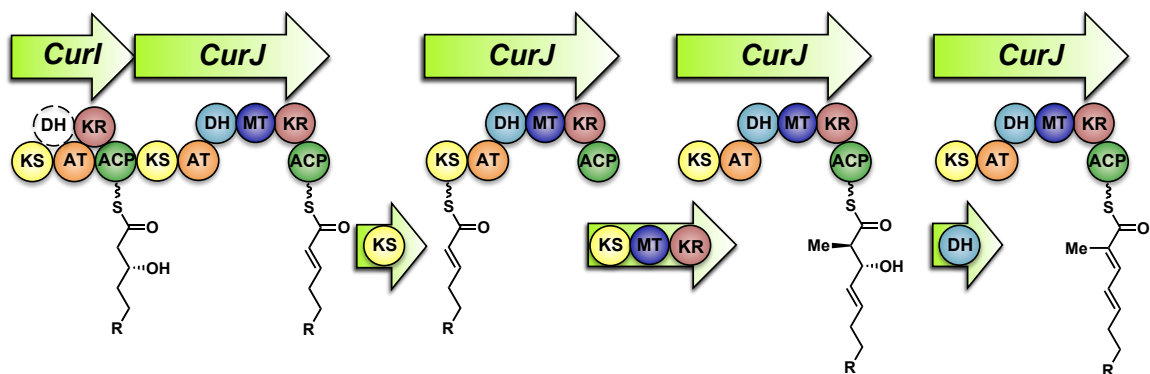


Figure 4.2. A depiction of stuttered dehydration. The CurI domain, lacking the dehydratase necessary to process its formed alcohol product, shuttles the β -hydroxythioester to CurJ's ACP for processing by the CurJ DH. The substrate is then sent back to the ketosynthase in CurJ for normal Claisen reaction followed by reduction and elimination to give the intermediary dienolate.

4.2 Chemical Strategy and Rationale

The stage was set for the *in-vitro* characterization of the atypical domain architecture of the curacin PKS. At the onset of the project we decided it would be most efficient to investigate the potential CurJ module DH substrates first as this module has a clear dehydratase present. Based on empirical, bioinformatic predictions on stereochemistry in the native substrate (**4.1**) the potential substrate **4.2** was designed (**Figure 4.3**). We also planned to synthesize the remaining three diastereomers (**4.3**, **4.4**, and **4.5**) to test the stereoselectivity of this dehydration. The *trans-trans*-dienoate **4.6** was also targeted to provide an authentic product standard. The same, proven strategy of truncation used in CurK (**Chapter 3**) was applied to the design of all CurJ substrates. Analogous work for CurI could determine if a stuttering mechanism was in affect based on the results for CurJ.

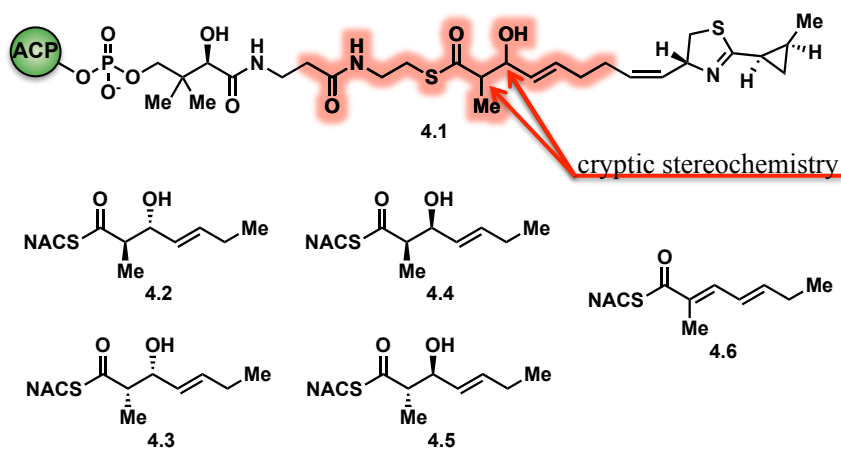
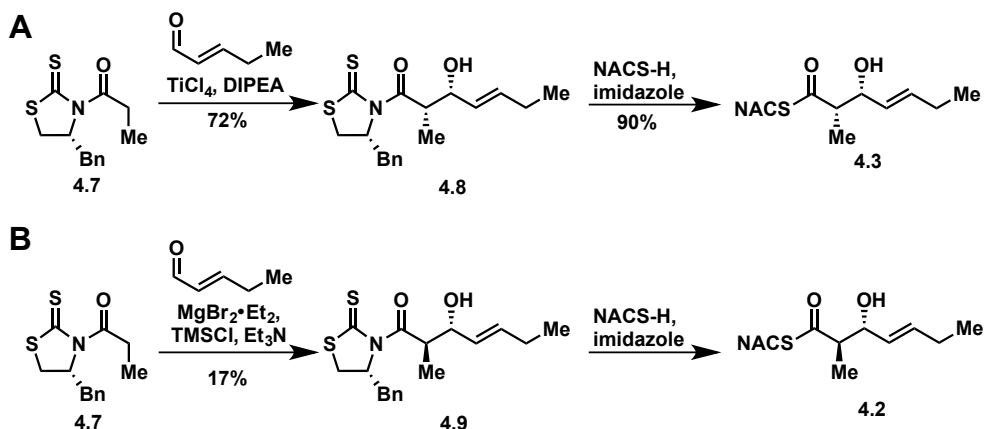


Figure 4.3. The predicted full length CurJ DH substrate (**4.1**) and designed small molecule substrates. The truncated region of the full-length substrate is shown highlighted in coral with the cryptic stereogenic centers shown. The four possible stereoisomers of the truncated substrate are displayed (**4.2–4.5**). Additionally, the dehydration product **4.6** is also shown.

4.3 Synthesis of truncated CurJ DH substrates

We decided to employ a synthetic strategy based on known thiazolidinethione chiral auxiliary chemistry (**Scheme 4.1**).^{73,74} This strategy would allow us to obtain all the desired diastereomers while relying on only two chiral auxiliaries derived from L- and D-phenylalanine. The propionyl thiazolidinethione **3.7** was submitted to anti-Evans *syn*-aldol reaction with TiCl_4 and 2-pentenaldehyde. The resulting aldol adduct was converted to the corresponding *N*-acetylcysteamine thioester by facile thiazolidinethione displacement to yield CurJ substrate analog **4.3** (**Scheme 4.1**, panel A). The anti-aldol products were synthesized utilizing a chlorotrimethylsilane-catalyzed aldol reaction developed by D. A. Evans and coworkers. As previously reported, the reaction provided the desired aldol adduct in poor yield for aldehyde substrates with a saturated γ -proton. Presumably under the reaction conditions the aldehyde is able to polymerize which outcompetes the desired aldol reaction. We were able to obtain enough of the aldol adduct to carry on to form the desired thioester **4.2** (**Scheme 4.1**, panel B). The remaining two diastereomers (**4.4** and **4.5**) were synthesized through identical procedures utilizing the corresponding chiral auxiliary antipode.

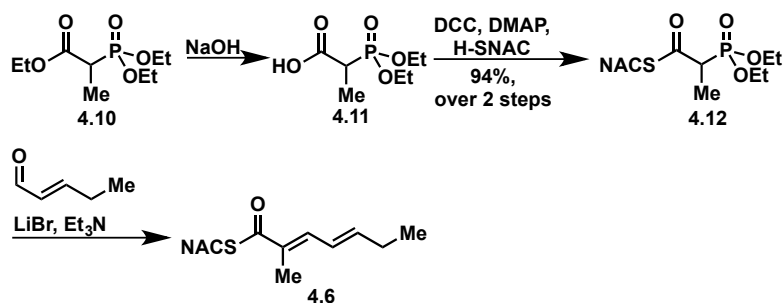
Scheme 4.1. Synthesis of CurJ DH substrates **4.2** and **4.3**.



The predicted CurJ DH product **4.6** was synthesized through use of thioester Horner

Wadsworth-Emmons (HWE) reagent **4.12** (Scheme 4.2).^{75,76} The unique HWE reagent was synthesized from triethyl 2-phosphonopropionate in two steps. Due to the nucleofugality of the *N*-acetylcysteine thioester, we chose to conduct the olefination under previously developed, mild reaction conditions.^{76,77} In the key transformation, the HWE enolate was preformed through use of lithium bromide and triethylamine. To the enolate solution at ambient temperature was added 2-pentenaldehyde in a dropwise fashion. After workup and purification, the CurJ product dienolate **4.6** was obtained in moderate yield.

Scheme 4.2. Synthetic route towards CurJ DH product **4.6**.



4.4 Comparative analysis of curacin DHs and predicted CurJ substrates

With the CurJ substrates and products in hand, we were prepared to analyze the pathway dehydratases for possible activity. Substrates (1 mM) were incubated overnight (12 h) with CurF-DH, H, J, and K DHs (5 μ M). The enzymatic reactions were halted upon addition of quench solution MeCN–H₂O(1:1), centrifuged to precipitate protein and injected and analyzed via LC-MS/MS. The CurJ-DH substrate with stereogenic centers matching the bioinformatic prediction (**4.2**) was only eliminated in the presence of CurF-DH or CurK-DH (**Figure 4.4**, panel A). The experiment highlights the syn nature of the elimination in CurK. This result forced us to consider if the bioinformatics prediction, in fact, incorrectly assigned the substrate's absolute stereochemistry. Surprisingly, the curacin pathway dehydratases could not eliminate any of the remaining

diastereomers (4.3–4.5) (Figure 4.4, panels B–D). Disheartened by the failure of CurJ to process any of the synthesized substrates we sought to reevaluate the curacin pathway in its entirety to rationalize these data.

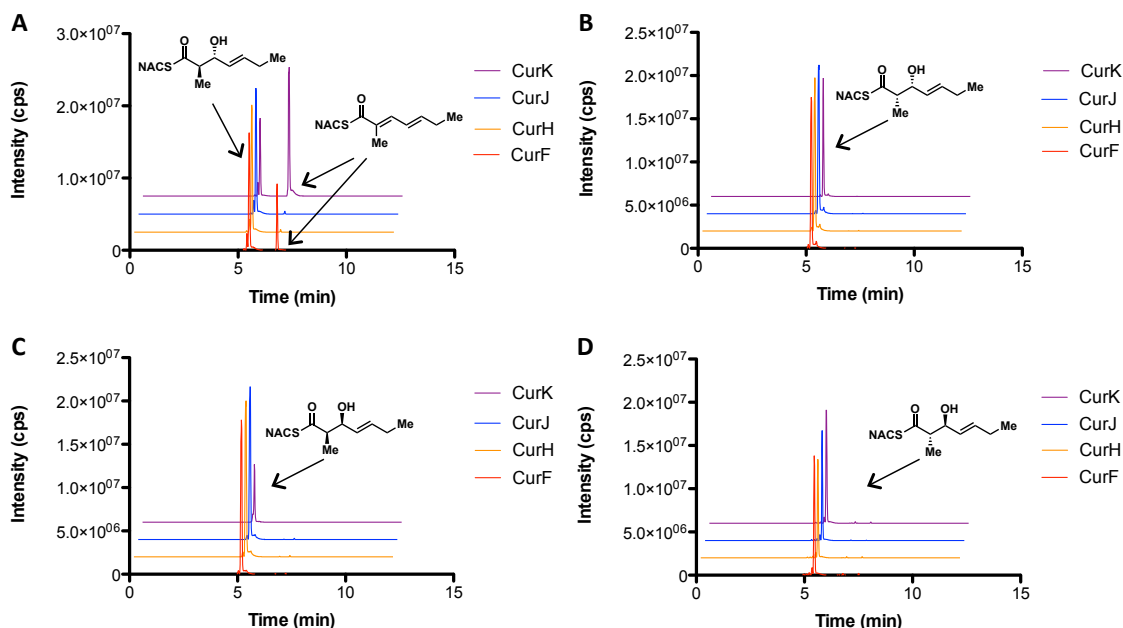


Figure 4.4. LC-MS/MS analysis of predicted CurJ DH substrate activity. The four panels (A, B, C and D) correspond to substrates 4.2, 4.3, 4.4 and 4.5, respectively. The transition 242→95 was used to monitor both substrate and product. The substrate peak remaining after 24 h incubation is shown with retention time of about 5 min. The product 4.6 has a retention time of 6.8 min.

4.5 Vinylogous dehydration theory of anomalous elimination

The failure of CurJ to process its predicted substrate necessitated a new hypothesis for dehydration in the curacin pathway. More specifically, the inability to process substrate 4.2 seemed to rule out the ‘domain stuttering’ mechanism proposed in other biosynthetic pathways (see Figure 4.2). We observed that the modules lacking distinct DH domains (CurG and CurI) always have a dehydratase present in the subsequent, downstream

module (CurH and CurJ). Our working hypothesis was that each module lacking a DH processes its substrate to the β -hydroxy-intermediate (**Figure 4.5**). This is chain extended in the next module by Claisen reaction with a malonyl-unit. The substrate is β -processed through reduction and elimination in the normal fashion. Finally, a DH-catalyzed vinylogous elimination furnishes the necessary diene in the biosynthetic pathway. In addition to removing the awkward stuttering steps present in past proposals, this theory accommodates for the inactivity towards previously synthesized CurJ substrates as these lack the distal hydroxyl moieties from carried over from CurI.

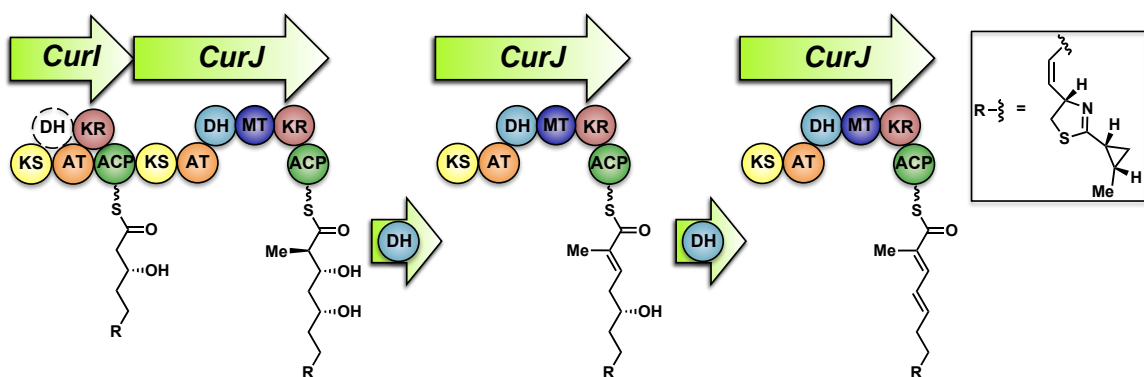


Figure 4.5. Vinylogous elimination catalyzed by the CurJ module. Normal chain elongation occurs with reduction of the formed Claisen condensation product. Following canonical elimination by CurJ DH, vinylogous elimination affords the crucial diene intermediate for curacin biosynthesis.

4.6 Chemical strategy and rationale for vinylogous elimination substrates

The new vinylogous elimination hypothesis necessitated a new series of synthetic substrates to examine if it actually was in effect in the curacin biosynthetic pathway. We chose to test our proposal by two distinct compound designs. Firstly, we required truncated vinylogous substrates **4.13** and **4.14** to test the CurJ module dehydratase's ability to catalyze the critical elimination (**Figure 4.6**). This would allow us to examine any inherent stereoselectivity in the dehydration. We also proposed to synthesize the

thioether substrate **4.15**. This substrate would allow us to examine both proposed elimination events while avoiding instabilities inherent in δ -hydroxyl- α,β -saturated substrates which are prone to intramolecular cyclization (**Scheme 4.3**). Additionally, we hypothesized that the pendant primary alcohol of **4.15** may mimic the hydrogen bonding elements missing from the previous, unsuccessful CurJ substrates (**4.2-4.5**).

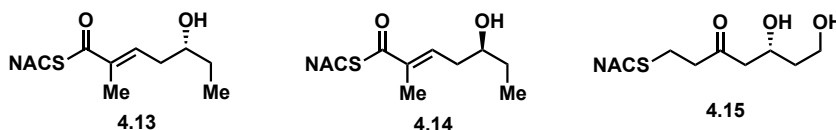
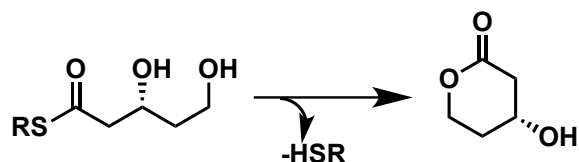


Figure 4.6. Designed vinylogous elimination substrates for CurJ DH.

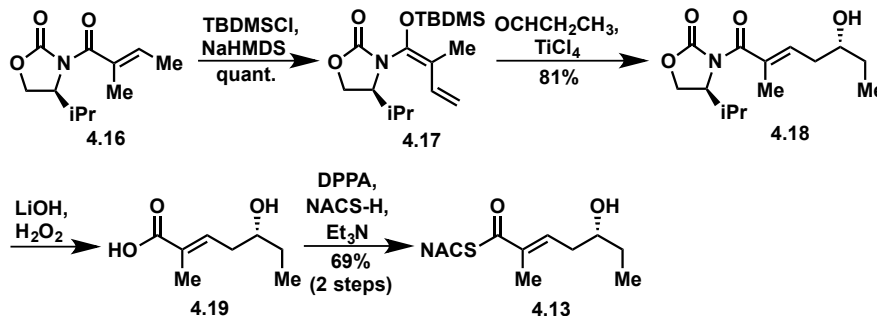
Scheme 4.3. Intramolecular cyclization of δ -hydroxyl-thioesters.



4.7 Synthesis of CurJ DH vinylogous elimination substrates

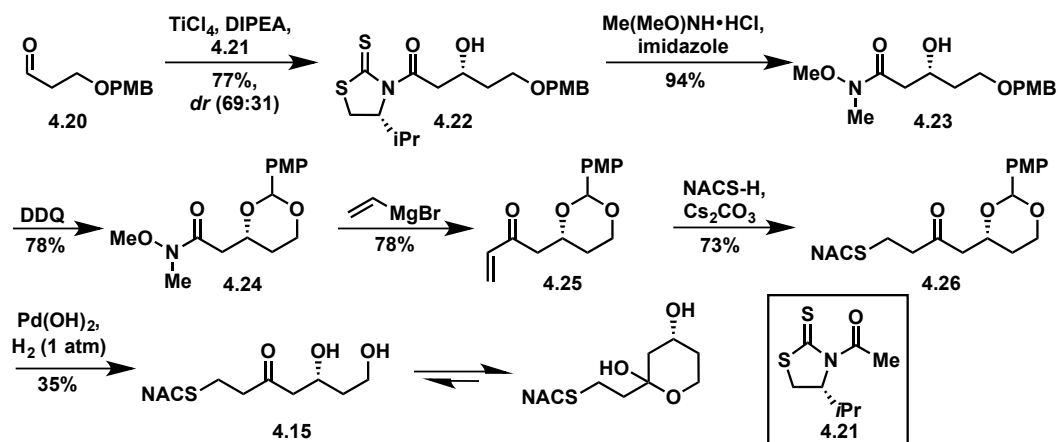
The synthesis of **4.13** began with deprotonation of known acyl oxazolidinone **4.16** and trapping of the resulting enolate with tert-butyldimethylsilyl chloride (**Scheme 4.4**). The resulting *N,O*-silyl ketene acetal (**4.17**) was submitted to vinylogous Mukaiyama aldol reaction with propionaldehyde.³⁰ The vinylogous aldol adduct **4.18** was saponified and coupled with *N*-acetylcysteamine to afford the D-alcohol substrate **4.13**. The enantiomeric compound **4.14** was synthesized in an identical manner starting with the D-valine derived enantiomer of **4.16** (*ent*-**4.16**).

Scheme 4.4. The short synthesis of vinylogous dehydration substrate **4.13**.



The synthesis of the diol substrate **4.15** commenced with known aldehyde **4.20**, itself derived in two steps from 1,3-propanediol (**Scheme 4.5**).⁷⁸ Acetate aldol reaction with Nagao's D-valine-derived acetyl thiazolidinethione (**4.21**) yielded aldol adduct **4.22** and its diastereomer (not shown) in a ratio of 69:31 favoring the desired **4.22**.³² The major diastereomer was submitted to thiazolidinethione displacement with methanol giving the known methyl ester to confirm the alcohol stereocenter (Not shown, see **Chemistry experimental section**).^{79,80} Facile thiazolidinethione displacement with *N,O*-dimethylhydroxylamine afforded Weinreb amide **4.23**. Benzylic oxidation of the *para*-methoxybenzyl ether with 2,3-dichloro-5,6-dicyano-1,4-benzoquinone (DDQ) served to protect the β -hydroxyl group. The fully protected Weinreb amide **4.24** was converted to the vinyl ketone **4.25** via action of vinylmagnesium bromide.³⁴ Michael addition of *N*-acetylcysteamine served to install the pantetheine-mimicking portion of the substrate. A final deprotection of **4.26** with Pearlman's catalyst under an atmosphere of hydrogen afforded the desired diol substrate in low yields. A substantial amount of starting material was recovered in this reaction (~35%). Given the markedly slow reaction rate we rationalized that the thioether is most likely poisoning the catalyst, thereby increasing the reaction time and allowing for decomposition. The desired product **4.15** was obtained in sufficient quantities for full characterization and was found to exist in equilibrium of both open chain and hemi-ketal forms.

Scheme 4.5. The synthesis of di-dehydration substrate **4.15**.



4.8 Comparative analysis of vinylogous elimination in the curacin pathway

Having completed the synthesis of all potential substrates for vinylogous elimination we were poised to test for the hypothetical dehydration using recombinant curacin dehydratase domains. Following a similar procedure to that utilized for prior CurJ substrates, all substrate-enzyme combinations were tested in parallel and analyzed via LC-MS/MS. Similar to trends observed for canonical elimination all enzymes were unable to process L-alcohol substrate **4.14**, but module CurH and CurJ dehydratases were proficient at eliminating D-alcohol **4.13**, forming diene **4.6** (Figure 4.7, panels A and B). Although the conversion was quite low (~3%) we were encouraged by the stereoselective nature of the enzyme-catalyzed reaction. Moreover, the fact that module CurF and CurK DHs were unable to catalyze the reaction fit well into the theory of vinylogous elimination in the curacin pathway as neither of these follows a module lacking a dehydratase.

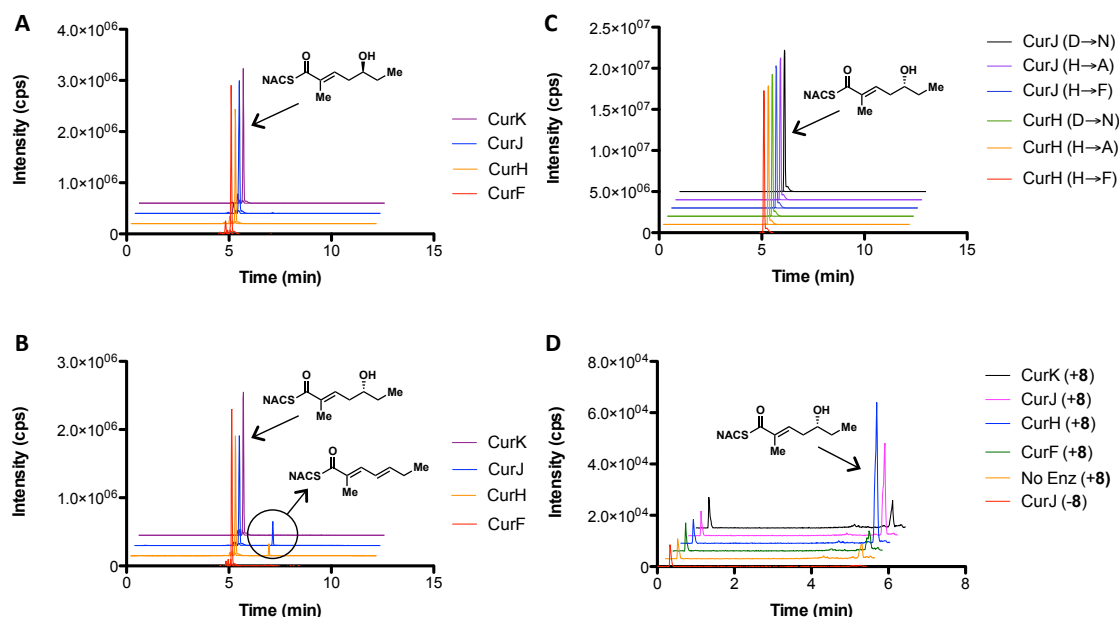


Figure 4.7. Incubation of substrates 4.13 and 4.14 with the curacin dehydratases. Panels A and B display the traces resulting from incubation vinylogous substrates 4.14 and 4.13, respectively. The loss of activity towards substrate 4.13 resulting from dyad-mutants is shown in panel C. Detection of the reverse reaction from diene 4.7 to form 4.13 is presented in Panel D. The diene was detected from the transition 242→95. The vinylogous substrate was detected scanning for the transition 260→141.

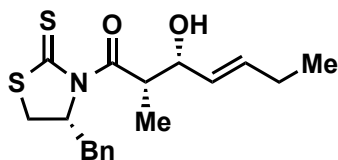
In a similar fashion to the CurK DH we tested several potential knockout mutants of the CurH and CurJ dehydratases (Figure 4.7, panel C). These mutants were created by single-point mutation of the recombinant curacin dehydratases by our collaborator Gregory Dodge (Dr. Janet L. Smith lab, University of Michigan- Life Sciences Institute). Knockout mutations of the catalytic dyad (His and Asp residues) completely ablated vinylogous elimination activity. This indicates a similar mechanism between canonical α,β -elimination and vinylogous dehydration.

Given the poor turnover of the substrate we wanted to investigate the ability of the enzymes to catalyze the reverse reaction. In this case, the net reaction would be hydration

of the diene **4.6** in across the distal, γ,δ -olefin. We incubated each enzyme overnight with the diene and scanned for alcohol formation using its known transition and retention time. Judging by the LC/MS-MS traces we could see alcohol formation with both CurK and CurF DHs at levels consistent with the control without enzyme (**Figure 4.7**, panel **D**). In contrast, incubation with CurH and CurJ dehydratases led to a significant increase in the amount of alcohol **4.13**, consistent with enzyme-catalyzed hydration. Not unlike the dehydration, we only saw fractional turnover to the hydrated substrate in the reverse reaction. As we are unable to reach a stable equilibrium, we proposed a slow forward, dehydration reaction with disfavored binding of product compared to substrate.

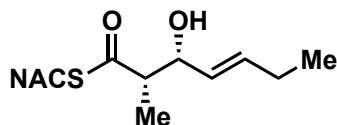
Unfortunately, we were unable to detect any product formation (mono- or di-dehydration) when incubating substrate **4.15** with any of the curacin dehydratase domains. We hypothesized two possible reasons for this result: 1) Diol **4.15**, being significantly more polar than the native substrate, is unable to gain access to the hydrophobic substrate tunnel or 2) The equilibrium between hemi-ketal and open chain forms precludes substrate binding of the latter in the enzyme active site. Additionally, substrate **4.15** is a severely truncated version of the native substrate for CurH and CurJ, which may inhibit binding and enzyme-catalyzed dehydration.

4.9 Chemistry experimental section



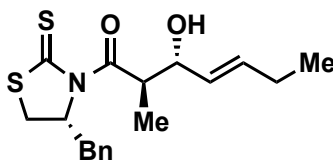
(2*S*,3*R*,*E*)-1-((*R*)-4-Benzyl-2-thioxothiazolidin-3-yl)-3-hydroxy-2-methylhept-4-en-1-one (4.8). To a flask containing thiazolidinethione **4.7** (0.250 g, 0.940 mmol, 1.00 equiv) under argon atmosphere was added CH₂Cl₂ (4.00 mL). The bright yellow solution was placed in ice-water bath (0 °C) and supplemented with TiCl₄ (0.110 mL, 0.990 mmol, 1.05 equiv). The resulting bright orange, opaque solution was stirred for 9 min. To the

reaction mixture was added freshly distilled $i\text{Pr}_2\text{NEt}$ ⁵⁶ (0.183 mL, 1.05 mmol, 1.12 equiv). The reaction was stirred at 0 °C for 40 min. To the dark red mixture was slowly added freshly distilled 2-pentenaldehyde⁵⁶ (0.138 mL, 1.41 mmol, 1.50 equiv) causing a color change to dark brown. After 2 h, the reaction was halted via addition of a saturated NH_4Cl (5.00 mL). The biphasic mixture was warmed to room temperature and the layers separated. The aqueous layer was extracted with CH_2Cl_2 (3×10.0 mL) and the combined organic layers were dried over Na_2SO_4 and filtered. The filtrate was concentrated under reduced pressure and purified flash chromatography (20% EtOAc/hexanes). The title compound (0.252 g, 0.677 mmol, 72 %) was isolated as viscous, yellow oil. TLC: R_f = 0.20 (20% EtOAc/hexanes); $[\alpha]_D^{23} = -191.6$ (c 1.00, CHCl_3); ^1H NMR (CDCl_3 , 400 MHz) δ 7.37–7.27 (m, 5H), 5.82 (ddt, J = 15.6, 6.4, 1.2 Hz, 1H), 5.50 (ddt, J = 15.2, 6.0, 1.2 Hz, 1H), 5.39 (ddd, J = 10.6, 6.8, 4 Hz, 1H), 4.79 (dq, J = 6.8, 3.2 Hz, 1H), 4.59–4.54 (m, 1H), 3.37 (dd, J = 11.6, 6.8 Hz, 1H), 3.24 (dd, J = 13.2, 4.0 Hz, 1H), 3.04 (dd, J = 13.2, 10.4 Hz, 1H), 2.88 (d, J = 11.6 Hz, 1H), 2.74 (d, J = 2.8 Hz, 1H), 2.08 (app. quint, J = 7.2, 2H), 1.19 (d, J = 6.8 Hz, 3H), 1.01 (t, J = 7.6 Hz, 3H); ^{13}C NMR (CDCl_3 , 100 MHz) δ 201.8, 177.8, 136.6, 135.0, 129.6, 129.1, 127.9, 127.4, 72.5, 69.1, 43.5, 37.1, 31.9, 25.5, 13.6, 11.6; HRMS (ESI-TOF) m/z : $[\text{M} + \text{Na}]^+$ Calcd for $\text{C}_{18}\text{H}_{23}\text{NO}_2\text{S}_2\text{Na}$ 372.1062, found 372.1087 (Δ = 6.7 ppm).



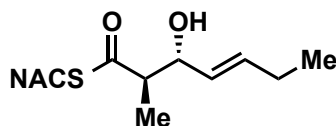
***S*-(2-Acetamidoethyl) (2*S*,3*R*,*E*)-3-hydroxy-2-methylhept-4-enethioate (4.3).** To a flask was added the aldol adduct **4.8** (25.2 mg, 0.0721 mmol, 1.00 equiv) and CH_2Cl_2 (5.00 mL). The bright yellow solution was supplemented with *N*-acetylcysteamine (8.43 μL , 0.0793 mmol, 1.10 equiv) and imidazole (14.7 mg, 0.216 mmol, 3.00 equiv). The reaction mixture was at ambient temperature for 21 h. The reaction mixture was evaporated by nitrogen stream and purified by flash chromatography (5% MeOH/ CH_2Cl_2). The title compound (16.9 mg, 0.0652 mmol, 90%) was isolated as a

colorless, viscous oil. TLC: R_f = 0.20 (5% MeOH/CH₂Cl₂); $[\alpha]_D^{24}$ = 27.6 (c 0.87, CHCl₃); ¹H NMR (CDCl₃, 400 MHz) 5.79 (br s, 1H), 5.77 (ddt, J = 15.2, 6.4, 1.2 Hz, 1H), 5.44 (ddt, J = 15.2, 6.8, 1.6 Hz, 1H), 4.37 (br s, 1H), 3.52–3.34 (m, 2H), 3.10–2.96 (m, 2H), 2.84–2.75 (m, 1H), 2.06 (app. quint, J = 6.8 Hz, 2H), 1.96 (s, 3H), 1.22 (d, J = 6.4 Hz, 3H), 0.99 (t, J = 7.2 Hz, 3H); ¹³C NMR (CDCl₃, 100 MHz) δ 203.6, 170.5, 135.7, 128.0, 73.6, 54.0, 39.6, 28.7, 25.4, 23.4, 13.5, 12.0; HRMS (ESI-TOF) m/z : $[M + Na]^+$ Calcd for C₁₂H₂₁NO₃SNa 282.1134, found 282.1136 (Δ = 0.7 ppm).

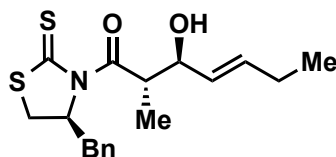


(2R,3R,E)-1-((R)-4-Benzyl-2-thioxothiazolidin-3-yl)-3-hydroxy-2-methylhept-4-en-1-one (4.9). To a flask was added MgBr₂•OEt₂ (14.6 mg, 0.0566 mmol, 0.100 equiv). The flask was charged with acyl thiazolidinethione **4.7** (0.150 g, 0.566 mmol, 1.00 equiv), EtOAc (1.4 mL) and freshly distilled 2-pentenaldehyde⁵⁶ (60.9 μ L, 0.623 mmol, 1.10 equiv). The yellow solution was supplemented with distilled Et₃N (0.158 mmol, 1.13 mmol, 2.00 equiv) and TMSCl⁵⁶ (0.108 mL, 0.849 mmol, 1.50 equiv). The reaction mixture was stirred under inert atmosphere at room temperature for 26 h. The reaction was filtered through a silica gel plug (2.00 cm), washed with Et₂O (20.0 mL) and concentrated under reduced pressure. The crude residue was dissolved in a biphasic mixture of THF (10.0 mL) and aqueous HCl (1.00 N, 2.00 mL) and vigorously stirred at ambient temperature for 2 h. The reaction was halted via addition of aqueous NaHCO₃ (10.0 mL) and the biphasic solution was separated. The aqueous layer was extracted with EtOAc (3x 15.0 mL) and the combined organic fractions were dried over Na₂SO₄ and filtered. The crude residue obtained from concentration under reduced pressure was purified by flash chromatography (20% EtOAc/hexanes) furnishing the title compound (35.8 mg, 0.0962 mmol, 17% yield) as a viscous, yellow oil. TLC: R_f = 0.28 (20% EtOAc/hexanes); $[\alpha]_D^{24}$ = -297.1 (c 1.00, CHCl₃); ¹H NMR (CDCl₃, 400 MHz) δ 7.37–7.27 (m, 5H), 5.79 (dt, J = 15.2, 5.6 Hz, 1H), 5.42 (ddt, J = 15.2, 7.2, 1.6 Hz, 1H), 5.25

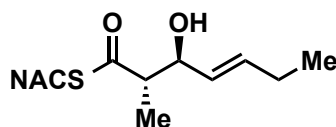
(ddd, $J = 10.8, 6.8, 3.6$ Hz, 1H), 4.34 (dq, $J = 7.6, 6.8$ Hz, 1H), 4.26 (t, $J = 7.6$ Hz, 1H), 3.39 (dd, $J = 11.2, 6.8$ Hz, 1H), 3.26 (dd, $J = 13.2, 3.6$ Hz, 1H), 3.06 (dd, $J = 12.8, 10.8$ Hz, 1H), 2.90 (d, $J = 11.6$ Hz, 1H), 2.16 (br s, 1H), 2.06 (app. quint, $J = 6.4$, 2H), 1.22 (d, $J = 6.8$ Hz, 3H), 1.00 (t, $J = 7.2$ Hz, 3H); ^{13}C NMR (CDCl_3 , 100 MHz) δ 201.5, 178.2, 136.7, 136.3, 129.6, 129.3, 129.0, 127.3, 76.7, 69.2, 45.2, 36.8, 32.8, 25.4, 14.9, 13.5; HRMS (ESI-TOF) m/z : $[\text{M} + \text{Na}]^+$ Calcd for $\text{C}_{18}\text{H}_{23}\text{NO}_2\text{S}_2\text{Na}$ 372.1062, found 372.1049 ($\Delta = 3.4$ ppm).



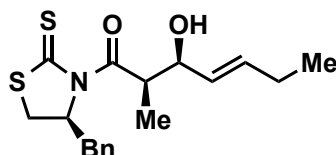
***S*-(2-acetamidoethyl) (2*R*,3*R*,*E*)-3-hydroxy-2-methylhept-4-enethioate (4.2).** To a flask was added the acyl thiazolidine **4.9** (31.1 mg, 0.0890 mmol, 1.00 equiv) in CH_2Cl_2 (4.00 mL). The resulting bright yellow solution was supplemented with imidazole (18.2 mg, 0.267 mmol, 3.00 equiv) and *N*-acetylcysteamine (10.4 μL , 0.0980 mmol, 1.10 equiv). The reaction mixture was vigorously stirred under argon at ambient temperature for 21 h. The crude reaction mixture was concentrated under reduced pressure and purified by flash chromatography (5% MeOH/ CH_2Cl_2). The title compound (16.8 mg, 0.0596 mmol, 67%) was furnished as a slightly yellow, viscous oil. TLC: $R_f = 0.30$ (5% MeOH/ CH_2Cl_2); $[\alpha]_D^{24} = -34.5$ (c 0.29, CHCl_3); ^1H NMR (CDCl_3 , 400 MHz) δ 6.00 (br s, 1H), 5.76 (dt, $J = 15.6, 6.0$ Hz, 1H), 5.40 (ddt, $J = 15.6, 6.4, 1.2$ Hz, 1H), 4.19 (t, $J = 7.6$ Hz, 1H), 3.55–3.37 (m, 2H), 3.13–2.98 (m, 2H), 2.76 (app. quint, $J = 7.2$ Hz, 1H), 2.42 (br s, 1H), 2.06 (app. quint, $J = 7.6$ Hz, 2H), 1.94 (s, 3H), 1.11 (d, $J = 6.8$ Hz, 3H), 1.00 (t, $J = 7.6$ Hz, 3H); ^{13}C NMR (CDCl_3 , 100 MHz) δ 203.6, 170.6, 136.6, 128.8, 75.5, 54.5, 39.5, 28.7, 25.4, 23.3, 15.1, 13.5; HRMS (ESI-TOF) m/z : $[\text{M} + \text{Na}]^+$ Calcd for $\text{C}_{12}\text{H}_{21}\text{NO}_3\text{SNa}$ 282.1134, found 282.1153 ($\Delta = 6.7$ ppm).



(2*S*,3*S*,*E*)-1-((*S*)-4-Benzyl-2-thioxothiazolidin-3-yl)-3-hydroxy-2-methylhept-4-en-1-one (*ent*-4.9). The desired aldol product was obtained an analogous method as the enantiomer, **4.9**, affording the title compound (10%) as a viscous yellow oil. $[\alpha]_D^{24} = 302.6$ (*c* 1.00, CHCl₃). The title compound was identical to its enantiomer, **4.9**, in all remaining aspects.

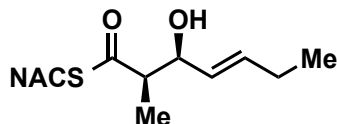


***S*-(2-Acetamidoethyl) (2*S*,3*S*,*E*)-3-hydroxy-2-methylhept-4-enethioate (4.4).** The thioester **4.4** was synthesized in an analogous manner to that of the prior thioester **4.2** furnishing the title compound as a colorless oil (42%). $[\alpha]_D^{24} = 37.3$ (*c* 0.35, CHCl₃). **4.4** was found to be identical to its enantiomer (**4.2**) in all remaining aspects.

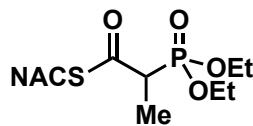


(2*R*,3*S*,*E*)-1-((*S*)-4-benzyl-2-thioxothiazolidin-3-yl)-3-hydroxy-2-methylhept-4-en-1-one (*ent*-4.8). The desired aldol product was obtained an analogous method as the enantiomer, **4.8**. The alcohol was a viscous, yellow oil (78%). $[\alpha]_D^{23} = 199.3$ (*c* 1.00, CHCl₃). The compound matched its enantiomer, **4.8**, in all remaining aspects.

The total yield was 86% from the 91:6:3 mixture of diastereomers.

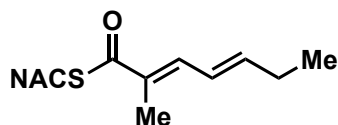


***S*-(2-Acetamidoethyl) (2*R*,3*S*,*E*)-3-hydroxy-2-methylhept-4-enethioate (4.5).** The thioester **4.5** was synthesized in an analogous manner to that of the thioester **4.3** yielding a colorless oil (63%). $[\alpha] = -24.1$ (c 0.58, CHCl_3). The compound matched its enantiomer (**4.3**) in all other aspects.

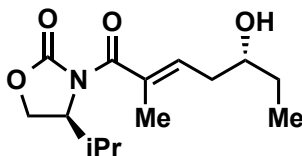


***S*-(2-Acetamidoethyl) 2-(diethoxyphosphoryl)propanethioate (4.12).** A flask containing triethyl 2-phosphonopropionate **4.10** (1.00 mL, 4.66 mmol, 1.00 equiv) in H_2O (2.00 mL) was cooled via ice water bath ($0\text{ }^\circ\text{C}$). To the chilled mixture was slowly added a cooled ($4\text{ }^\circ\text{C}$), aqueous NaOH solution (10.0 N, 0.490 mL, 4.90 mmol, 1.05 equiv). The reaction mixture was allowed to slowly warm to room temperature and stirred for 20 h. The reaction was quenched upon addition of aqueous HCl (1.00 M) until the pH was 1.00. The resulting solution was saturated with NaCl and extracted with CH_2Cl_2 (4×10.0 mL). The combined organic layers were dried over Na_2SO_4 , filtered and the solvent removed under reduced pressure. The crude residue was dissolved in CH_2Cl_2 (40.0 mL) and cooled by placing in an ice water bath ($0\text{ }^\circ\text{C}$). To the chilled solution was added DMAP (57.0 mg, 0.467 mmol, 0.100 equiv) and DCC (1.01 g, 4.89 mmol, 1.05 equiv) and the solution was stirred for 2 min. *N*-acetylcysteamine (0.644 mL, 6.06 mmol, 1.30 equiv) was added to the reaction mixture. The resulting solution was allowed to warm to ambient temperature and stirred 22 h. The reaction mixture was supplemented with Et_2O (40.0 mL) and filtered to remove the urea precipitate. The filtrate was concentrated under reduced pressure and the resulting crude residue was purified by flash chromatography (100% EtOAc) affording the title compound (1.36 g, 4.37 mmol, 94%) as a clear colorless oil. TLC: $R_f = 0.15$ (100% EtOAc); ^1H NMR (CDCl_3 , 400 MHz) δ 6.30 (br s, 1H), 4.21–4.09 (m, 4H), 3.54–3.37 (m, 2H), 3.29 (dq, $J = 22.4, 7.2$ Hz, 1H),

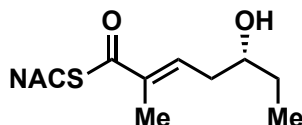
3.20–3.12 (m, 1H), 3.04–2.95 (m, 1H), 1.96 (s, 3H), 1.45 (dd, $J = 18.0, 7.2$ Hz, 3H), 1.34 (t, $J = 7.2$ Hz, 6H); ^{13}C NMR (CDCl_3 , 100 MHz) δ 196.1, 196.0, 170.6, 63.34, 63.27, 63.0, 62.9, 49.2, 47.9, 39.2, 29.4, 23.2, 16.54, 16.48, 12.51, 12.45; HRMS (ESI-TOF) m/z : $[\text{M} + \text{Na}]^+$ Calcd for $\text{C}_{11}\text{H}_{22}\text{NO}_5\text{PSNa}$ 334.0849, found 334.0847 ($\Delta = 0.6$ ppm).



***S*-(2-Acetamidoethyl) (2*E*,4*E*)-2-methylhepta-2,4-dienethioate (4.6).** To a flask containing LiBr (0.132 g, 1.52 mmol, 3.16 equiv) was added THF (6.00 mL). To the resulting solution was added the phosphono-thioester **4.12** (0.150 g, 0.482 mmol, 1.00 equiv). The solution was stirred vigorously at ambient temperature for 10 min. To the reaction mixture was Et_3N (0.212 mL, 1.52 mmol, 3.16 equiv) resulting in the formation of a cloudy, colorless solution that was stirred at ambient temperature for 15 min. To the reaction vessel was added freshly distilled 2-pentenaldehyde⁵⁶ (99.0 μL , 1.02 mmol, 2.11 equiv) in a dropwise fashion. After stirring for 24 h, the reaction mixture was quenched upon addition of H_2O (30.0 mL). The biphasic solution was separated and the aqueous layer was repeatedly extracted with EtOAc (4×10.0 mL). The combined organic fractions were dried over Na_2SO_4 , filtered and concentrated under reduced pressure. The crude product residue was purified by flash chromatography (50% EtOAc/hexanes) yielding the title compound (49.5 mg, 0.205 mmol, 43%) as a cloudy oil. TLC: $R_f = 0.30$ (5% MeOH/ CH_2Cl_2); ^1H NMR (CDCl_3 , 400 MHz) δ 7.17 (d, $J = 10.8$ Hz, 1H), 6.35 (dd, $J = 14.8, 11.2$ Hz, 1H), 6.22 (dt, $J = 5.6, 15.2$ Hz, 1H), 6.01 (br s, 1H), 3.52–3.40 (m, 2H), 3.15–3.03 (m, 2H), 2.30–2.16 (m, 2H), 1.97 (s, 6H), 1.07 (t, $J = 6.8$ Hz, 3H); ^{13}C NMR (CDCl_3 , 100 MHz) δ 193.9, 170.8, 146.9, 138.5, 132.6, 124.8, 40.2, 28.5, 26.7, 23.4, 13.2, 12.7; HRMS (ESI-TOF) m/z : $[\text{M} + \text{Na}]^+$ Calcd for $\text{C}_{12}\text{H}_{19}\text{NO}_2\text{SNa}$ 264.1029; Found 264.1043 ($\Delta = 5.3$ ppm).



(S)-3-((R,E)-5-Hydroxy-2-methylhept-2-enoyl)-4-isopropylloxazolidin-2-one (4.18). A flask containing CH_2Cl_2 (15.0 mL) was supplemented with freshly distilled propionaldehyde⁵⁶ (0.443 mL, 6.14 mmol, 2.00 equiv) and cooled by dry ice–acetone bath ($-78\text{ }^\circ\text{C}$). To the reaction mixture was added TiCl_4 (0.338 mL, 3.07 mmol, 1.00 equiv). To the resulting yellow reaction mixture was slowly added the *N,O*-silyl ketene acetal **4.17**⁸¹ (1.00 g, 3.07 mmol, 1.00 equiv) as a solution in CH_2Cl_2 (14.6 mL). The reaction mixture was transferred to a dry ice–MeCN bath ($-40\text{ }^\circ\text{C}$) and stirred for 7 h. The reaction was halted via sequential addition of a saturated aqueous potassium sodium tartrate (10.0 mL) and a saturated, aqueous NaHCO_3 (10.0 mL). The resulting cloudy mixture was vigorously stirred at room temperature for 1 h. The biphasic solution was separated and the aqueous layer was extracted with CH_2Cl_2 ($3 \times 20.0\text{ mL}$). The combined organic layers were dried over Na_2SO_4 , filtered and concentrated under reduced pressure. The crude product residue was purified by flash chromatography (30% EtOAc/hexanes) affording the title compound (0.673 g, 2.49 mmol, 81%) as a white amorphous solid. TLC: $R_f = 0.20$ (30% EtOAc/hexanes); $[\alpha]_D^{24} = 46.0$ (c 1.00, CHCl_3); ^1H NMR (CDCl_3 , 400 MHz) δ 6.03 (t, $J = 7.6\text{ Hz}$, 1H), 4.56 (dt, $J = 8.8, 4.8\text{ Hz}$, 1H), 4.33 (t, $J = 8.8\text{ Hz}$, 1H), 4.9 (dd, $J = 8.8, 5.2\text{ Hz}$, 1H), 3.70–3.60 (m, 1H), 2.53 (br s, 1H), 2.43–2.26 (m, 3H), 1.94 (s, 3H), 1.65–1.47 (m, 2H), 0.98 (t, $J = 7.6\text{ Hz}$, 3H), 0.92 (t, $J = 6.8\text{ Hz}$, 6H); ^{13}C NMR (CDCl_3 , 100 MHz) δ 171.7, 154.4, 135.4, 133.2, 72.2, 63.6, 58.3, 36.5, 29.9, 28.5, 18.0, 15.3, 13.9, 10.4, 7.3; HRMS (ESI-TOF) m/z : $[\text{M} + \text{Na}]^+$ Calcd for $\text{C}_{14}\text{H}_{23}\text{NO}_4\text{Na}$ 292.1519, found 292.1529 ($\Delta = 3.4\text{ ppm}$).



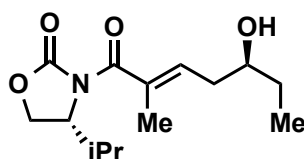
S-(2-Acetamidoethyl) (R,E)-5-hydroxy-2-methylhept-2-enethioate (4.13). To a flask

was added the imide **4.18** (0.190 g, 0.707 mmol, 1.00 equiv). The solid was dissolved in a THF–H₂O (2:1, 6.43 mL) solution and vigorously stirred in ice–water bath (0 °C). To the chilled reaction mixture was added H₂O₂ (30% in water, 0.219 mL, 1.93 mmol, 3.00 equiv) followed by LiOH•H₂O (80.9 mg, 1.93 mmol, 3.00 equiv). The reaction mixture was vigorously stirred overnight, slowly warming to ambient temperature. After 24 h, an additional aliquot of H₂O₂ (80.0 µL, 0.707 mmol, 1.00 equiv) and LiOH•H₂O (29.7 mg, 0.707 mmol, 1.00 equiv) were added to the reaction mixture at 0 °C. The reaction mixture was allowed to warm to ambient temperature over 36 h. The crude solution was concentrated under reduced pressure, removing all ethereal solvents. The resulting aqueous solution was supplemented with aqueous saturated NaHCO₃ (1.00 mL) and washed with Et₂O (2 × 10.0 mL). The aqueous fraction was acidified with aqueous HCl (2 M) to pH 2 and extracted with Et₂O (4 × 10.0 mL). The combined organics were concentrated to dryness under reduced pressure and the crude colorless oil (0.112 g) was submitted directly to the next reaction.

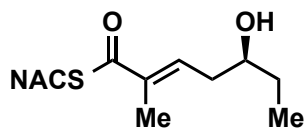
To a flask containing a portion of the crude acid **4.19** (82.2 mg, 0.520 mmol, 1.00 equiv) was added anhydrous DMF (2.73 mL). The reaction flask was cooled via ice–water bath (0 °C) and allowed to dissolve with stirring. To the chilled solution was sequentially added DPPA (0.168 mL, 0.780 mmol, 1.50 equiv) and Et₃N (145 µL, 1.04 mmol, 2.00 equiv). The reaction mixture was stirred at 0°C for 2 h. An aliquot of *N*-acetylcysteamine (55.3 µL, 0.520 mmol, 1.00 equiv) was added to the reaction mixture at 0°C. The slightly yellow solution was allowed to gradually warm to ambient temperature and stirred 5 h 30 min. The reaction mixture was quenched upon addition of H₂O (3.00 mL) and EtOAc (10.0 mL) and the biphasic solution was separated. The aqueous layer was extracted with EtOAc (4 × 10.0 mL). The combined organic fractions were dried over Na₂SO₄, filtered and concentrated under reduced pressure. The crude product residue was purified via flash chromatography (5–10% MeOH/CH₂Cl₂) yielding the title compound (92.6 mg, 0.357 mmol, 69% over 2 steps) as a clear, colorless oil. TLC: *R_f* = 0.20 (5% MeOH/CH₂Cl₂); $[\alpha]_{\text{D}}^{24} = -15.3$ (*c* 1.00, CHCl₃); ¹H NMR (CDCl₃, 400 MHz) δ 6.86 (t, *J*

= 7.2 Hz, 1H), 5.87 (br s, 1H), 3.78–3.69 (m, 1H), 3.45 (q, J = 6.0 Hz, 2H), 3.07 (t, J = 6.4 Hz, 2H), 2.47–2.32 (m, 2H), 1.97 (s, 3H), 1.91 (s, 3H), 1.60–1.46 (m, 2H), 0.98 (t, J = 7.2, 3H); ^{13}C NMR (CDCl_3 , 100 MHz) δ 194.0, 170.4, 138.0, 137.8, 72.5, 39.9, 36.4, 30.3, 28.7, 23.4, 12.9, 10.0; HRMS (ESI-TOF) m/z : $[\text{M} + \text{Na}]^+$ Calcd for $\text{C}_{12}\text{H}_{21}\text{NO}_3\text{SNa}$ 282.1134, found 282.1136 (Δ = 0.7 ppm).

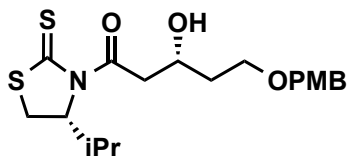
The above compound matches that synthesized by another alternative and previously reported route in all respects.⁸²



(*R*)-3-((*S,E*)-5-Hydroxy-2-methylhept-2-enoyl)-4-isopropylloxazolidin-2-one (*ent*-4.18). The target alcohol was synthesized from *N*, *O*-vinyl ketene acetal *ent*-4.17 via an analogous route to that of the enantiomer, 4.18. The title compound was produced as a clear, colorless oil (88%). $[\alpha]_{\text{D}}^{24} = -44.5$ (c 1.00, CHCl_3). Additional properties matched those of the enantiomer 4.18.

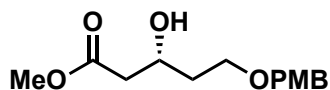


***S*-(2-Acetamidoethyl) (*S,E*)-5-hydroxy-2-methylhept-2-enethioate (4.14).** The thioenoate substrate 4.14 was synthesized in an analogous route to that of the enantiomer 4.13 starting from acyl oxazolidinone *ent*-4.18. The title compound was afforded as a clear, colorless oil (69% over 2 steps). $[\alpha]_{\text{D}}^{24} = 14.0$ (c 1.00, CHCl_3). All other properties matched those of the enantiomer, compound 4.14.

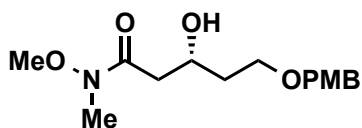


(R)-3-Hydroxy-1-((R)-4-isopropyl-2-thioxothiazolidin-3-yl)-5-((4-methoxybenzyl)oxy)pentan-1-one (4.22). To a flask (50 mL) containing thiazolinethione **4.21** (0.504 g, 2.48 mmol, 1.50 equiv) was added CH₂Cl₂ (12.4 mL). The resulting bright yellow solution was placed in a dry ice–MeCN bath (-40 °C). To the chilled solution was slowly added TiCl₄ (0.289 mL, 2.64 mmol, 1.60 equiv). The resulting red-orange solution was stirred at -40 °C for 27 min. To the reaction mixture was added *i*Pr₂NEt (0.460 mL, 2.64 mmol, 1.60 equiv), resulting in a sudden color change to blood red. The reaction mixture was stirred for 1 h 20 min then cooled via dry ice–acetone bath (-78 °C). To the chilled solution was added the aldehyde **4.20**⁷⁸ (0.320 g, 1.65 mmol, 1.00 equiv) in CH₂Cl₂ (2.10 mL) slowly over 5 min. The reaction mixture was stirred for 4 h 40 min at -78 °C prior to quenching with a saturated aqueous NH₄Cl solution (8.00 mL). The biphasic solution was warmed to ambient temperature and the layers were separated. The aqueous was extracted with CH₂Cl₂ (3 × 15.0 mL). The combined organics were dried over Na₂SO₄ and concentrated under reduced pressure. The crude product residue was purified by silica gel flash chromatography (30% EtOAc/hexanes) furnishing the title compound (0.353 g, 0.889 mmol, 54%) as a yellow oil. TLC: *R_f* = 0.19 (30% EtOAc/hexanes); [α]_D²⁴ = -253.0 (*c* 1.00, CHCl₃); ¹H NMR (CDCl₃, 400 MHz) δ 7.25 (d, *J* = 8.8 Hz, 2H), 6.87 (d, *J* = 8.8 Hz, 2H), 5.15 (t, *J* = 7.2 Hz, 1H), 4.45 (s, 2H), 4.40–4.31 (m, 1H), 3.80 (s, 3H), 3.70–3.69 (m, 2H), 3.54 (dd, *J* = 13.6, 2.8 Hz, 1H), 3.51–3.47 (m, 1H), 3.28 (dd, *J* = 17.6, 8.8 Hz, 1H), 3.01 (d, *J* = 10.8 Hz, 1H), 2.36 (app. sext, *J* = 6.8 Hz, 1H), 1.88–1.80 (m, 2H), 1.06 (d, *J* = 6.8 Hz, 3H), 0.97 (d, *J* = 7.2, 3H); ¹³C NMR (CDCl₃, 100 MHz) δ 203.1, 172.8, 159.4, 130.3, 129.5, 114.0, 73.1, 71.6, 67.8, 67.0, 55.4, 45.6, 36.1, 31.0, 30.8, 19.2, 18.0; HRMS (ESI-TOF) *m/z*: [M + Na]⁺ Calcd for C₁₉H₂₇NO₄S₂Na 420.1274, found 420.1253 (Δ = 5.0 ppm).

The diastereomer was also recovered as a bright yellow oil (0.156 g, 0.365 mmol, 22%).

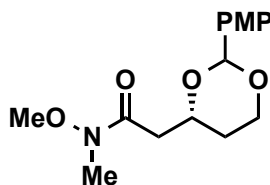


Methyl (*R*)-3-hydroxy-5-((4-methoxybenzyl)oxy)pentanoate (4.27). To a small glass containing the aldol product **4.22** (45.7 mg, 0.115 mmol, 1.00 equiv) at 0 °C (ice–water bath) was added MeOH (2.00 mL). To the resulting, bright yellow solution was added K₂CO₃ (5.00 mg, 0.0362 mmol, 0.315 equiv) in one portion. The resulting mixture was allowed to warm to ambient temperature with vigorous stirring for 21 h. The reaction mixture was supplemented with H₂O (10.0 mL) and Et₂O (10.0 mL). The resulting biphasic solution was separated and the aqueous layer was extracted with Et₂O (3 × 10.0 mL). The combined organic fractions were dried over Na₂SO₄, filtered and concentrated under reduced pressure. The crude oil was purified by flash column chromatography (40% EtOAc/hexanes) and the title compound (30.8 mg, 0.115 mmol, quant.) was isolated as a clear, colorless oil (30.8 mg, 0.115 mmol, quant.). TLC: R_f = 0.25 (40% EtOAc/hexanes); $[\alpha]_D^{24}$ = –12.8 (c 1.00, CHCl₃) (literature = $[\alpha]_D^{24}$ = –20.9 (c 3.10, CHCl₃))⁸⁰; ¹H NMR (CDCl₃, 400 MHz) δ 7.24 (d, J = 8.4 Hz, 2H), 6.87 (d, J = 8.4 Hz, 2H), 4.44 (s, 2H), 4.23 (app. quin, J = 6.4 Hz, 1H), 3.79 (s, 3H), 3.69 (s, 3H), 3.68–3.58 (m, 2H), 2.49 (d, J = 6.4 Hz, 2H), 1.84–1.72 (m, 2H); ¹³C NMR (CDCl₃, 100 MHz) δ 172.9, 159.4, 130.2, 129.4, 114.0, 73.0, 67.8, 67.3, 55.4, 51.8, 41.5, 36.1; HRMS (ESI-TOF) m/z : [M + Na]⁺ Calcd for C₁₄H₂₀O₂₀Na 291.1203, found 291.1200 (Δ = 1.0 ppm).



(*R*)-3-Hydroxy-*N*-methoxy-5-((4-methoxybenzyl)oxy)-*N*-methylpentanamide (4.24). To a flask containing acyl thiazolidinethione (0.255 g, 0.641 mmol, 1.00 equiv) under argon atmosphere was added CH₂Cl₂ (4.00 mL). The resulting bright yellow solution was supplemented with HN(OMe)Me•HCl (0.188 mg, 1.92 mmol, 3.00 equiv) and imidazole (0.231 g, 0.385 mmol, 6.00 equiv). The reaction mixture was stirred at ambient temperature for 42 h. The reaction was halted upon addition of saturated aqueous NH₄Cl (2.00 mL). The biphasic solution was separated and the aqueous layer was extracted with

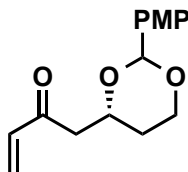
EtOAc (3 × 15.0 mL). The combined organic extracts were dried over Na₂SO₄, filtered and concentrated under reduced pressure. The crude reaction residue was purified via silica flash column (100% EtOAc) yielding the title compound (0.178 g, 0.601 mmol, 94%) as a colorless, clear. TLC: R_f = 0.17 (50% EtOAc/hexanes); $[\alpha]_D^{24}$ = -22.5 (c 1.00, CHCl₃); ¹H NMR (CDCl₃, 400 MHz) δ 7.25 (d, J = 8.4 Hz, 2H), 6.86 (d, J = 8.4 Hz, 2H), 4.44 (s, 2H), 4.27–4.18 (m, 1H), 3.79 (s, 3H), 3.70–3.58 (m, 5H), 3.18 (s, 3H) 2.69–2.50 (m, 2H), 1.88–1.74 (m, 2H); ¹³C NMR (CDCl₃, 100 MHz) δ 173.6, 159.3, 130.5, 129.4, 113.9, 73.0, 67.6, 66.6, 61.4, 55.4, 38.6, 36.5, 32.0; HRMS (ESI-TOF) m/z : [M + Na]⁺ Calcd for C₁₅H₂₃NO₅Na 320.1468, found 320.1481 (Δ = 4.1 ppm).



***N*-Methoxy-2-((4*R*)-2-(4-methoxyphenyl)-1,3-dioxan-4-yl)-*N*-methylacetamide**

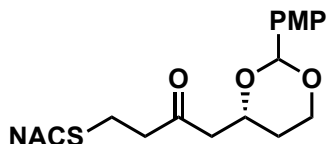
(4.24). To a flask containing the weinreb amide **4.23** (0.131 g, 0.440 mmol, 1.00 equiv) in CH₂Cl₂ (4.00 mL) at -10 °C (NaCl–ice bath) was added activated molecular sieves (4 Å, ~0.100 g). The reaction was stirred for 30 min. To the chilled solution was added DDQ (0.120 g, 0.529 mmol, 1.20 equiv) in one portion. The resulting dark green solution was allowed to warm to 4 °C (cold room) and stirred for 2h 10 min. The reaction was quenched via filtration through a short pad of celite (2.00 cm). The pad was rinsed with CH₂Cl₂ (25.0 mL). The filtrate was washed sequentially with saturated NaHCO₃ (2 × 15.0 mL) and brine (20.0 mL). The resulting organic solution was dried over Na₂SO₄, filtered and concentrated under reduced pressure. The crude residue was purified by flash chromatography (50–100% EtOAc/hexanes) affording the title compound (0.101 g, 0.342 mmol, 78% (85% BRSM)) as a colorless oil. TLC: R_f = 0.23 (50% EtOAc/hexanes); $[\alpha]_D^{24}$ = 5.9 (c 1.00, CHCl₃); ¹H NMR (CDCl₃, 400 MHz) δ 7.38 (dd, J = 8.4, 2.0 Hz, 2H), 6.85 (dd, J = 8.4, 2.0 Hz, 2H), 5.50 (s, 1H), 4.43–4.33 (m, 1H), 4.27–4.19 (m, 1H), 3.98 (tt, J = 12.0, 2.0 Hz, 1H), 3.77 (s, 3H), 3.66 (s, 3H), 3.18 (s, 3H), 3.03–2.88 (m, 1H), 2.54

(dd, $J = 16.0, 6.0$ Hz, 1H), 1.83 (dq, $J = 12.4, 4.8$ Hz, 1H), 1.73–1.65 (m, 1H); ^{13}C NMR (CDCl_3 , 100 MHz) δ 171.5, 159.9, 131.3, 127.4, 113.6, 101.3, 73.9, 66.9, 61.5, 55.3, 38.4, 32.1, 31.4; HRMS (ESI-TOF) m/z : $[\text{M} + \text{Na}]^+$ Calcd for $\text{C}_{15}\text{H}_{21}\text{NO}_5\text{Na}$ 318.1312, found 318.1308 ($\Delta = 1.3$ ppm).



1-((4R)-2-(4-Methoxyphenyl)-1,3-dioxan-4-yl)but-3-en-2-one (4.25). To a flask containing the weinreb amide **4.24** (50.0 mg, 0.169 mmol, 1.00 equiv) was added THF (10.0 mL). After allowing the solution to dissolve, the clear mixture was cooled to 0 °C (ice–water bath). To the chilled solution was slowly added a THF solution (1.0 M) of vinylmagnesium bromide (0.508 mL, 0.508 mmol, 3.00 equiv). The reaction mixture was stirred for 4.5 h at 0 °C. An additional amount of vinylmagnesium bromide (84.7 μL , 0.0847 mmol, 0.500 equiv) was added to the reaction. After stirring for an additional 40 min, the reaction was quenched upon addition of a saturated aqueous NH_4Cl (10.0 mL). The biphasic solution was allowed to warm to ambient temperature and the layers were separated. The aqueous layer was extracted with EtOAc (4×20.0 mL) and the combined organics were dried over Na_2SO_4 , filtered and concentrated under reduced pressure. The resulting crude residue was purified by silica column chromatography (30% EtOAc/hexanes) yielding the title compound (34.6 mg, 0.132 mmol, 78%) as a clear, colorless oil. TLC: $R_f = 0.36$ (30% EtOAc/hexanes); $[\alpha]_{\text{D}}^{24} = -16.0$ (c 1.00, CHCl_3); ^1H NMR (CDCl_3 , 400 MHz) δ 7.38 (d, $J = 8.4$ Hz, 2H), 6.87 (d, $J = 8.4$ Hz, 2H), 6.38 (dd, $J = 18.0, 10.8$ Hz, 1H), 6.25 (d, $J = 17.6$ Hz, 1H), 5.88 (d, $J = 10.4$ Hz, 1H), 5.50 (s, 1H), 4.44–4.35 (m, 1H), 4.25 (dd, $J = 11.6, 4.8$ Hz, 1H), 3.99 (dt, $J = 12.0, 2.4$ Hz, 1H), 3.79 (s, 3H), 3.09 (dd, $J = 16.4, 6.4$ Hz, 1H), 2.73 (dd, $J = 16.4, 6.4$ Hz, 1H), 1.81 (ddd, $J = 25.2, 12.8, 4.8$ Hz, 1H), 1.66 (dq, $J = 12.8, 2$ Hz, 1H); ^{13}C NMR (CDCl_3 , 100 MHz) δ 198.3, 160.0, 137.1, 131.2, 129.1, 127.4, 113.7, 101.3, 73.4, 66.9, 55.4, 45.6, 31.4; HRMS (ESI-TOF) m/z : $[\text{M} + \text{Na}]^+$ Calcd for $\text{C}_{15}\text{H}_{18}\text{O}_4\text{Na}$ 285.1097, found 285.1095 ($\Delta =$

0.7 ppm).



***N*-(2-((4-((4*R*)-2-(4-Methoxyphenyl)-1,3-dioxan-4-yl)-3-oxobutyl)thio)ethyl)acetamide (4.26).** To a flask (100 mL) containing the vinyl ketone **4.25** (65.7 mg, 0.251 mmol, 1.00 equiv) was added THF (20.0 mL). To the clear solution was added cesium Cs_2CO_3 (~ 5 mg, catalytic) and *N*-acetylcysteamine (32.0 μL , 0.301 mmol, 1.20 equiv). The resulting solution was stirred at ambient temperature for 2 h 35 min. The reaction was halted upon addition of saturated, aqueous NH_4Cl solution (15.0 mL). The biphasic mixture was separated and the aqueous layer was extracted with EtOAc (4 \times 15.0 mL). The combined organics were dried over Na_2SO_4 , filtered and concentrated under reduced pressure. The crude thioether was purified by flash chromatography (5% MeOH/ CH_2Cl_2) affording the title compound (70.0 mg, 0.184 mmol, 73%) as a clear, viscous oil. TLC: R_f = 0.31 (5% MeOH/ CH_2Cl_2); $[\alpha]_{\text{D}}^{24} = -15.4$ (c 1.00, CHCl_3); ^1H NMR (CDCl_3 , 400 MHz) δ 7.37 (dd, J = 6.4, 2.0 Hz, 2H), 6.87 (dd, J = 6.8, 2.0 Hz, 2H), 5.96 (br s, 1H), 5.48 (s, 1H), 4.38–4.30 (m, 1H), 4.24 (dd, J = 11.6, 4.4 Hz, 1H), 3.97 (dt, J = 12.0, 2.8 Hz, 1H), 3.79 (s, 3H), 3.39 (q, J = 6.4 Hz, 2H), 2.85 (dd, J = 16.0, 7.6 Hz, 1H), 2.80–2.71 (m, 4H), 2.61 (t, J = 6.4 Hz, 2H), 2.56 (dd, J = 15.6, 4.8 Hz, 1H), 1.97 (s, 3H), 1.81 (ddd, J = 24.2, 12.8, 5.2 Hz, 1H), 1.59 (d, J = 14.0 Hz, 1H); ^{13}C NMR (CDCl_3 , 100 MHz) δ 206.9, 170.3, 160.1, 131.0, 127.4, 113.7, 101.3, 73.5, 66.9, 55.4, 49.1, 44.0, 38.5, 32.3, 31.2, 25.2, 23.4; HRMS (ESI-TOF) m/z : $[\text{M} + \text{Na}]^+$ Calcd for $\text{C}_{19}\text{H}_{27}\text{NO}_5\text{SNa}$ 404.1502, found 404.1491 (Δ = 2.7 ppm).



***(R)*-N-(2-((5,7-Dihydroxy-3-oxoheptyl)thio)ethyl)acetamide (4.15).** To a flask containing the acetal **4.25** (17.5 mg, 0.0459 mmol, 1.00 equiv) and *i*PrOH (6.00 mL) was

added Pd(OH)₂ (20% w/w, wet) (19.0 mg). The black solution was purged with hydrogen atmosphere and stirred for 26 h at ambient temperature. The reaction was filtered through a pad of Celite® (2.00 cm). The filtrate was concentrated under reduced pressure. The crude residue was purified by flash chromatography (5–10% MeOH/CH₂Cl₂) furnishing the title compound (4.10 mg, 0.0156 mmol, 34%, 52% BRSM) as a clear oil. TLC: *R_f* = 0.26 (10% MeOH/CH₂Cl₂); [α]_D²⁴ = -11.0 (*c* 0.27, CHCl₃); (the compound exists in linear and cyclic forms. Peaks listed are for the major isomer only) ¹H NMR (CDCl₃, 400 MHz) δ 5.97 (br s, 1H), 4.39–4.30 (m, 1H), 4.25 (t, *J* = 12.4 Hz, 1H), 3.87–3.81 (m, 1H), 3.44 (q, *J* = 6.8 Hz, 2H), 2.79 (s, 2H), 2.73–2.63 (m, 4H), 2.00 (s, 3H), 1.94–1.82 (m, 2H), 1.76–1.58 (m, 4H); ¹³C NMR (CDCl₃, 100 MHz) δ 209.7, 170.5, 67.8, 61.2, 49.9, 43.4, 38.7, 38.0, 32.1, 25.2, 23.4; HRMS (ESI-TOF) *m/z*: [M + Na]⁺ Calcd for C₁₁H₂₁NO₄Na 286.1083, found 289.1105 (Δ = 7.7 ppm).

4.10 Biology Experimental Section

Recombinant protein was expressed and purified as previously reported for the curacin dehydratases.⁶⁷ The dehydratases (5 μ M) were incubated with substrate (1 mM) in a 100 μ L of Tris buffer (50 mM Tris, 150 mM NaCl, pH 8.0) at ambient temperature for 12 h. A small aliquot of the reaction mixture (5 μ L) was added to a MeCN–H₂O (1:1, 495 μ L) quench solution and briefly vortexed to mix. The solution was centrifuged and a small portion (60 μ L) was added to an HPLC vial. The solution was injected and analyzed by LC-MS/MS as discussed in **Chapter 3**. The monitored transitions and retention times are given in **Table 4.1**. The LC-MS/MS traces were extracted with SCIEX Analyst[®] software and were input into GraphPad Prism software to generate **Figures 4.4** and **4.7**

Table 4.1. LC-MS/MS data for **4.2–4.6**, **4.13** and **4.14**.

Analyte	HPLC retention time (min)	Transition
4.6	6.80	242→95
4.2 or 4.5	5.52	242→95
4.3 or 4.4	5.24	242→95
4.13 or 4.14	5.11	260→141

Chapter 5: Curacin Module G dehydratase substrates

5.1 Formation of the *cis*-alkene within curacin biosynthetic pathway

The *cis* olefin-generation in curacin biosynthesis remains the last unexplained transformation in the biosynthetic pathway. Undoubtedly there is a polyketide chain elongation event in module G following the CurF NRPS module. This results in a β -ketothioester intermediate, which is the substrate for the CurG ketoreductase (**Figure 5.1**). Bioinformatic prediction categorizes this ketoreductase as A-type, capable of forming an L-alcohol. This is a tentative assignment of stereochemistry as the absolute configuration is rendered cryptic by dehydration. However, this prediction matches well with the hypothesis that only substrates of L-orientation seem to form *cis*-double bonds, while D-alcohols form *trans*-alkenes in polyketides.¹⁷ Although this mnemonic seems to hold true for many PKSs, it remains empirical, as *cis*-olefin generation by a dehydratase has never been observed *in-vitro*. Further complicating matters is the absence of a dehydratase in the CurG module. It has been proposed that either CurF or CurH, the abutting modules in the biosynthetic pathway, house the dehydratase that catalyzes this elimination, forming the α,β -unsaturated intermediate. Presumably this occurs via a ‘domain stuttering’ mechanism as put forth for similar cases in other pathways (See **Chapter 4**).

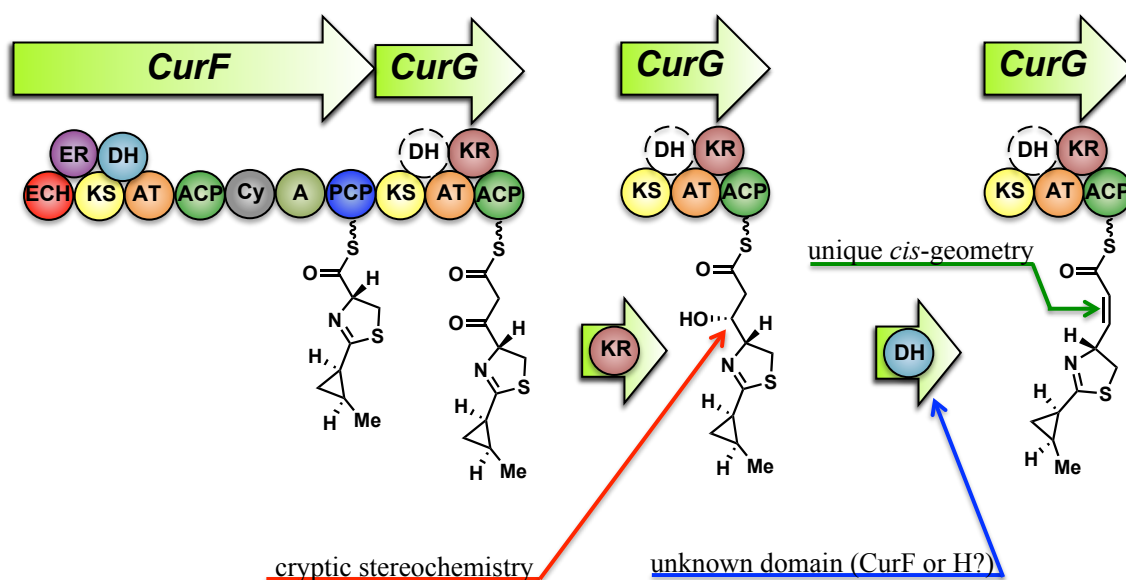


Figure 5.1. The actions of the CurF-CurG di-module from the curacin pathway. The key biosynthetic chain intermediates are shown attached to their respective ACP domains. The product of the ketoreductase is predicted to be an L-alcohol, but it is rendered cryptic by elimination in the pathway. The DH domain predicted for CurG was found to be nonexistent and is shown as a colorless circle with a dotted line. An unknown dehydratase, postulated to be in either CurF or CurH modules, generates the *cis*-olefin present in the ultimate CurG module product.

5.2 Chemical strategy and rationale

We wanted to interrogate the pathway for the identity of the CurG dehydratase. This would allow us to conduct the first *in-vitro* characterization of a *cis*-olefin-generating dehydratase. Our strategy in this regard was to synthesize analogs of the native CurG dehydratase substrate (**5.1**) for incubation with the CurF, H, J and K DHs (**Figure 5.2**). The products would be detected based on their parent mass and fragmented to verify their molecular identity. Further verification of the gross structure and olefin geometry could be determined through synthesis of the products after initial detection of enzymatic dehydration. The substrates **5.2** and **5.2** represent molecularly simplified substrates in two aspects. Firstly, we adopted *N*-acetylcysteamine thioesters as surrogates for the

phosphopantetheine-ACP thioester in the natural product. This was analogous to previous studies (i.e. **Chapters 2, 3, and 4**) giving us a reasonable degree of confidence that these small molecules could serve as substrates. The second simplification was the deletion of the pendant methyl substituent. This subtle change would eliminate two stereogenic centers in the substrates and, in so doing, greatly abridge their synthesis. We anticipated that the enzyme would tolerate this alteration, as no hydrogen bonds would be modified in the process. Moreover, our established LC-MS/MS detection method would allow us to perceive even small amounts of substrate production in the event of poor enzyme catalysis.

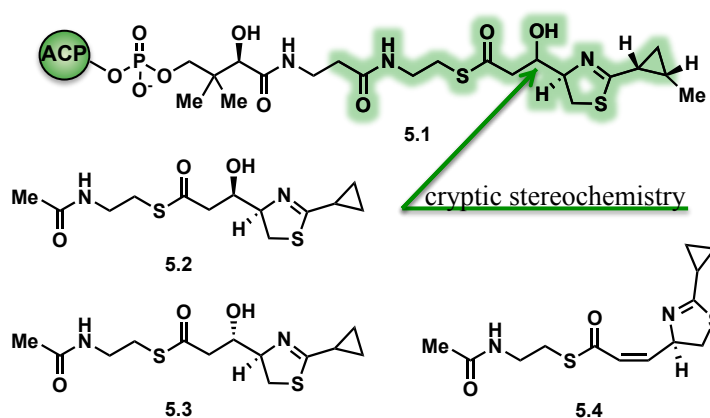


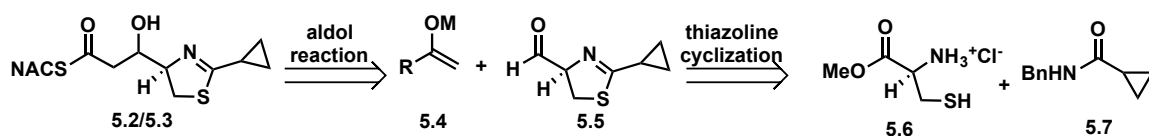
Figure 5.2. Design of synthetic CurG dehydratase product and substrate. The native substrate for CurG dehydration (**5.1**) is shown with green highlighting the basis for small molecule substrates. Substrates **5.2** and **5.3** were designed by simplifying the phosphopantetheine arm as well as eliminating the pendant methyl group. The product **5.4** would be synthesized in the event of positive LC-MS/MS results to corroborate product formation.

5.3 Synthesis and activity of the putative CurG dehydratase substrate

The retrosynthesis of the proposed CurG DH substrates is shown in **Scheme 5.1**. A late-stage aldol reaction between either a simple ester or acylated chiral auxiliary enolate and key aldehyde **5.5** would efficiently create a key carbon-carbon bond and install one of the

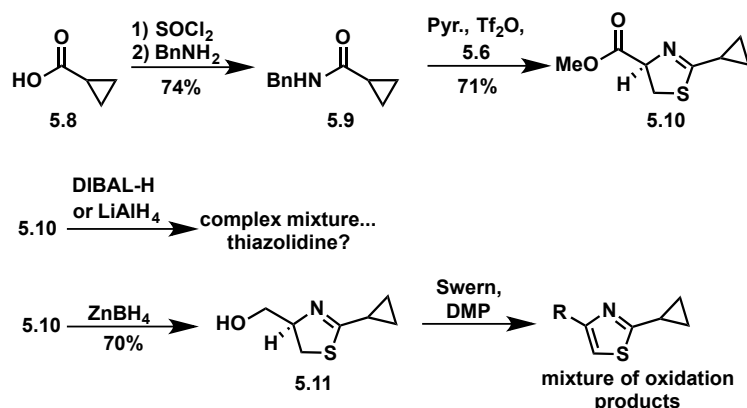
two stereogenic centers in the substrate. The resulting aldol product could undergo straightforward hydrolysis and thioester bond formation to give the desired product. We envisioned aldehyde **5.5**. The thiazoline can be obtained from the commercially available L-cysteine methyl ester hydrochloride and the known amide **5.7**.⁸³ This step relies on cyclization chemistry developed by Charette and coworkers.⁸⁴ The resulting ester could be reduced to the aldehyde **5.5**.

Scheme 5.1. Retrosynthetic analysis of CurG DH substrates **5.2/5.3**.



In the forward sense, the cyclopropane carboxylic acid was converted to cyclopropyl amide **5.7** through a two-step, one-pot procedure involving exposure to thionyl chloride and reaction of the acid chloride with excess benzylamine (**Scheme 5.2**). Conveniently, the cyclopropyl carboxamide could be readily recrystallized from a mixture of ethyl acetate–hexane, avoiding the need for column chromatography. Tf₂O-promoted thiazoline cyclization afforded the desired heterocycle **5.10** in modest yield, similar to that previously reported.⁸⁴ With ester **5.10** in hand we wanted to investigate partial reduction to key aldehyde **5.5**. Unfortunately, reductions with both LiAlH₄ and DIBAL-H resulted in complex product mixtures that seemed to lack the thiazoline unsaturation. Presumably, the thiazoline has a comparable reduction potential to that of the methyl ester. In line with a similar, previous report, complete reduction with zinc borohydride produced the alcohol **5.11**.⁸⁵ Attempted Swern or DMP oxidations of **5.11** failed to produce the desired aldehyde. The complex product mixtures exhibited higher UV absorbance on TLC and extraneous aromatic peaks in ¹H-NMR, indicative of over oxidation to the thiazoline. Aldehydes similar to **5.5** have been a targeted intermediate by several labs but still remain unobtainable by all reports in the literature.⁸⁵⁻⁸⁷

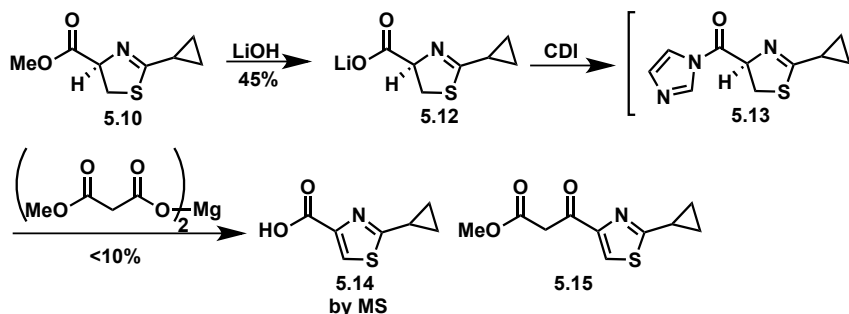
Scheme 5.2. Failed synthesis of key aldehyde **5.5**.



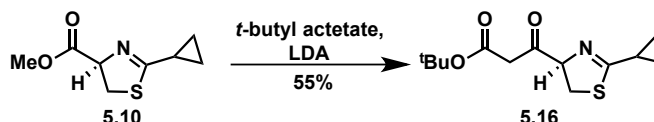
Disappointed by failed attempts to obtain the crucial aldehyde **5.5**, we sought an alternative strategy to avoid this intermediate entirely. Due to the nature of polyketide ketosynthase domains, we rationalized that ester **5.10** (or a similar, activated compound) might be a willing partner in a Claisen condensation (**Scheme 5.3**). The β -ketoester resulting could be reduced under mild conditions to afford the β -hydroxyester intermediate, itself just two standard transformations away from the desired DH substrate **5.2** or **5.3**. Concerned by potential instability of the thiazoline to harsh enolate-forming conditions, we elected to utilize Masamune's mild decarboxylative Claisen reaction.⁸⁸ The methyl ester **5.10** was saponified with lithium hydroxide. Surprisingly, we were unable to isolate the desired acid after aqueous hydrochloric acid workup. We hypothesized that the thiazoline is susceptible to hydrolysis under conditions necessary for carboxylic acid protonation. We were able to isolate the lithium carboxylate (**5.12**) in modest yields after quenching the reaction mixture with acetone and collection of the white precipitate via filtration. The necessary acyl imidazole species (**5.13**) was obtained *in-situ* through reaction with CDI and the imidazole hydrochloride. Unfortunately, addition of the magnesium salt of methylmalonate half ester failed to produce the desired β -ketoester. A small amount of the oxidized carboxylate and β -ketoester thiazoles were obtained as judged by mass spectroscopy of the crude mixture. We reasoned that prolonged reaction conditions necessary for the Masamune claisen reaction allowed oxidation of the substrate to occur. Rationalizing that hard enolization conditions would provide shorter reaction conditions, we submitted the methyl ester **5.10** to reaction with

the lithium enolate of *tert*-BuOAc. To our delight, the reaction afforded the desired product **5.16** in modest yields. (**Scheme 5.4**)

Scheme 5.3. Failed decarboxylative Claisen reaction.



Scheme 5.4. Successful Claisen condensation to form **5.16**.



With the key ketone **5.16** in hand, we investigated conditions for its reduction and completion of the CurG dehydratase substrates **5.2** and **5.3** (**Scheme 5.5**). During the course of our initial studies we noticed a large amount of thiazole formation during reduction with sodium borohydride, yielding an aromatic alcohol. We later traced this back to an inherent instability of β -ketoester **5.16** when stored above -78 C and under argon atmosphere for more than 2 days. Due to its oxidative susceptibility, the purified Claisen product was immediately carried on to the reduction reaction, reducing undesired thiazole product formation. The diastereomer ratio of reduction products obtained with sodium borohydride was found to be strongly dependent on temperature (**Table 5.1**). The mixture of diastereomers (2:1, obtained at 0 °C) was carried forward in the synthesis. We wanted to test both **5.2** and **5.3** because the CurG stereochemistry is cryptic and the mixture would allow us to synthesize and test both in unison. The *tert*-butyl ester was removed via addition of anhydrous TFA. The labile thiazoline is remarkably stable to

these conditions, affording the acid as the TFA salt **5.19/5.20**. The crude salt was coupled with *N*-acetylcysteamine to afford the putative dehydratase substrates **5.2** and **5.3** as a diastereomeric mixture (2:1).

Scheme 5.5. Completion of CurG DH substrates **5.2/5.3**.

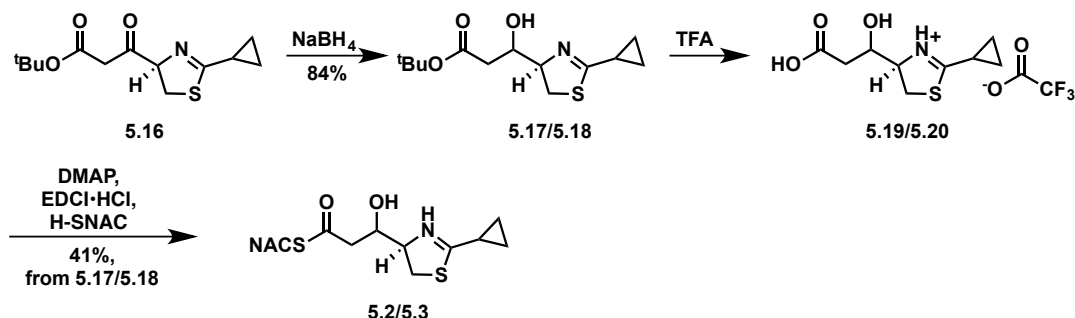


Table 5.1. Temperature-dependent diastereomeric ratio of ketone reduction.

Temperature (°C)	Diastereomer Ratio
0	2:1
-20	4:1
-40	8:1

We were interested in testing the postulated CurG DH substrates with all of the dehydratases from the curacin biosynthetic pathway. The purified mixture of **5.2** and **5.3** was incubated overnight with CurF, CurH, CurJ and CurK DHs. Crude mass detection of all four reactions failed to indicate any product formation (i.e. loss of water, $[\text{M}-18]^+$). We rationalized that, although synthetic **5.2/5.3** differs from the native substrate by lacking the full phosphopantetheine arm as well as the pendant methyl group, we might gain more insight by reassessing the early dehydration processes of the curacin pathway.

5.4 A holistic hypothesis for curacin biosynthesis

Given the precedence for both canonical (CurK DH) and non-canonical (CurJ DH) dehydration in the curacin A pathway we were extremely skeptical of the proposed CurG substrate. The truncated dehydratase substrate **5.2/5.3** was similar to failed CurJ DH substrates **4.2-4.5 (Chapter 4)** in the sense that they assume canonical elimination. Moreover, all the dehydratases (from CurF, CurH, CurJ and CurK modules) were unable to dehydrate synthesized these truncated substrates. These striking similarities led us to deduce that the CurG module intermediate, similar to the CurI KR product, is not directly dehydrated by any module. The β -hydroxythioester product of the CurG module ketoreductase is directly loaded onto the CurH ketosynthase domain and undergoes extension through a decarboxylative Claisen condensation (**Figure 5.3**). The δ -hydroxy- β -ketothioester intermediate is reduced to the diol and shuttled to the dehydratase domain (CurH DH). A standard, α , β -elimination occurs followed by a non-canonical γ , δ -elimination furnishing a diene intermediate. An enoyl reductase (ER) domain in CurH reduces α , β -olefin. This product, still containing the distal olefin, is loaded onto the KS domain in module I for another round of extension. The CurI module produces a β -hydroxythioester which, as put forth in chapter 3, is loaded onto CurJ for extension, normal processing and vinylogous elimination. Module K faithfully carries out a normal series of polyketide reactions with proven, cryptic D-alcohol and *E*-olefin configurations (**Chapter 2**). Finally, CurL and CurM modules carry out the final two extensions, complete with processing events and decarboxylative cleavage of the mature intermediate, forming curacin A. We propose that the DH domain in module F is vestigial and possibly originates from a gene duplication event in *Moorea producens*' evolutionary history. The overall process with module terminating intermediates is displayed in **Figure 5.4**.

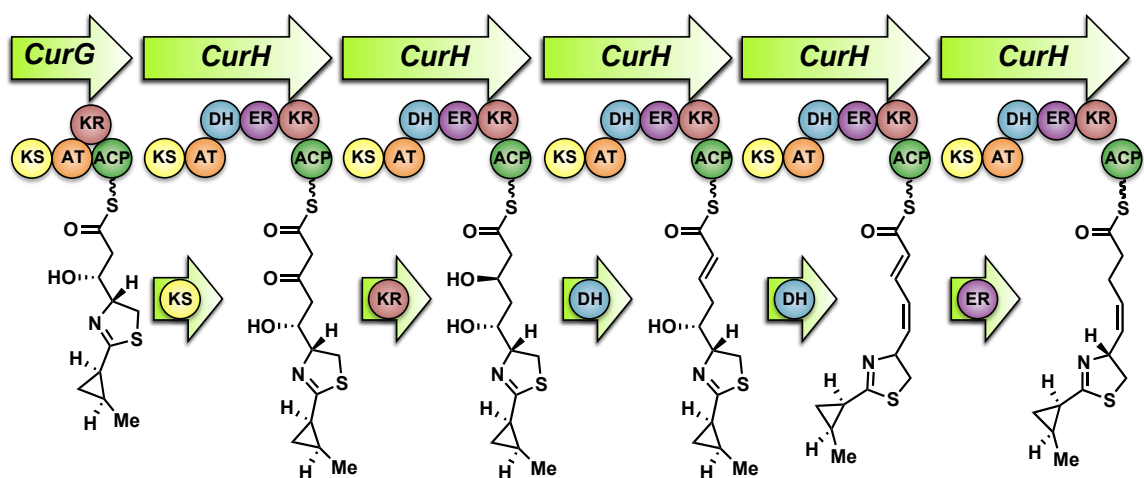


Figure 5.3. Proposed vinylogous elimination between modules CurG and CurH. All extension and processing steps between CurG ketoreductase action and CurH ER reduction are displayed.

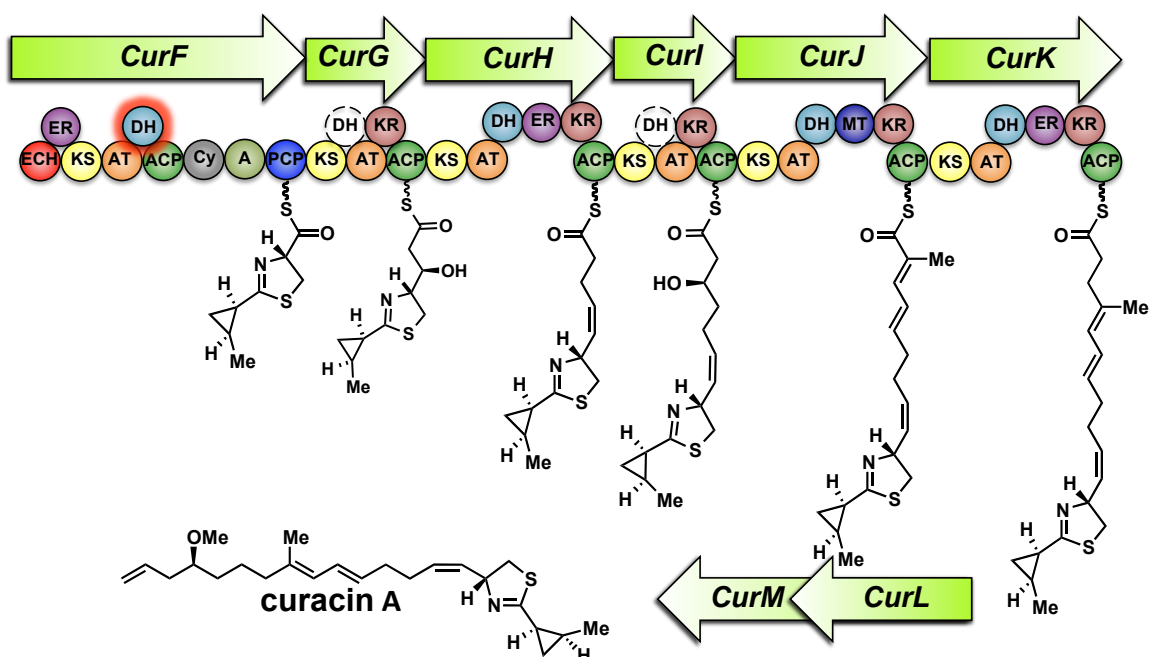


Figure 5.4. Proposed pathway incorporating vinylogous eliminations for curacin A biosynthesis. The DH domain in CurF and highlighted in red is predicted to serve no catalytic function in the pathway. The missing dehydratases not present in curacin A biosynthesis are denoted as white circles with hashed lines. The β -hydroxythioester products of modules G and I are extended and processed by modules H and J, respectively.

5.5 Vinylogous dehydration-Unknowns and future directions

Several mechanistic questions still remain unanswered about the novel vinylogous elimination. Firstly, it is unknown if the reaction utilizes a *syn*-elimination mechanism, similar to that seen in the FabA isomerization of fatty acids.⁸⁹ This could be elucidated by dehydration experiments utilizing selectively γ -deuterated vinylogous substrates. Secondly, does the catalytic dyad's function differ between canonical and non-canonical eliminations? Although the key histidine and aspartate residues for α , β -elimination were shown to be necessary for γ , δ -elimination, we have yet to discover the exact orientation, and role played by these residues and the substrate. Continued efforts by our

collaborators, Dr. Janet Smith and Gregory Dodge at the University of Michigan, seek to illuminate these questions through a co-crystal structure between substrates and His or Asp knockout mutants. Third, what is the mechanism dictating *cis* vs. *trans* olefin formation in vinylogous elimination? Although our work suggests the *cis* olefin in curacin A is put into place by vinylogous elimination, we observed *trans* olefin bond formation by the CurH DH on the vinylogous CurJ substrate. Additionally, the stereoselectivity observed in CurH for the CurJ DH substrate opposes the predicted L-alcohol furnished from the CurG KR. We predict that this discrepancy is actually a clue as to the mechanism of olefin bond preference. Specifically, a clear difference between the CurJ and CurH vinylogous DH substrates is the presence of a trisubstituted olefin in the case of CurJ. This α -methyl group imposes a restraint on the conformational freedom of rotation along the β - γ bond via 1,3-allylic ($A^{1,3}$) strain (**Figure 5.5**). This impacts the orientation of the two prochiral γ -protons and, in so doing, the accessibility for deprotonation by the catalytic base. In contrast, the putative vinylogous substrate of the CurH DH lacks the α -methyl, affording greater flexibility and choice in which proton the enzyme may abstract for elimination. In this system, $A^{1,2}$ strain is the predominant factor in determining preferred conformations. By abstraction of the pro-*S* proton, a *syn*-elimination of the D-alcohol occurs with a transition state favoring the *cis* olefin (**Figure 5.6**). The enhanced flexibility may also be propagated to the δ -center, allowing for tolerance of the predicted L-alcohol substrate. In this case, the pro-*R* proton would be deprotonated setting up a transition state resulting in *cis* olefin formation. Obviously an anti-elimination mechanism could also be considered but, as the enzyme apparently uses the same enzymes and displays a strict stereochemical bias, we are operating under the assumption that a *syn*-dehydration is still at play. This mechanism could be elucidated through synthesis of truncated CurH vinylogous dehydration substrates and deuterium labeling experiments.

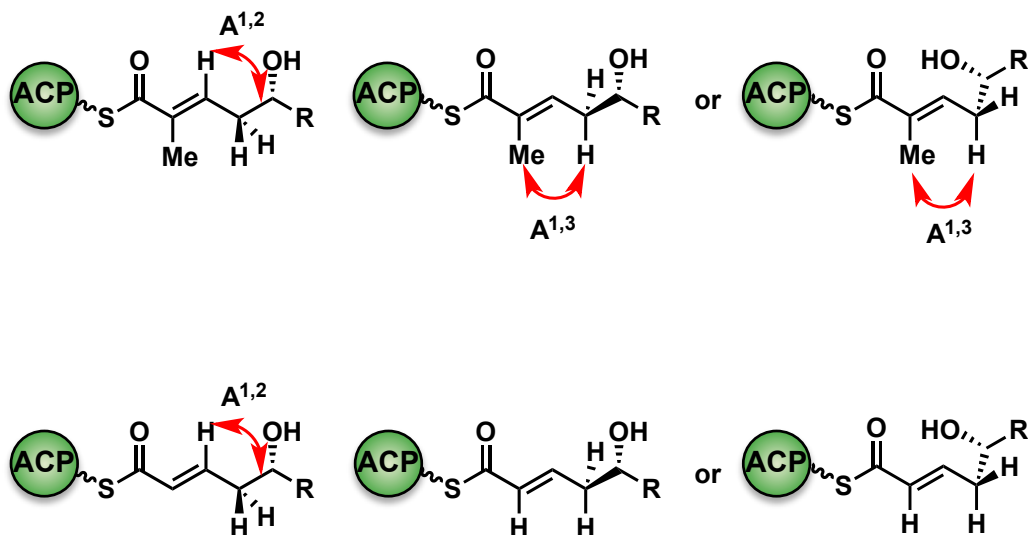


Figure 5.5. Depiction of allylic strain in vinylogous dehydration substrates. The trisubstituted (top) and disubstituted (bottom) conformations differ in terms of $A^{1,3}$ strain. In disubstituted substrates, $A^{1,2}$ strain is predicted to be an important factor in the relative distribution of conformers.

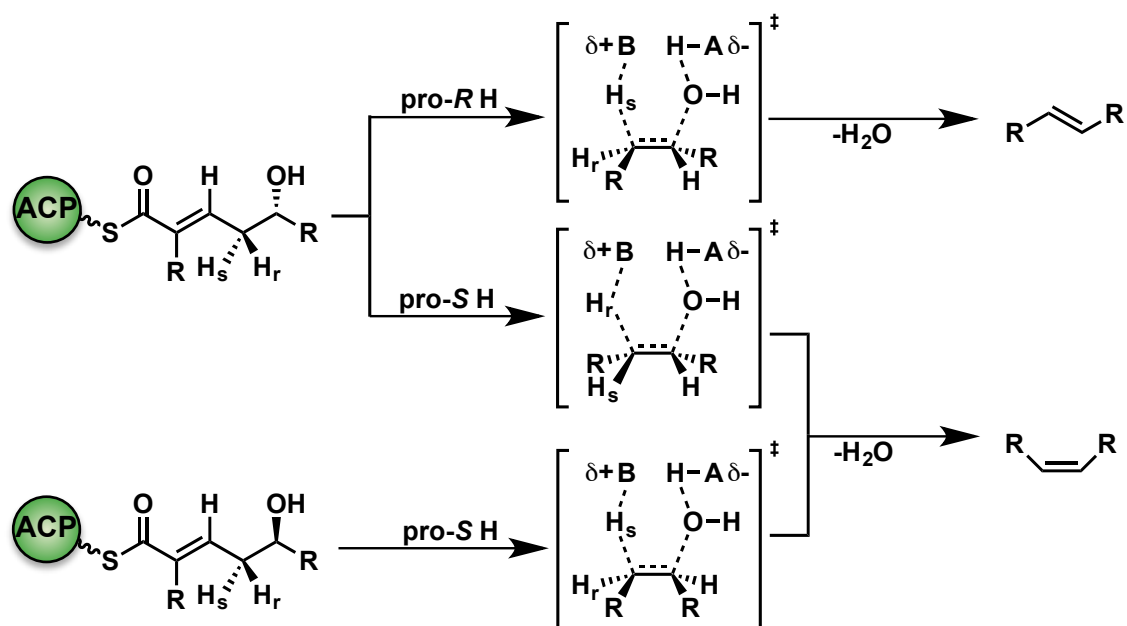
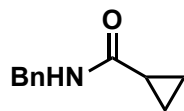
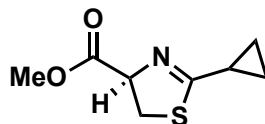


Figure 5.6. The proposed mechanistic basis for *cis* alkene formation through vinylogous elimination. Deprotonation of the *pro-R* or *pro-S* proton from the D-alcohol substrate and *syn*-elimination yields a *trans* or *cis* olefin, respectively. A *cis* olefin is obtained through *syn*-elimination of an L-alcohol only if the dehydratase deprotonates the *pro-S* proton.

5.6 Chemistry experimental section

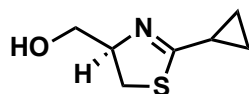


***N*-Benzylcyclopropanecarboxamide (5.9).** To a flask equipped with reflux condenser containing toluene (5.00 mL) under argon atmosphere was added SO_2Cl_2 (0.932 mL, 12.8 mmol, 1.10 equiv) and the mixture was heated to 40 °C (oil bath). To the warm mixture was slowly added cyclopropanecarboxylic acid (0.925 mL, 11.6 mmol, 1.00 equiv) dropwise over 2 min. The reaction mixture was heated to 80–85°C for 2h 15 min. The slightly yellow solution was cooled to –10°C (ice– NH_4Cl). To the chilled solution was added BnNH_2 (4.40 mL, 40.6 mmol, 3.50 equiv) in one portion. The yellow slurry was allowed to warm to ambient temperature over 2 h. The resulting mixture was quenched upon addition of saturated aqueous NH_4Cl (5.00 mL) and extracted with EtOAc (4 × 10.0 mL). The organic fractions were dried under reduced pressure, yielding a bright yellow amorphous solid. The solid was recrystallized from EtOAc–hexanes providing the title compound (1.51 g, 8.60 mmol, 75%) as tan crystal needles. TLC: R_f = 0.14 (30% EtOAc/hexanes); ^1H NMR (CDCl_3 , 400 MHz) δ 7.37–7.28 (m, 5H), 5.85 (br s, 1H), 4.47 (d, J = 5.6 Hz, 2H), 1.39–1.31 (m, 1H), 1.02 (dt, J = 6.8, 4.0 Hz, 2H), 0.76 (dq, J = 8, 3.6 Hz, 2H); ^{13}C NMR (CDCl_3 , 100 MHz) δ 173.5, 138.6, 128.8, 128.0, 127.6, 44.0, 14.9, 7.4. Data collected matches the known compound.⁸³



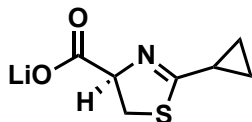
Methyl (*R*)-2-cyclopropyl-4,5-dihydrothiazole-4-carboxylate (5.10). To a flask containing cyclopropylcarboxamide **5.9** (0.790 g, 4.51 mmol, 1.00 equiv) under argon atmosphere was added CH_2Cl_2 (45.1 mL). The clear solution was cooled by a dry ice–MeCN bath (–40 °C). A solution of freshly distilled pyridine (1.09 mL, 13.5 mmol, 3.00 equiv) was added to the reaction mixture. An aliquot of TiF_4 (0.986 mL, 5.86 mmol, 1.30 equiv) was added dropwise over 10 min. The reaction mixture was allowed to

slowly warm to 0 °C over 2 h. After 4 h at 0 °C, the reaction was cooled to –30 °C. To the red-orange solution was quickly added crushed L-cysteine methyl ester–HCl (1.16 g, 6.77 mmol, 1.50 equiv) followed by another aliquot of pyridine (1.09 mL, 13.5 mmol, 3.00 equiv). The solution slowly developed a golden hue. After 6 h, the reaction was vacuum filtered through silica gel plug (2.00 cm). The plug was washed with EtOAc–hexanes (1:1, 40 mL). The resulting organic solution was concentrated under reduced pressure and the product residue was purified by flash chromatography (30–50% EtOAc/hexanes) affording the title compound (0.595 g, 3.21 mmol, 71%) as a light yellow oil. TLC: R_f = 0.27 (30% EtOAc/hexanes); ^1H NMR (CDCl_3 , 400 MHz) δ 5.02 (t, J = 8.8 Hz, 2H), 3.80 (s, 3H), 3.50 (dq, J = 11.2, 8.8 Hz, 2H), 1.98 (app. quin, J = 7.2 Hz, 1H), 1.67–1.59 (br s, 1H), 1.05–0.94 (m, 4H); ^{13}C NMR (CDCl_3 , 100 MHz) δ 177.1, 171.5, 77.7, 52.6, 35.0, 15.3, 9.3; HRMS (ESI-TOF) m/z : $[\text{M} + \text{Na}]^+$ Calcd for $\text{C}_8\text{H}_{11}\text{NO}_2\text{SNa}$ 208.0403; found 208.0409 (Δ = 2.9 ppm).

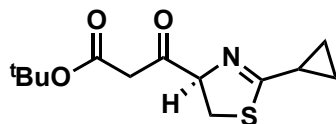


(*R*)-(2-Cyclopropyl-4,5-dihydrothiazol-4-yl)methanol (5.11). To a flask containing the thiazoline **5.10** (63.0 mg, 0.340 mmol, 1.00 equiv) was added Et_2O (10.0 mL). To the faintly yellow solution was added $\text{Zn}(\text{BH}_4)_2$ in Et_2O (0.147 M, 4.60 mL, 0.68 mmol, 2.00 equiv) over 3 min. The reaction mixture developed a cloudy, white appearance. After 2.75 h, another aliquot of $\text{Zn}(\text{BH}_4)_2$ in Et_2O (1.50 mL, 0.22 mmol) was added. After 1 h, the reaction was quenched via saturated aqueous NH_4Cl (10.0 mL). The biphasic mixture was separated and the aqueous extracted with Et_2O (6×20 mL). The organic layers were dried over Na_2SO_4 , filtered and concentrated under reduced pressure. The crude residue was purified by flash chromatography (5% MeOH/ CH_2Cl_2) yielding the title compound (37.0 mg, 0.236 mmol, 70%) as a clear, colorless oil. TLC: R_f = 0.29 (5% MeOH/ CH_2Cl_2); ^1H NMR (CDCl_3 , 400 MHz) (contaminated with MeOH) δ 4.53–4.42 (m, 1H), 3.68 (dd, J = 11.2, 4.8 Hz, 1H), 3.63–3.54 (m, 1H), 3.36 (dd, J = 11.2, 8.8 Hz, 1H), 3.24 (dd, J = 11.2, 8.8 Hz, 1H), 1.96–1.87 (m, 1H), 1.18 (t, J = 7.2 Hz, 1H), 1.02–

0.86 (m, 4H).

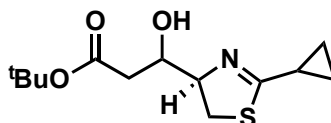


Lithium (*R*)-2-cyclopropyl-4,5-dihydrothiazole-4-carboxylate (5.12). To a flask containing the methyl ester **5.11** (127.5 mg, 0.690 mmol, 1.00 equiv) in MeOH (3.45 mL) in an ice–water bath (0 °C) was added an aqueous solution of LiOH (1N, 0.69 mmol, 1.00 equiv) dropwise over 2 min. The mixture was allowed to warm to room temperature for 1.5 h. The reaction was quenched by the addition of acetone (13.8 mL). The white precipitate was vacuum filtered and dried under reduced pressure affording the title compound (74.6 mg, 0.421 mmol, 61%) as a white, flakey solid. ¹H NMR ((CD₃)₂SO, 400 MHz) δ 4.52 (t, *J* = Hz, 1H), 3.40–3.25 (m, 2H), 1.85–1.76 (m, 1H), 0.92–0.75 (m, 4H).

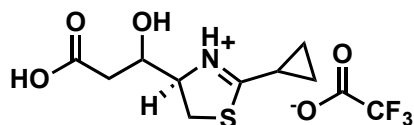


***tert*-Butyl (*R*)-3-(2-cyclopropyl-4,5-dihydrothiazol-4-yl)-3-oxopropanoate (5.16).** A flask containing *i*Pr₂NH (0.361 mL, 2.58 mmol, 2.20 equiv) in THF (10.0 mL) was equilibrated in dry ice–MeCN bath (–78 °C). To the cooled solution was slowly added *n*-BuLi (2.39M, 1.08 mL, 2.58 mmol, 2.20 equiv) and the reaction mixture was stirred for 1.5 h. An aliquot of *t*-BuOAc (0.346 mL, 2.58 mmol, 2.20 equiv) was added slowly over 5 min. A THF solution (2.00 mL) of methyl ester **5.10** (0.217 g, 1.17 mmol, 1.00 equiv) was added over 3 min. After 1h 40 min, the reaction was quenched by addition of aqueous saturated NH₄Cl (5.00 mL). The quenched reaction was warmed to ambient temperature and the layers were separated. The aqueous layer was extracted with EtOAc (4 × 15.0 mL). The organic fractions were concentrated under reduced pressure. The crude residue was purified by flash chromatography (15% EtOAc/hexanes) affording the title compound (0.174 g, 0.642 mmol, 55%) as a colorless cloudy oil. TLC: *R*_f = 0.39

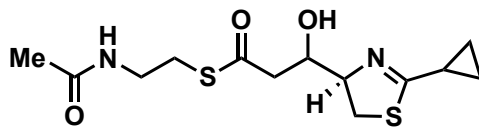
(30% EtOAc/hexanes); ^1H NMR (CDCl_3 , 400 MHz) δ 5.08 (dd, $J = 9.6, 7.6$ Hz, 1H), 3.72–3.53 (m, 3H), 3.42 (t, $J = 10.0$ Hz, 1H), 1.98–1.90 (m, 1H), 1.47 (s, 9 H), 1.15–0.96 (m, 4H); ^{13}C NMR (CDCl_3 , 100 MHz) δ 202.2, 176.5, 166.5, 84.5, 82.1, 48.7, 33.5, 28.1, 15.1, 9.71, 9.65; HRMS (ESI-TOF) m/z : $[\text{M} + \text{Na}]^+$ Calcd for $\text{C}_{13}\text{H}_{19}\text{NO}_3\text{SNa}$ 292.0978; found 292.0990 ($\Delta = 4.1$ ppm). (In practice this compound was reduced immediately after isolation to combat undesired thiazoline oxidation to the corresponding thiazole).



tert-Butyl 3-((*R*)-2-cyclopropyl-4,5-dihydrothiazol-4-yl)-3-hydroxypropanoate (5.17/5.18). To a flask containing β -ketoester **5.16** (87.7 mg, 0.326 mmol, 1.00 equiv) was added MeOH (10.0 mL). The resulting clear, colorless solution was cooled to 0 °C (ice–water). To the chilled solution was added NaBH_4 (37.0 mg, 0.978 mmol, 3.00 equiv) in one portion. The reaction was stirred for 35 min and quenched upon addition of saturated aqueous NH_4Cl (5.00 mL). The biphasic solution was warmed to ambient temperature and extracted with EtOAc (4×10.0 mL). The combined organic layers were dried over Na_2SO_4 , filtered and concentrated under reduced pressure. The crude residue was purified by flash chromatography (30–40% EtOAc/hexanes) affording a 2:1 mixture of title compounds (74.0 mg, 0.273 mmol, 84%) as a slightly yellow oil. TLC: $R_f = 0.35$ and 0.34 (30% EtOAc/hexanes); ^1H NMR (CDCl_3 , 400 MHz) δ 4.50–4.41 (m, 0.33H), 4.38–4.28 (m, 0.66H), 4.18–4.10 (m, 0.33 H), 4.07–4.00 (m, 0.66H), 3.34–3.29 (m, 1H), 3.28–3.16 (m, 1H), 2.73 (ddd, $J = 16.4, 4.4, 3.2$ Hz, 0.66H), 2.61–2.42 (m, 1.33H), 1.95–1.84 (m, 1H), 1.48 (s, 2 H), 1.47 (s, 4H), 1.06–0.90 (m, 4H); HRMS (ESI-TOF) m/z : $[\text{M} + \text{Na}]^+$ Calcd for $\text{C}_{13}\text{H}_{21}\text{NO}_3\text{SNa}$ 294.1134; found 294.1126 ($\Delta = 2.7$ ppm).



(4*R*)-4-(2-Carboxy-1-hydroxyethyl)-2-cyclopropyl-4,5-dihydrothiazol-3-ium trifluoroacetate (5.19/5.20). A flask containing *tert*-butyl ester **5.17/5.18** (2:1 diastereomer mixture, 45.9 mg, 0.169 mmol, 1.00 equiv) in CH₂Cl₂ (4.50 mL) was cooled to 0 °C (ice–water). TFA (0.500 mL, 6.53 mmol, 38.6 equiv) was added dropwise and the reaction mixture was stirred at ambient temperature for 18 h. The reaction was quenched upon addition of MeOH (1.00 mL) and concentrated under reduced pressure affording the crude mixture (2:1) of title compounds (56.0 mg, 101%) as an off-white amorphous solid. TLC: *R_f* = 0.0 (10% MeOH/CH₂Cl₂); ¹H NMR (CD₃OD, 400 MHz) δ 4.75 (dt, *J* = 8.4, 3.6 Hz, 1H), 4.34 (app. quin, *J* = 4.8 Hz, 0.66H), 4.17 (dt, *J* = 8.0, 4.8 Hz, 0.33H), 3.80 (dd, *J* = 11.6, 10.0 Hz, 0.33H), 3.71–3.64 (m, 1.66 H), 3.57 (dd, *J* = 12, 7.2 Hz, 0.33 Hz), 2.68–2.52 (m, 1.33H), 2.46 (dd, *J* = 16.0, 8.4 Hz, 0.66H), 2.42–2.27 (m, 1H), 1.56–1.44 (m, 2H), 1.33–1.20 (m, 2H).



***S*-(2-Acetamidoethyl) 3-((*R*)-2-cyclopropyl-4,5-dihydrothiazol-4-yl)-3-hydroxypropanethioate (5.2/5.3).** To a flask containing the crude acid **5.19/5.20** (0.169 mmol, based on quant. yield for the prior deprotection) was added CH₂Cl₂ (20.0 mL) at 0 °C (ice–water). The resulting white opaque solution was supplemented with *N*-acetylcysteamine (35.9 μL, 0.338 mmol, 2.00 equiv). DMAP (22.7 mg, 0.186 mmol, 1.10 equiv) was slowly added to the mixture resulting in a colorless, clear solution. To the reaction mixture was added EDCI•HCl (38.6 mg, 0.202 mmol, 1.19 equiv) and the solution was slowly warmed to ambient temperature over 1 h 10 min. The reaction was quenched upon addition of saturated aqueous NH₄Cl (5.00 mL) and the biphasic solution was separated. The aqueous layer was extracted with EtOAc (4 × 10 mL) and the combined organic layers were dried over Na₂SO₄, filtered and concentrated under

reduced pressure. The crude residue was purified by flash chromatography (5–10% MeOH/CH₂Cl₂) affording a 2:1 mixture of the title compounds (21.7 mg, 0.0686 mmol, 41%) as a cloudy colorless oil. TLC: R_f = 0.34 (10% MeOH/CH₂Cl₂); ¹H NMR (CDCl₃, 400 MHz) δ 6.48 (br s, 0.33H), 6.19 (br s, 0.66H), 4.53 (app. quin, J = 5.2 Hz, 0.66H), 4.38 (d, J = 5.6, 0.33H), 4.30 (dd, J = 8.4, 2.8 Hz, 0.33H), (dt, J = 8.0, 6.0 Hz, 0.66H), 3.75–3.60 (m, 1H), 3.55 (q, J = 6.4, 0.66H), 3.41 (q, J = 6.0 Hz, 0.66H), 3.32–3.17 (m, 1H), 3.12–2.78 (m, 4H), 2.69–2.63 (m, 0.66H), 2.63–2.54 (m, 1H), 2.53–2.46 (m, 0.66H), 2.01 (s, 1H), 2.00 (s, 2H), 1.14–1.08 (m 0.66H), 1.00–0.95 (m, 0.66H), 0.72–0.63 (m, 1.2H), 0.63–0.56 (m, 0.66H), 0.51–0.44 (m, 0.66H); HRMS (ESI-TOF) m/z : [M + Na]⁺ Calcd for C₁₃H₂₀N₂O₃S₂Na 339.0808; found 339.0795, (Δ = 3.8 ppm).

References:

- (1) Wiley, P. F.; Gerzon, K.; Flynn, E. H.; Sigal, M. V.; Quarck, U. C. *J. Am. Chem. Soc.* **1955**, *77*, 3677.
- (2) Collie, J. N. *J. Chem. Soc.* **1907**, *91*, 1806.
- (3) Collie, N.; Myers, W. S. *J. Chem. Soc.* **1893**, *63*, 122.
- (4) Birch, A.; Massy-Westropp, R.; Moye, C. *Aust. J. Chem.* **1955**, *8*, 539.
- (5) Poust, S.; Phelan, R. M.; Deng, K.; Katz, L.; Petzold, C. J.; Keasling, J. D. *Angew. Chem., Int. Ed.* **2015**, *54*, 2370.
- (6) Xie, X.; Garg, A.; Keatinge-Clay, A. T.; Khosla, C.; Cane, D. E. *Biochemistry* **2016**, *55*, 1179.
- (7) Cane, D. E.; Liang, T. C.; Taylor, P. B.; Chang, C.; Yang, C. C. *J. Am. Chem. Soc.* **1986**, *108*, 4957.
- (8) Keatinge-Clay, A. T. *Chem. Biol.* **2007**, *14*, 898.
- (9) Valenzano, C. R.; You, Y.-O.; Garg, A.; Keatinge-Clay, A.; Khosla, C.; Cane, D. E. *J. Am. Chem. Soc.* **2010**, *132*, 14697.
- (10) Kwan, D. H.; Sun, Y.; Schulz, F.; Hong, H.; Popovic, B.; Sim-Stark, J. C. C.; Haydock, S. F.; Leadlay, P. F. *Chem. Biol.* **2008**, *15*, 1231.
- (11) Kwan, D. H.; Leadlay, P. F. *ACS Chem. Biol.* **2010**, *5*, 829.
- (12) Khare, D.; Hale, Wendi A.; Tripathi, A.; Gu, L.; Sherman, David H.; Gerwick, William H.; Håkansson, K.; Smith, Janet L. *Structure* **2015**, *23*, 2213.
- (13) Rosenthal, R. G.; Vogeli, B.; Quade, N.; Capitani, G.; Kiefer, P.; Vorholt, J. A.; Ebert, M.-O.; Erb, T. J. *Nat. Chem. Biol.* **2015**, *11*, 398.
- (14) Rosenthal, R. G.; Ebert, M.-O.; Kiefer, P.; Peter, D. M.; Vorholt, J. A.; Erb, T. J. *Nat. Chem. Biol.* **2014**, *10*, 50.
- (15) Kim, B. S.; Cropp, T. A.; Beck, B. J.; Sherman, D. H.; Reynolds, K. A. *J. Biol. Chem.* **2002**, *277*, 48028.
- (16) Claxton, H. B.; Akey, D. L.; Silver, M. K.; Admiraal, S. J.; Smith, J. L. *J. Biol. Chem.* **2009**, *284*, 5021.
- (17) Reid, R.; Piagentini, M.; Rodriguez, E.; Ashley, G.; Viswanathan, N.; Carney, J.; Santi, D. V.; Hutchinson, C. R.; McDaniel, R. *Biochemistry* **2003**, *42*, 72.
- (18) Kandziora, N.; Andexer, J. N.; Moss, S. J.; Wilkinson, B.; Leadlay, P. F.; Hahn, F. *Chem. Sci.* **2014**, *5*, 3563.
- (19) Bonnett, S. A.; Whicher, J. R.; Papireddy, K.; Florova, G.; Smith, J. L.; Reynolds, K. A. *Chem. Biol.* **2013**, *20*, 772.
- (20) Alhamadsheh, M. M.; Palaniappan, N.; DasChouduri, S.; Reynolds, K. A. *J. Am. Chem. Soc.* **2007**, *129*, 1910.
- (21) Wu, J.; Zaleski, T. J.; Valenzano, C.; Khosla, C.; Cane, D. E. *J. Am. Chem. Soc.* **2005**, *127*, 17393.
- (22) Li, Y.; Fiers, W. D.; Bernard, S. M.; Smith, J. L.; Aldrich, C. C.; Fecik, R. A. *ACS Chem. Biol.* **2014**, *9*, 2914.
- (23) Caffrey, P. *ChemBioChem* **2003**, *4*, 654.
- (24) Cundliffe, E.; Bate, N.; Butler, A.; Fish, S.; Gandeche, A.; Merson-Davies, L. A. *Van Leeuw. J. Microb.* **2001**, *79*, 229.
- (25) Piasecki, S. K.; Taylor, C. A.; Detelich, J. F.; Liu, J.; Zheng, J.;

- Komsoukaniants, A.; Siegel, D. R.; Keatinge-Clay, A. T. *Chem. Biol.* **2011**, *18*, 1331.
- (26) Vergnolle, O.; Hahn, F.; Baerga-Ortiz, A.; Leadlay, P. F.; Andexer, J. N. *ChemBioChem* **2011**, *12*, 1011.
- (27) Castonguay, R.; Valenzano, C. R.; Chen, A. Y.; Keatinge-Clay, A.; Khosla, C.; Cane, D. E. *J. Am. Chem. Soc.* **2008**, *130*, 11598.
- (28) Liu, Y. Q.; Li, Z.; Vederas, J. C. *Tetrahedron* **1998**, *54*, 15937.
- (29) Li, Y.; Dodge, G. J.; Fiers, W. D.; Fecik, R. A.; Smith, J. L.; Aldrich, C. C. *J. Am. Chem. Soc.* **2015**, *137*, 7003.
- (30) Shirokawa, S.; Kamiyama, M.; Nakamura, T.; Okada, M.; Nakazaki, A.; Hosokawa, S.; Kobayashi, S. *J. Am. Chem. Soc.* **2004**, *126*, 13604.
- (31) Shirokawa, S.; Shinoyama, M.; Ooi, I.; Hosokawa, S.; Nakazaki, A.; Kobayashi, S. *Org. Lett.* **2007**, *9*, 849.
- (32) Nagao, Y.; Hagiwara, Y.; Kumagai, T.; Ochiai, M.; Inoue, T.; Hashimoto, K.; Fujita, E. *J. Org. Chem.* **1986**, *51*, 2391.
- (33) Gonzalez, A.; Aiguade, J.; Urpi, F.; Vilarrasa, J. *Tetrahedron Lett.* **1996**, *37*, 8949.
- (34) Nahm, S.; Weinreb, S. M. *Tetrahedron Lett.* **1981**, *22*, 3815.
- (35) Batt, F.; Bourcet, E.; Kassab, Y.; Fache, F. *Synlett* **2007**, 1869.
- (36) Firouzabadi, H.; Ghaderi, E. *Tetrahedron Lett.* **1978**, 839.
- (37) Ball, S.; Goodwin, T. W.; Morton, R. A. *Biochem. J.* **1948**, *42*, 516.
- (38) Bartlett, S. L.; Beaudry, C. M. *J. Org. Chem.* **2011**, *76*, 9852.
- (39) Ema, T.; Sugiyama, Y.; Fukumoto, M.; Moriya, H.; Cui, J.-N.; Sakai, T.; Utaka, M. *J. Org. Chem.* **1998**, *63*, 4996.
- (40) Winkler, J. D.; Oh, K.; Asselin, S. M. *Org. Lett.* **2005**, *7*, 387.
- (41) Keatinge-Clay, A. T.; Stroud, R. M. *Structure* **2006**, *14*, 737.
- (42) Zheng, J.; Gay, D. C.; Demeler, B.; White, M. A.; Keatinge-Clay, A. T. *Nat. Chem. Biol.* **2012**, *8*, 615.
- (43) Keatinge-Clay, A. *J. Mol. Biol.* **2008**, *384*, 941.
- (44) Valenzano, C. R.; You, Y. O.; Garg, A.; Keatinge-Clay, A.; Khosla, C.; Cane, D. E. *J. Am. Chem. Soc.* **2010**, *132*, 14697.
- (45) Gay, D.; You, Y. O.; Keatinge-Clay, A.; Cane, D. E. *Biochemistry* **2013**, *52*, 8916.
- (46) Mukaeda, Y.; Kato, T.; Hosokawa, S. *Org. Lett.* **2012**, *14*, 5298.
- (47) Hari, T. P.; Labana, P.; Boileau, M.; Boddy, C. N. *ChemBioChem* **2014**, *15*, 2656.
- (48) Kapur, S.; Lowry, B.; Yuzawa, S.; Kenthirapalan, S.; Chen, A. Y.; Cane, D. E.; Khosla, C. *Proc. Natl. Acad. Sci. U. S. A.* **2012**, *109*, 4110.
- (49) Kapur, S.; Chen, A. Y.; Cane, D. E.; Khosla, C. *Proc. Natl. Acad. Sci. U. S. A.* **2010**, *107*, 22066.
- (50) Haines, A. S.; Dong, X.; Song, Z.; Farmer, R.; Williams, C.; Hothersall, J.; Ploskon, E.; Wattana-amorn, P.; Stephens, E. R.; Yamada, E.; Gurney, R.; Takebayashi, Y.; Masschelein, J.; Cox, R. J.; Lavigne, R.; Willis, C. L.; Simpson, T. J.; Crosby, J.; Winn, P. J.; Thomas, C. M.; Crump, M. P. *Nat. Chem. Biol.* **2013**, *9*, 685.
- (51) Whicher, J. R.; Dutta, S.; Hansen, D. A.; Hale, W. A.; Chemler, J. A.; Dosey, A. M.; Narayan, A. R.; Hakansson, K.; Sherman, D. H.; Smith, J. L.; Skiniotis, G.

Nature **2014**, 510, 560.

(52) Dutta, S.; Whicher, J. R.; Hansen, D. A.; Hale, W. A.; Chemler, J. A.; Congdon, G. R.; Narayan, A. R.; Hakansson, K.; Sherman, D. H.; Smith, J. L.; Skiniotis, G. *Nature* **2014**, 510, 512.

(53) Heathcote, M. L.; Staunton, J.; Leadlay, P. F. *Chem. Biol.* **2001**, 8, 207.

(54) Butler, A. R.; Bate, N.; Cundliffe, E. *Chem. Biol.* **1999**, 6, 287.

(55) Claxton, H. B.; Akey, D. L.; Silver, M. K.; Admiraal, S. J.; Smith, J. L. *J. Biol. Chem.* **2009**, 284, 5021.

(56) Armarego, W. L. F.; Perrin, D. D. *Purification of laboratory chemicals*; 4th ed.; Butterworth Heinemann: Oxford ; Boston, 1996.

(57) Schmauder, A.; Muller, S.; Maier, M. E. *Tetrahedron* **2008**, 64, 6263.

(58) Cane, D. E.; Tan, W.; Ott, W. R. *J. Am. Chem. Soc.* **1993**, 115, 527.

(59) Gerwick, W. H.; Proteau, P. J.; Nagle, D. G.; Hamel, E.; Blokhin, A.; Slate, D. L. *J. Org. Chem.* **1994**, 59, 1243.

(60) Gu, L.; Wang, B.; Kulkarni, A.; Geders, T. W.; Grindberg, R. V.; Gerwick, L.; Hakansson, K.; Wipf, P.; Smith, J. L.; Gerwick, W. H.; Sherman, D. H. *Nature* **2009**, 459, 731.

(61) Gu, L.; Wang, B.; Kulkarni, A.; Gehret, J. J.; Lloyd, K. R.; Gerwick, L.; Gerwick, W. H.; Wipf, P.; Håkansson, K.; Smith, J. L.; Sherman, D. H. *J. Am. Chem. Soc.* **2009**, 131, 16033.

(62) Gu, L.; Eisman, E. B.; Dutta, S.; Franzmann, T. M.; Walter, S.; Gerwick, W. H.; Skiniotis, G.; Sherman, D. H. *Angew. Chem., Int. Ed.* **2011**, 50, 2795.

(63) McCarthy, J. G.; Eisman, E. B.; Kulkarni, S.; Gerwick, L.; Gerwick, W. H.; Wipf, P.; Sherman, D. H.; Smith, J. L. *ACS Chem. Biol.* **2012**, 7, 1994.

(64) Khare, D.; Wang, B.; Gu, L.; Razelun, J.; Sherman, D. H.; Gerwick, W. H.; Håkansson, K.; Smith, J. L. *Proc. Natl. Acad. Sci. U. S. A.* **2010**, 107, 14099.

(65) Gu, L.; Geders, T. W.; Wang, B.; Gerwick, W. H.; Håkansson, K.; Smith, J. L.; Sherman, D. H. *Science* **2007**, 318, 970.

(66) Whicher, J. R.; Smaga, S. S.; Hansen, D. A.; Brown, W. C.; Gerwick, W. H.; Sherman, D. H.; Smith, J. L. *Chem. Biol.* **2013**, 20, 1340.

(67) Akey, D. L.; Razelun, J. R.; Tehranisa, J.; Sherman, D. H.; Gerwick, W. H.; Smith, J. L. *Structure* **2010**, 18, 94.

(68) Gehret, J. J.; Gu, L.; Gerwick, W. H.; Wipf, P.; Sherman, D. H.; Smith, J. L. *J. Biol. Chem.* **2011**, 286, 14445.

(69) Geders, T. W.; Gu, L.; Mowers, J. C.; Liu, H.; Gerwick, W. H.; Håkansson, K.; Sherman, D. H.; Smith, J. L. *J. Biol. Chem.* **2007**, 282, 35954.

(70) Yoo, H.-D.; Gerwick, W. H. *J. Nat. Prod.* **1995**, 58, 1961.

(71) Chang, Z.; Sitachitta, N.; Rossi, J. V.; Roberts, M. A.; Flatt, P. M.; Jia, J.; Sherman, D. H.; Gerwick, W. H. *J. Nat. Prod.* **2004**, 67, 1356.

(72) Moss, S. J.; Martin, C. J.; Wilkinson, B. *J. Nat. Prod.* **2004**, 21, 575.

(73) Evans, D. A.; Downey, C. W.; Shaw, J. T.; Tedrow, J. S. *Org. Lett.* **2002**, 4, 1127.

(74) Crimmins, M. T.; Chaudhary, K. *Org. Lett.* **2000**, 2, 775.

(75) Wadsworth, W. S.; Emmons, W. D. *J. Am. Chem. Soc.* **1961**, 83, 1733.

(76) Rathke, M. W.; Nowak, M. *J. Org. Chem.* **1985**, 50, 2624.

- (77) Blanchette, M. A.; Choy, W.; Davis, J. T.; Essenfeld, A. P.; Masamune, S.; Roush, W. R.; Sakai, T. *Tetrahedron Lett* **1984**, 25, 2183.
- (78) Batt, F.; Fache, F. *Eur. J. Org. Chem.* **2011**, 2011, 6039.
- (79) Nakatsuka, M.; Ragan, J. A.; Sammakia, T.; Smith, D. B.; Uehling, D. E.; Schreiber, S. L. *J. Am. Chem. Soc.* **1990**, 112, 5583.
- (80) Holson, E. B.; Roush, W. R. *Org. Lett.* **2002**, 4, 3719.
- (81) Shirokawa, S.-i.; Kamiyama, M.; Nakamura, T.; Okada, M.; Nakazaki, A.; Hosokawa, S.; Kobayashi, S. *J. Am. Chem. Soc.* **2004**, 126, 13604.
- (82) Kinoshita, K.; G Williard, P.; Khosla, C.; Cane, D. E. *J. Am. Chem. Soc.* **2001**, 123, 2495.
- (83) Yang, Y.-H.; Shi, M. *J. Org. Chem.* **2005**, 70, 8645.
- (84) Charette, A. B.; Chua, P. *J. Org. Chem.* **1998**, 63, 908.
- (85) Lai, J.-Y.; Yu, J.; Mekonnen, B.; Falck, J. R. *Tetrahedron Lett* **1996**, 37, 7167.
- (86) White, J. D.; Kim, T.-S.; Nambu, M. *J. Am. Chem. Soc.* **1997**, 119, 103.
- (87) Wipf, P.; Xu, W. *J. Org. Chem.* **1996**, 61, 6556.
- (88) Brooks, D. W.; Lu, L. D. L.; Masamune, S. *Angew. Chem., Int. Ed.* **1979**, 18, 72.
- (89) Schwab, J. M.; Klassen, J. B. *J. Am. Chem. Soc.* **1984**, 106, 7217.

Appendix

^1H NMR and ^{13}C NMR data for synthetic compounds are provided following the order of their synthetic route in the text.

